BEACH AND DUNE EROSION ALONG THE COAST OF RICHARDS BAY, SOUTH AFRICA AND IMPLICATIONS FOR THE MANAGEMENT OF SHORELINE CHANGE

Suvana Alakram
40907481

DFGGR91
SUPERVISOR: PROF. DAVID WILLIAM HEDDING

DEPARTMENT OF GEOGRAPHY
UNIVERSITY OF SOUTH AFRICA

Submitted in partial fulfilment of the requirements for the degree
MASTER OF SCIENCE (GEOGRAPHY)

January 2026

BEACH AND DUNE EROSION ALONG THE COAST OF RICHARDS BAY, SOUTH AFRICA AND IMPLICATIONS FOR THE MANAGEMENT OF SHORELINE CHANGE

Student: Suvana Alakram
Supervisor: Prof D.W. Hedding
Department: Geography, University of South Africa
Degree: Master of Science (Geography)

Abstract

Sandy beaches are dynamic in nature and are subject to natural and anthropogenic processes that influence its evolution. One of the key drivers of coastal evolution is the erosion of the coastline. Sandy beaches are more susceptible to erosion because its fine sand is easily erodible. Since approximately 80% of South Africa's coastline consists of sandy beaches, including environmentally sensitive dune systems, the impetus is to improve our knowledge and understanding of processes taking place at the coastal zone to aid in coastal zone management and planning for future hazards. This research integrated the use of geographical information systems (GIS), remote sensing, and modelling techniques to contribute knowledge on the interrelationships between the spatial and temporal dynamics of shoreline changes along the coast of Richards Bay, South Africa. Shoreline change rates were quantified over a 45 year period between 1977 and 2022 using the United States Geological Survey's Digital Shoreline Analysis System. The historical data was then used to estimate future shoreline positions 10 and 20 years into the future. The results of the shoreline analysis revealed consistent erosion north of the Richards Bay harbour with a net shoreline movement of 167.80 m in some areas. The beaches south of the harbour recorded an accretional trend with a net shoreline movement of 98.90 m in some areas. The study verified that the development of the port breakwaters has caused an interruption the longshore sediment transport pattern, resulting in accretion on the updrift side (South), and erosion on the downdrift (North). The shoreline change rate statistics were used to predict future shoreline positions using the Extrapolated Linear Regression method 10 and 20 years into the future. In the context of climate change and associated sea level rise, model based approaches in ArcGIS Pro were used to assess the vulnerability of the study area to inundations caused by storm

surges. The inundation screening was initated for four different surge levels using a high resolution DEM as input. The results indicated that during a 9 and 10 m storm surge, 60 and 68% of the study area respectively was inundated which serves as important baseline information for disaster risk assessments. This dissertation also explored possible pathways to coastal resilience and proposed strategies to mitigate coastal erosion and flooding in a changing environment.

Samevatting

Strande is dinamies en onderhewig aan natuurlike en antropogeniese prosesse wat die evolusie daarvan beïnvloed. Een van die belangrikste dryfkragte van kusevolusie is erosie van die kuslyn. Strande is meer vatbaar vir erosie omdat fyn sand maklik erodeerbaar is. Ongeveer 80% van Suid-Afrika se kuslyn bestaan uit hoofsaaklik sand dominante strande wat omgewings belangrikke duinstelsels behels. Dus is die doel van hierdie projek om ons kennis en begrip van kussoonprosesse te verbeter asook om te help met kussonebestuur en beplanning vir toekomstige gevare. Hierdie navorsing maak gebruik van ‘n metode wat geografiese inligtingstelsels (GIS), afstandswaarneming en modelleringstegnieke behels. Met die doel om die onderliggende verband tussen die ruimtelike en temporale dinamika van kuslynveranderinge langs die kus van Richardsbaai, Suid-Afrika, beter te verstaan. Die kuslynveranderingstempo's is oor 'n tydperk van 45 jaar, tussen 1977 en 2022, gekwantifiseer met behulp van die Verenigde State se Geologiese Opname se Digitale Kuslynanalisestelsel (DSAS). Hierdie historiese data was gebruik om die toekomstige kuslynposisies te skat oor 10 en 20 jaar. In sommige gebiede het die studie erosie noord van die Richardsbaai-hawe uitgewys met 'n totale kuslynbeweging van 167.80 m. Strande suid van die hawe het 'n akkresionele tendens vertoon met 'n netto kuslynbeweging van 98.90 m in sommige gebiede. Met klimaatverandering en stygende seevlaktes ingedagte, was ArcGIS Pro gebruik om die kwesbaarheid van die studiegebied vir stormvloede te modeleer en assesseer. Vier verskillende stormvloed scenarios was getoets met behulp van hoë resolusie DEMs. Die resultate wys dat 60 of 68 persent van die studiegebied sal vloed met ‘n 9 of 10 m stormvloed scenario en dien as ‘n belangrikke basislyn for toekomstige ramp en risikoassesering. Verder, ondersoek hierdie navorsing opsies om kusveerkragtigheid te

verbeter en stel strategië voor om die impak van kuserosie en vloede te versag in ‘n area wat klimaatverandering ondervind.

Declaration

I, Suvana Alakram, declare that the thesis is my own work and that all the sources that I have used or quoted have been indicated and acknowledged by means of complete references, and that any use of Artificial Intelligence (AI) has been fully disclosed.

I further declare that I submitted the thesis to the appropriate originality detection system which is endorsed by Unisa and that it falls within the accepted requirements for originality.

I further declare that I have not previously submitted this work, or part of it, for examination at Unisa for another qualification or at any other higher education institution.

I further declare that where Artificial Intelligence (AI) tools have been used in the preparation of this thesis/dissertation, their use has been limited to ethical permissible support, has been fully disclosed, and does not replace my own original research, my independent critical thinking and analysis, or authorship responsibilities.

I understand that failure to disclose AI use, plagiarism and/or lack of academic integrity may constitute academic misconduct under Unisa's policies.

Signature:

Date:
26/01/2026

Acknowledgments

The role of fortune, both positive and negative, has shaped my life and given me an opportunity to increase my knowledge, and for that I am grateful to God.

I express my profound gratitude to my husband, Avesh, for the love, devotion and support towards my success. Without you, this would not be possible. I am forever grateful to my son Areev, for being a patient and pleasant child while I spent endless hours at my desk. I appreciate you both. This is dedicated to you.

Appreciation and immense gratitude goes to my supervisor, Professor David Hedding for the guidance, valuable advice and constant, timely support which was critical to my goal.

I thank Rachael Henderson of the United States Geological Survey (USGS) for the input on the extrapolated linear regression method for shoreline forecasting and the numerous messages of support.

I am equally thankful to Professor Thomas Balstrom of the University of Copenhagen, Denmark for support provided on the models used in the storm surge analysis. For rectifying the errors on the models and creating the python scripts. Your willingness and patience provided a deeper motivation for me.

Finally, Stellenbosch University is acknowledged and thanked for providing the high-resolution Digital Elevation Model of the study area.

Table of Contents

Acronyms

- CD – Chart Datum
- CI – Confidence Inerval
- DALRRD – Department of Agriculture, Land Reform and Rural Development
- DSAS – Digital Shoreline Analysis System
- DTM – Digital Terrain Model
- ELR – Extrapolated Linear Regression
- EMP – Estuarine Management Plan
- EPR – End Point Rate
- EPRunc – Uncertainty of the end point rate
- ESRI – Environmental Systems Research Institute
- GIS – Geographical Information System
- ha – Hectare
- HAT – Highest Astronomical Tide
- HWL – High Water Line
- KZN – KwaZulu Natal province
- ID – Identifier
- km – Kilometre
- LAT – Lowest Astronomical Tide
- LiDAR – Light Detection and Ranging
- LCI – Confidence interval of linear regression
- LNC – Lunar Nodal Cycle
- LPS – Lunar Perigean Subharmonic
- LRR – Linear Regression Rate
- LR^2 – R-squared of linear regression
- LSE – Standard error of linear regression
- LWL – Low Water Line
- MAP – Mean Annual Precipitation
- MAR – Mean Annual Runoff
- MHW – Mean High Water
- m – Metre
- m^3 – cubic metres
- NPA – National Ports Act

- NGI – National Geospatial Information
- NSM – Net Shoreline Movement
- SCE – Shoreline Change Envelope
- SDGs – Sustainable Development Goals
- SLR – Sea level rise
- TNPA – Transnet National Ports Authority
- USGS – United States Geological Survey
- WCI – Confidence interval of weighted linear regression
- WDL – Wet-dry line
- WLR – Weighted Linear Regression
- WSE – Standard error of weighted linear regression
- WR^2 – R-squared of weighted linear regression

Definitions

- Arenaceous Member – a specific layer or unit within a large rock formation that is primarily composed of sand or sand-like material.
- Backshore – The portion of the beach subject to wave action only during storms.
- Barrier lagoon complex – a coastal feature, characterised by a long, narrow island (a barrier island), that is separated from the mainland by a shallow, sheltered body of water called a lagoon. This system is shaped by processes like wave action, wind, and sediment transport.
- Beach/sand nourishment – a coastal engineering technique where sand is added to an eroded beach to restore its width and volume.
- Breakwater / groyne – a barrier built out into the sea to protect a coast or harbour from the forces of waves and limit the movement and loss of beach sand.
- Chart Datum – The water level surface serving as origin of depths displayed on a nautical chart.
- Dolos (plural dolosse) – A type of concrete breakwater block shaped like a ships anchor designed to break wave energy.
- Dredging – Clearing the bed of a harbour, river or any body of water, by scooping sand, stones, weeds, or mud with a dredge.
- Extrapolated linear regression (ELR) – a statistical technique used to predict values outside the range of observed data. It assumes that the relationship between two variables remains constant and linear even beyond the observed range.
- Foreshore – The portion of the beach subject to wave action during non-storm conditions.
- Geographical Information System (GIS) – is a spatial system that creates, manages, analyses and maps all types of data.
- High Water Line (HWL) – A point that represents the maximum rise of a body of water over land.
- Intertidal zone – The zone between the high and low water tide.
- KwaZulu-Natal Bight – a small, widening coastal shelf region on South Africa's northeast coast, stretching from Richards Bay to Durban.
- Lignite – a soft brownish coal showing traces of plant structure, intermediate between bituminous coal and peat.
- Linear regression – shows the relationship between two variables by assuming they have a straight-line relationship.

- Littoral drift – The rate at which sediment is moved parallel to the coast in the littoral zone
- Littoral zone – The portion of the coastal profile where sediment can be transported by wave action.
- River impoundment – the creation of a reservoir or lake by obstructing a river's natural flow, typically through the construction of a dam or weir.
- Semi-diurnal tides – A coastal area that experiences two high and two low tides of approximately equal size every lunar day.
- Surf zone – The zone of broken waves extending from the breaker zone to the foreshore.
- Sustainable Development Goals (SDGs) – A set of interconnected global goals set up by the UN General Assembly in 2015, intended to serve as a blueprint for achieving a sustainable future for all.
- Swash zone – The zone of wave run-up on the beach and return of water in the form of backwash.
- Wave refraction – is the bending of waves as they pass from one medium to another, typically as they move from deeper to shallower water.

List of Figures

List of Tables

Chapter 1: Introduction

1.1 Background

Human population density is intensifying all over the world, specifically along coastal areas where there is an appetence for scenic beauty, idyllic climate, and economic and recreational activities. Consequently, the vulnerability of coastal areas to anthropogenic changes is increasing. Currently, it is estimated that approximately 40% of the worlds' population live within 100 km of the coast (United Nations, 2017) and, as such, the exploitation of coastal regions for urban development and tourism activities results in the phenomena known as "coastal squeeze". This process of coastal squeeze reduces the area available for natural processes to take place; thereby making the coastline more vulnerable to erosion (KZN EDTEA, 2023). Moreover, sea level rise linked to climate change will ultimately intensify this situation (Luijendijk et al., 2018).

Erosion can be described as the removal and deposition of soil, rock or dissolved particles from one place to another and occurs across all landscapes on the earth's surface. Coastal erosion is a process where the shoreline retreats in a landward direction due to a lack of sediment on a beach (Corbella & Stretch, 2012a; Smith et al., 2014; Esterhuizen, 2019; Murray et al., 2023). Coastal erosion results from a combination of various factors, both natural and anthropogenic. Natural forces include wave and wave regimes, ocean currents, tides, and sediment dynamics, while anthropogenic activities such as harbour construction, sand mining and tourism developments can cause significant changes to the coastal landscape. For example, the source of the sand on the beaches of Richards Bay comes from inland erosion from the Thukela (previously Tugela), uMhlathuze, and Mlalazi rivers and is washed onto the beaches by wave action (Simmonis, 2016). Consequently, sand mining in these rivers is impeding the delivery of sand to the coast, exacerbating the erosion problem (Fig.1.1). Regionally, agricultural expansion and dam construction are also impacting the transport of sediment to the coast which is affecting coastal erosion. Other factors that also impact coastal erosion include the nature and source of the sand, i.e. how easily it is eroded and local coastal geomorphology (Simmonis, 2016).

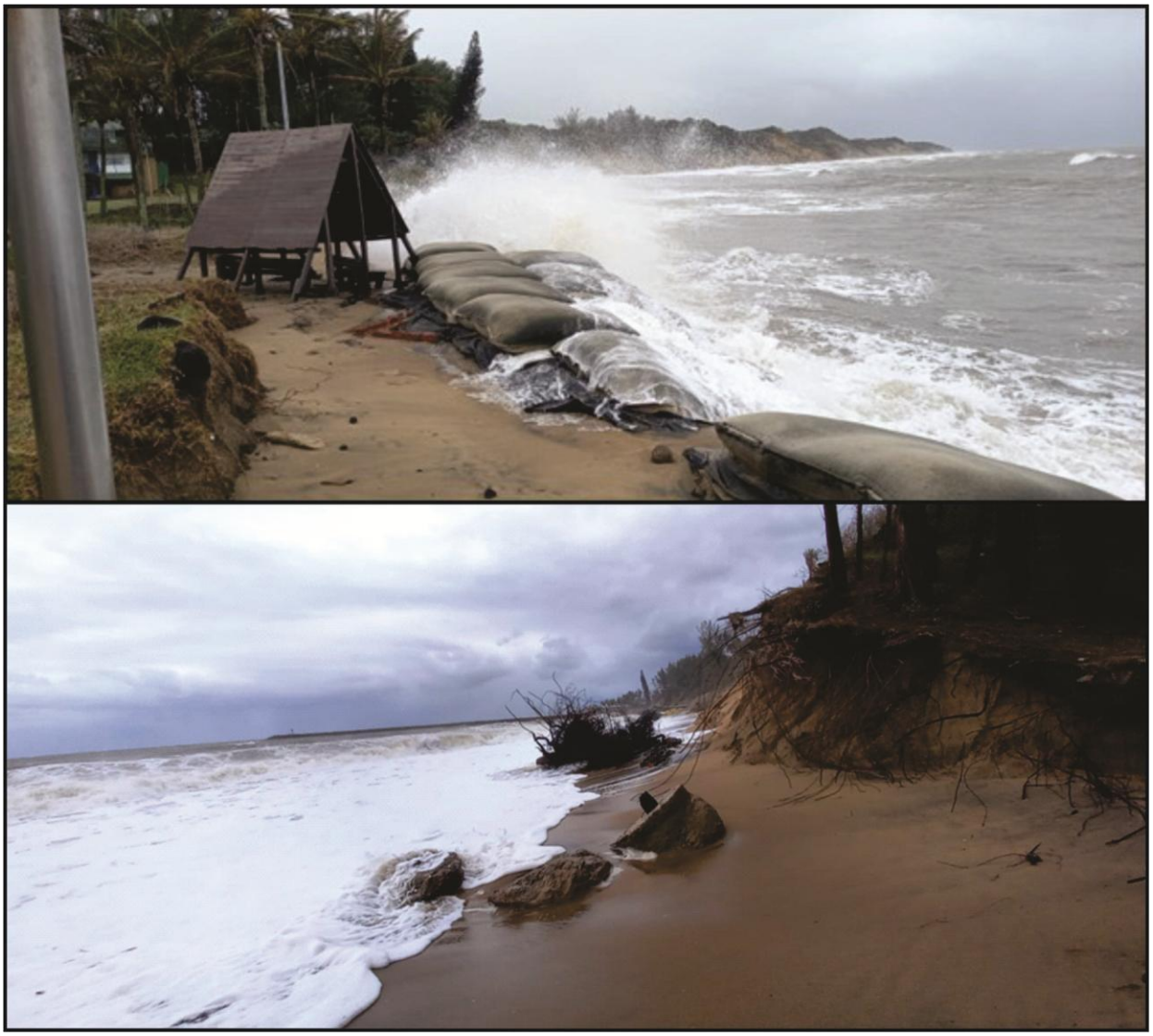

Figure 1.1: Shoreline retreat in Richards Bay, South Africa (Alakram, October 2023).

Globally, estimates of shoreline change vary greatly. Luijendijk et al. (2018) suggest that the reason for this is that there is no reliable global-scale assessment of their occurrence (i.e. erosion/accretion rates). Luijendijk et al. (2018) calculates that approximately 24% of sandy beaches worldwide are eroding while the previous estimate provided by Bird (1985) suggests that at least 70% of sandy beaches worldwide are eroding. More in line with the calculation for eroding coastal regions provided by Luijendijk et al. (2018), the recent study by Barbaro et al. (2022) asserts that 30% of the worlds' coasts are eroding. Similarly, a study by Bozzeda et al. (2023) revealed that one-fifth of the global beaches analysed were experiencing extreme, or intense erosion rates. The global coastline comprises of several different types of landforms (e.g. deltas, estuaries, lakeshores, rocky coasts and sandy coasts). The focus of this dissertation is on sandy

coasts which are dynamic in nature, sensitive to change and constitute a considerable portion of the world's coastline.

A large proportion of the coastline of the UK (17%) and Ireland (19.9%) is suffering from erosion as a result of seal level rise, reduced sediment supply, vulnerability to extreme storms and human activities. The Environmental Agency in the UK estimates that, without coastal protection, approximately 28000 properties could be vulnerable to coastal erosion in 50 years (Bodezza et al., 2023). In the Gulf of California 72% of the shoreline is undergoing steady erosion (Medina et al., 2023). Severe erosion of sandy beaches in Spain, as a result of extreme storm events, has led to the destruction of numerous ports and beachfront properties (Flor-Blanco et al., 2021).

In South Africa, studies have shown that most of the sandy beaches are in an erosional state due to human impacts (disturbance to terrestrial environments, and of inter- and subtidal environments), short term hazards (storm surges), long term processes (sea level rise) and other coastal processes (sediment dynamics) (Smith et al., 2014; Smith et al., 2016; Luck-Vogel et al., 2019; Murray et al., 2023). Within the Richards Bay study area, particularly in areas north of the harbour, main recreational beach areas have disappeared, wave overtopping has led to temporary inundations, infrastructure have been lost to the sea, and further north, eroding sea cliffs have caused large erosion volumes to occur within short timemscales.

Fine sand is easily eroded and, therefore, more susceptible to erosion. In South Africa, the threat of coastal erosion to coastal communities and infrastrutureis severe because 80% of the roughly 3000 km coastline consists of sandy beaches and coastal dune ecosystems (Tinley, 1985; Murray et al., 2023). In addition, there is a growing pressure for coastal development in South Africa (Goble & MacKay, 2013). South Africa's coastal resources contribute nearly USD 6.3 billion to national income and coastal goods and services contribute to nearly 35% of Gross Domestic Product (GDP) (Department of Forestry, Fisheries and Environment: Oceans and Coasts; Operation Phakisa, 2013).

The beach-dune system in sandy beaches is dynamic in nature and sensitive to change (Fig. 1.2). Dunes are a natural coastal defense against erosion and act as significant barriers to the land-sea interface. According to McGwynne et al. (1996: 1) "Beaches and dunes are inextricably linked through the exchange of sand into a coupled sand transport system and as a

unit form an integral part of the coastal zone, a highly sensitive transition between the land and the sea. In addition to beaches and dunes, the coastal zone incorporates diverse features that include inshore waters, the intertidal zone, coastal lakes, lagoons and estuaries". The most important ecological function of coastal dunes is to serve as a protective natural barrier between the land and sea where it offers protection against storm surges, wave attacks and rising sea levels (Tinley, 1985; McGwynne et al., 1996; Maun, 2009., Jackson, 2019; D'Alessandro et al., 2022). Tinley (1985) identified seven determinants to dune development along the coast, 1) wind regime, 2) sand supply, 3) coast trend and configuration of shorelines (degree of exposure and deflection of the effective winds), 4) rainfall regime, 5) plant colonization, 6) wave action and longshore drift, and 7) river mouth dynamics (change of flow and sand input). The urgency of the restoration and preservation of coastal sand dunes has been emphasized by many studies (i.e. Tinley, 1985; McGwynne et al., 1996; Hellemaa, 1999; Smith et al., 2016; Knight & Burningham, 2019). Coastal sand dunes near Richards Bay in the province of KwaZulu-Natal (KZN) face additional impacts from mining for heavy metals (Mol et al., 2013).

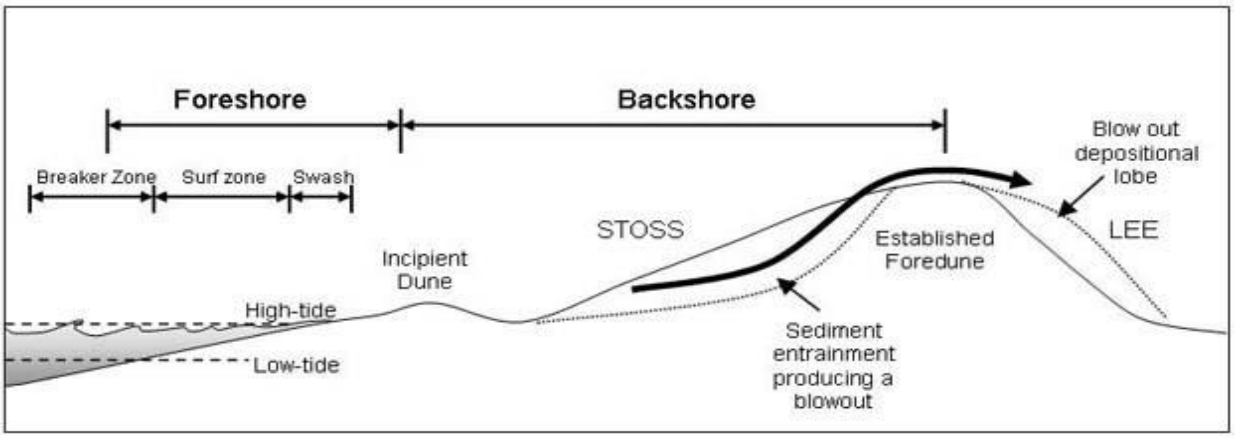

Figure 1.2: The beach-dune system (After du Pont, 2015).

Management of coastal environments for protection against coastal erosion demands a solid knowledge about the different processes which comprise coastal evolution. This knowledge is critical to categorize the different processes behind coastal evolution (Palalane, 2016). It can be simply described that the coast will erode and consequently the shoreline will recede, but we need to know what the eroded volume will be, and the range of expected recession to inform our decisions around different coastal protection interventions. Thus, predictions about future coastline changes, because of erosion, are valuable for the improvement of the protection of coastal sensitive systems (Palalane, 2016), spatial planning, mitigation of climate change impacts

along the coastline (Luijendijk et al., 2018; Enrique et al., 2019; Murray et al., 2023) and the use of soft approaches in coastal protection projects (Hellemaa, 1999).

The role of dune vegetation in protecting the coastal zone from erosion and storm damage is vital. The plants stabilize the dunes by trapping windblowm sand thus preventing erosion. Their roots also bind the soil together making it more resistant to wave action. “In a dune landscape, the geomorphological development of a beach depends on the ecological succession of plant communities.” (Hellemaa, 1999; p.9). The sand trapping efficiency of dune vegetation has profound impacts on coastal dune morphology and as a storm buffering function (Hellemaa, 1999; Jackson et al., 2019). Protecting and restoring coastal vegetation is essential for long-term coastal resilience and can aid in mitigating the effects of coastal erosion, storm ssurges and sea level rise.

1.2 Motivation

The Draft Umhlathuze/Richards Bay Estuarine Management Plan (Department of Forestry, Fisheries and the Environment: Oceans and Coasts, 2019) has identified key information gaps relating to erosion and sedimentation along the KZN coast. In particular, the Richards Bay cosatal zone is impacted by coastal infrastructure possibly having negative impacts on the natural sediment transport patterns, and activities including upstream dams in catchments draining into the sea, extensive sand mining activities, and also through the impacts of climate change (e.g.storm surges and seal level rise). In addition to this, the report’s objectives in terms of climate change are to prepare and implement coastal defense strategies to ensure community safety, infrastructure protection, and biodiversity protection.

Furthermore, the Draft Umhlathuze/Richards Bay Estuarine Management Plan (Department of Forestry, Fisheries and Environment: Oceans and Coasts, 2019) draws attention to the need for more research within the Richards Bay study area to build a stronger evidence-based knowledge system in support of the local Estuarine Management Plan (EMP). The proposed research aims to support the EMP by improving the knowledge base on coastal erosion and predicting future trends to aid in development planning, as well as to propose locations for the implementation of coastal defenses. While coastal erosion is a global threat, due to the dynamic nature of coastlines, modelling coastal evolution needs to be site specific and substantiated with an appropriate range of data so that effective coastal management can prevail in the area of interest (Murray et al., 2023).

Coastal management also contributes to the global Agenda 2030 Sustainable Development Goals (SDGs). Goal 14 states “to conserve and sustainably use our oceans, seas, and marine resources for sustainable development.” Target 14.2 of this SDG aims to “sustainably manage and protect marine and coastal ecosystems to avoid significant adverse impacts, including strengthening their resilience, and take action for their restoration in order to achieve healthy and productive oceans” by 2020 (UNEP, 2018).

After reviewing the literature, it has been determined that studies on shoreline dynamics on the coastal areas of KZN and especially to the north of Richards Bay are limited both in scope and number. On the KZN coast, shoreline changes and coastal dynamics were studied by Cooper (1991) and Esterhuizen (2019). Similar to the proposed research, Goble & MacKay (2013) conducted a study which incorporated the entire 580 km coastline of KZN. They used historical shoreline change for a period of 70 years to develop risk set back lines to ensure new developments are protected from coastal events. The study incorporated spatial analysis using Geographic Information Systems (GIS) software. This study’s main limitation is that episodic/extreme events leading to significant erosion could not be accounted for. In a similar way this research will make use of historical data to analyses the rates of change and to make forecast future shoreline positions for the coastal area of Richards Bay. This proposed study will also attempt to address the main limitations of the research by Goble & MacKay (2013) by conducting an inundation screening to model extreme weather events such as storm surges to aid in disaster management. The proposed inundation screening utilizes model-based approaches in ArcGIS Pro (Balstrom & Kirby, 2022) and no known study of this nature has hitherto been conducted in the Richards Bay coastal area or in South Africa at large.

1.3 Problem statement

In many low-lying coastal areas such as Richards Bay, human impacts have made a substantial contribution to the erosion problem. For example, the construction of the Port of Richards Bay has disrupted the longshore sediment transport patterns and, in turn, has resulted in erosion in some areas and accretion in other areas (Simmonis, 2016). The impact of illegal sand mining in rivers have resulted in less sand being deposited along the shores of Richards Bay and the KZN region in general (Department of Forestry, Fisheries and the Environment: Oceans and Coasts, 2019). At the same time, coastal populations are growing placing ever-increasing pressure of coastal regions, and this trend is set to continue. The threat of coastal erosion and consequent recession of the shoreline is predicted to intensify because of climate

change and associated sea level rise. In addition, the increase in the intensity and frequency of storm surges have exacerbated the situation with large quantities of sand dunes being lost to the sea. This raises the question – **What are the best responses to the problem of shoreline recession in the Richards Bay area?**

1.4 Aim and objectives of the study

The aim of the proposed research is to improve the understanding of long-term evolution and erosion of the Richards Bay coastline and to predict how it will change in the future.

- To investigate historical shoreline changes as indicators for describing coastal evolution using the Digital Shoreline Analysis System (DSAS) software.
- To predict the future range of expected recession of the current shoreline to aid in coastal zone management.
- To assess the vulnerability of the study area to inundations caused by storm surges using model-based approaches in ArcGIS Pro.
- To recommend mitigation and adaptation strategies to minimize coastal erosion in the study area.

1.5 Dissertation structure

Chapter 1 – provides a background to the study, the relevance of the concept of coastal erosion to the study area, and a detailed motivation for the study. The aims and objectives of the study are also described.

Chapter 2 – contains the literature review relating to the theory of coastal evolution, various methods of monitoring shoreline changes and shoreline forecasting. Theory on storm surges and their modelling as well as nature-based solutions are also presented.

Chapter 3 – provides a description of the Richards Bay area including its hydrology and geomorphology. Materials and methods used to conduct the study are also outlined in this chapter.

Chapter 4 – presents the results of the shoreline change analysis and shoreline forecasting as well as the storm surge inundation modelling.

Chapter 5 – discusses the results of the findings as described in Chapter 4 with a detailed analysis of the results. Recommendations on possible strategies to mitigate the effects of erosion in the study area are proposed.

Chapter 6 – provides a summary of the findings of the study and recommends actions for future research based on the findings and limitatations of the study.

Chapter 2: Literature review

2.1 Background

Coastal evolution resulting from erosion occurs when the action of wind, waves, and longshore currents move sand from the shore and deposit it somewhere else (Carter & Woodruff, 1997; Mafi-Gholami et al., 2017). “The sand can be moved to another beach, to the deeper ocean bottom, into an ocean trench, or onto the landside of a dune” (Mafi-Gholami et al., 2017:1). It can also be seen that because beaches and dunes get their sand supply from the transportation of rivers coming from inland (Esterhuizen, 2019), factors such as river regulation can impede the delivery of sand to the coast, making deposition a rare event.

Studies of coastal evolution examine and explore the reasons why the position and nature of the shoreline alter from time to time. (Carter & Woodruff, 1997). A classic example in coastal evolution studies is the Bruun Rule, first published in 1962 by Per Moller Bruun. The Bruun Rule was the first to give a relationship between sea level rise and shoreline recession (Bruun, 1954; Bruun, 1962) by the formula:

$$R = \frac{SL}{h + B} = \frac{S}{\tan \beta}$$

Where:

R = Shoreline recession, in metres

S = Sea level rise, in metres

L = Horizontal length of the bottom affected by the sea level rise (from the dune peak to depth of closure), in meters

h = depth of closure (the water depth beyond which significant sediment transport does not occur, in metres

B = dune height above sea level, in metres

β = average slope of the active profile

This model assumes that the shoreline will always strive towards an equilibrium profile and as sea levels rise, the profile translates landward and upward to preserve its shape relative to the new sea level (Cooper & Pilkey, 2004; Aargaard & Sorenson, 2012; Rosati et al., 2013). The widely quoted and globally utilized Bruun Rule has been subject to much academic debate since its conception, yet its application is still in use in coastal management today (with

modifications) (Cooper & Pilkey, 2004). Carter & Woodruff (1997) concluded that the Bruun Rule has, over the years, been proven unsuccessful because coastlines do not behave in a strict two-dimensional sense. Bruun himself acknowledged the characteristically simple rule and tried to widen its applicability (Bruun 1988; Aargaard & Sorenson, 2012). One of the biggest challenges that remain in terms of the application of the Bruun Rule is the isolation of forcing parameters at the coast such as wind and wave regimes, sediment dynamics (longshore and cross-shore transport), and tidal currents among others (Cooper & Pilkey, 2004; Rollason et al., 2010; Anderson et al., 2015). The Bruun Rule is a deterministic model used to calculate coastal erosion rates but does not consider coastal processes such as longshore transport. This study makes use of observed past changes to make predictions about the future as an alternative to computationally intense models.

2.2 Monitoring shoreline changes

The shoreline is situated at the interface between the atmosphere, ocean, and the land surface (Arnott, 2009). The interaction between these three different natural systems is responsible for shaping the shoreline thus making the coastal zone a highly dynamic one. Sustainable coastal management requires information about where the shoreline is, where it has been in the past, and where it is predicted to be in the future, to be able to assess the design and implementation of coastal protection measures, calibrate and verify numerical models, and to identify hazardous zones (Mafi-Gholami et al., 2017; Enriques et al., 2019; Saad et al., 2021). Jackson et al. (2014: 718) highlight that, “little work has been conducted on the contemporary form and dynamics of dunes along the dune-fringed KZN coast of South Africa, where vast amounts of sand are currently occupying modern dune fields along a relatively narrow coastal shelf environment.” The study area is a dune-fringed coast that has seen a significant loss of dunes due to coastal erosion and storm surges over the past decade (Fig. 2.1).

Figure 2.1: The dunes in the study area sits on top of the Port Dunford Formation (semi consolidated rock from the Pleistocene age) which gets exposed in eroding sea-cliffs as pictured above.

Threats to the natural environment, human life and infrastructure near the coastal zone owing to coastal flooding, storm surges and erosion, provide a new impetus to improve our knowledge and understanding of the changes taking place at the coast to effectively plan mitigation measures and improve adaptation strategies. One of the more widely used methods of doing this is by monitoring shoreline positions over time and providing rates of change statistics. Mafi-Goulami et al. (2017:1) state that “Shoreline geometry remains one of the key parameters in the detection of coastal erosion and deposition and the study of coastal morphodynamics”, and Farris et al. (2023:1) similarly assert that “the shoreline is a common metric used to monitor coastal evolution”.

The use of remote sensing in the mapping and monitoring of shoreline changes has a distinct advantage over traditional ground-based monitoring as it is more cost effective (Baig et al., 2020; Murray et al., 2023). Accurate and continuous monitoring of the shoreline position is necessary for the application of mitigation measures such as dune construction (nature-based solutions), building sea walls, and dikes (Nassar et al., 2019; Baig et al., 2020; Hossain et al., 2022). Sea walls and dikes (Fig. 2.2 and 2.3) are known as hard engineering structures that are designed to withstand and resist wave action and water overtopping (Singhvi *et al*., 2022). These man-made structures protect low-lying areas from flooding.

Figure 2.2: Armoured sea dikes in the Netherlands at low tide (Hanegan, 2010).

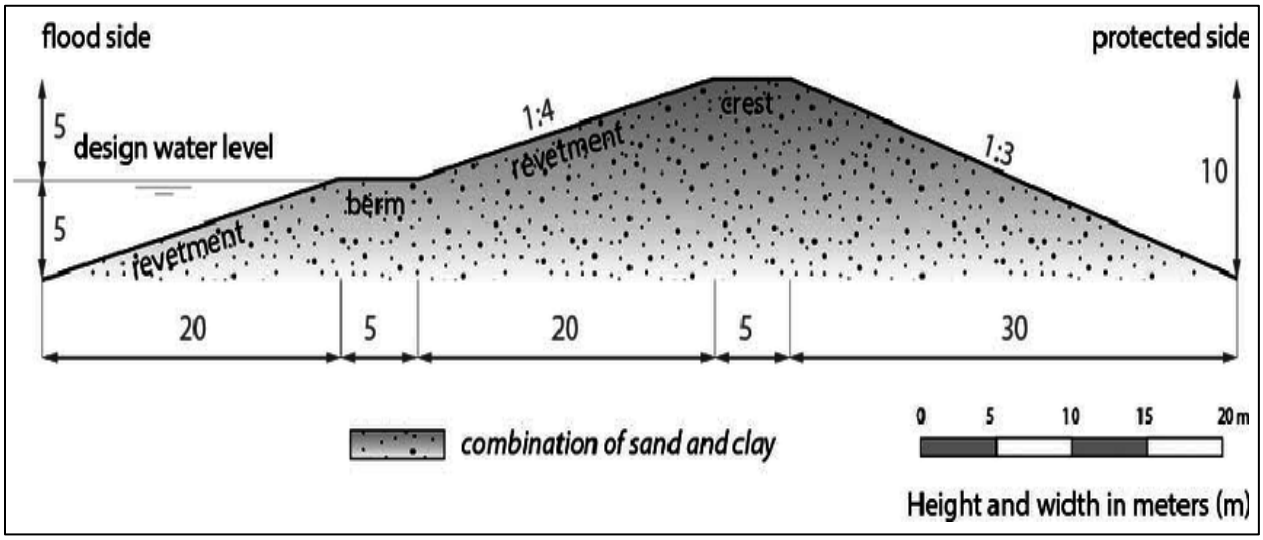

Figure 2.3: Schematic cross section of a typical sea dike in the Netherlands (Jonkman et al., 2013).

Shoreline variation has become vital in the context of climate change and sea level rise. Shoreline studies have already been conducted using remote sensing and GIS techniques for different spatial and temporal scales. Globally, shoreline dynamics has been addressed by numerous studies in the recent past (Oyedotun, 2014; Bheeroo *et al*., 2016; Mutaquin, 2017; Baig et al., 2020; Ferreira et al., 2021; Kilhar, 2022; Abd-Elhamid et al., 2023; Hoosen & Sultana, 2023) and in South Africa (Goble & MacKay, 2013; Smith et al., 2014; Murrary et al., 2023). The development of remote sensing technologies such as satellite imagery, aerial photography, airbourne LiDAR sensors and Synthetic Aperture Radar (SAR) sensors provide reliable data to monitor changes in shorelines (Ferreira et al., 2021; Kilhar, 2022). Although analysis of satellite imagery appears to be the most-commonly used technique to monitor shoreline changes (Kilhar, 2022; Tsai, 2022).

While most studies of spatiotemporal changes in coastlines have been conducted in areas of high anthropogenic influence, Ferreira et al. (2021) conducted a study in the Parnaiba Delta, Brazil, a sparsely populated and underdeveloped area. Using Landsat images (1984-2017) and the DSAS software, it was revealed that 52% of the coastline retreated under erosion while 48% accreted. Since the area has marginal anthropogenic influence, variability of natural factors such as river discharge and rainfall were concluded to be the main drivers proving that shorelines remain stable in areas of low human activity.

In South Africa, studies along the KZN coast (see Corbella & Stretch, 2012b; Smith et al., 2016) indicate that the main drivers of coastal erosion are sea level rise and reductions in the supply of beach sediment, suggesting that river regulation or illegal sand mining along rivers could be the factors why less sediment reaches the coastline. A study by Smith et al (2016) on the stability of the southeast African coastline highlighted and discussed errors when using aerial imagery in the analysis of coastal erosion with respect to the high water line. They conclude that the “decrease in coastal sand volume is likely to result in increased future erosion.” (Smith et al. 2016:1). During 2006-2007, the KZN coast was subjected to a number of large swells, with some coinciding with the spring tides resulting in severe erosion along parts of the coastline. In March 2007 the swells generated in Richards Bay, as recorded by data from the wave rider buoy, gave a maximum height of 14 m (Smith et al., 2010). During this event, the high water line retreated by 30 m and 5000 m^3 of sediment was displaced and transported 200 to 700 m further offshore and deposited at depths of approximately 21 m (Chart Datum) (Smith et al., 2010).

In Richards Bay, a 2006 study was conducted to investigate the cause of erosion inside the port after four groynes were constructed to stabilize the shoreline. Shoreline evolution in the vicinity if the groynes were documented and longshore sediment rates were estimated by means of beach surveys. Monitoring of the shoreline evolution involved documenting the tides, wave climate, wind, sand grain size, current regimes and beach slopes. The beach survey showed that progressive accretion occurs updrift, while erosion occurs downdrift of the groynes. This research provides important insight into a possible theory that groyne/breakwater construction interrupts the natural longshore drift of a particular area, resulting in accretion in some areas and erosion in others.

Similar to this study, Murray et al. (2023) conducted a study on the west coast of South Africa using remote sensing and the DSAS (Digital Shoreline Analysis System) software to quantify erosion rates over a 70-year period to determine the shoreline's vulnerability and predict its future position. The DSAS is a free software hosted by the United States Geological Survey (USGS). It enables a user to calculate rate-of-change statistics from multiple shoreline positions. The results conclude that the coastline changed tremendously, with a net erosion rate of 38 m. The study highlighted that since shorelines are highly dynamic environments, studies of this nature need to be site specific.

2.3 Shoreline forecasting

In addition to using shoreline geometry to measure rates of change over time, the historical data of shoreline geometry can also be used to predict its future positions for potential management actions. Typically, erosion rates are determined by performing a linear regression analysis and using the slope of the data to extrapolate the line into the future, thereby forecasting future shoreline positions based on the linear behavior of past shorelines. This type of time-series forecasting has some limitations in that they do not consider the relevant processes taking place at the coast e.g. accelerated erosion from storm surges, addition of coastal erosion infrastructure like groynes, interruptions in sediment transport, or sea-level rise (Calkoen et al., 2021). Even so, some states in the Unites States implicitly make use of this type of forecasting method to implement regulations based on 30-year erosion rates (Farris et al., 2023). In South Africa, this type of forecasting technique is also used by some municipalities to develop risk set back lines (Goble & McKay, 2013). Coastal risk set back lines are defined by a specific distance from the shoreline where development is prohibited to protect the coastline. In South Africa, the Integrated Coastal Management Act (ICM), Act 24 of 2008 refers to these as "Coastal Management Lines"

and are defined as, “designated boundaries along the coastline that mark the limit of development to protect coastal areas from natural hazards like erosion, flooding, and sea-level rise.”

A common method used to calculate future positions is the Kalman Filter model. This statistical forecasting method (Long & Plant, 2012) uses linear regression, calculated by DSAS, to generate 10- and/or 20-year forecasts. It has been applied in many recent studies (see Ciritci & Turk, 2020; Calkoen et al., 2021; Apostolopoulos et al., 2022; Islam & Crawford, 2022; Hoosen et al., 2023; Murray et al., 2023). Another method involves calculating an Extrapolated Linear Regression (ELR). According to Farris et al. (2023:2), this method “computes a shoreline rate by fitting a linear regression rate through all available data and then extrapolating the line to a specified future date”. Farris et al. (2023) compare the ELR method to the Kalman Filter model and found that both methods produced similar results. Calkoen et al. (2021) and Farris et al. (2023) agree that the ELR forecasting technique has many advantages because it is easy to compute, can be applied to large areas to compare vulnerabilities, and it can be used when temporal frequency of the data is inconsistent and/or wide.

Mathematical- and physics-based models are also used to model shoreline changes as well as predict its future position. These models consider hydro- and morpho-dynamic forces such as sediment transport patterns as well as wind, wave and tidal data to predict coastal change (Aargaard & Sorenson, 2011; Corbella & Stretch, 2012b; Hinkel et al., 2013; Palalane, 2016; Hugo & Luger, 2019; Farris et al., 2023). Enrique et al. (2019) demonstrated the importance of dunes as a coastal defense, reducing the shoreline retreat and dune vulnerability rates a few decades ahead. The methodology used was the numerical models XBeach and Q2D-morfo and applied in a sandy coast in the Mediterranean Sea, taking sediment transport into consideration. The GENESIS model is applicable to predicting generalized platform shoreline evolution specifically when alongshore gradients in sediment transport dominate (Mafi-Gholami et al., 2017). In Big Bay, Cape Town, the MIKE suite of numerical models was used to model sediment transport for a set of predetermined cases defined by the offshore wave conditions, the local water level and the longshore wind speed and direction to better understand the causes of beach erosion (Hugo & Luger, 2019). The results indicate that the erosion/accretion in Big Bay is likely to be caused by changes in wind direction as well as drought in Cape Town. While these models provide a more detailed analysis by taking into account geomorphic changes, they are usually very expensive, require large amounts of data, and “require large computational resources, which generally limits the spatial area over which the model can be applied” (Farris et al. 2023:2).

2.4 Storm surge analysis

The effects of climate change can be felt more rampantly near coastal areas where sea level rise presents a challenge for coastal management. These climate change impacts are expected to increase the exposure of coastal infrastructure and communities to storm surge hazards, resulting in an urgent need to study and understand the impact of storm surges on coastal zones (Kim et al., 2021). A storm surge occurs when high winds during a storm forces ocean water landward causing an abnormal rise in sea level. Single, independent, and isolated events such as storm surges may have an extremely important significance on coastal evolution. When these events are coupled with sea level rise, they can represent a twofold erosive force on beaches. For municipality planners and disaster management agencies to effectively plan and prepare for flooding caused by storm surges, information on what gets affected, how deep the inundated areas are, and where the surge enters are required (Balstrom & Kirby, 2022).

The ability of a beach to recover after a storm surge depends on the frequency of storms and the speed of beach recovery before the next storm occurs. A cluster of storms tend to worsen storm induced erosion of beach/dune systems because of insufficient recovery periods between storms resulting in rapid erosion. This is evidenced in a study by Dissanayake et al. (2015) on the Sefton coast, UK, where the numerical model X Beach was applied, demonstrating the impacts of storm clustering on beach/dune morpho-dynamics.

Globally, many recent examples have exemplified the significance of extreme events on coastal evolution. In the coastal regions of Bangladesh, a suite of Delft3D hydrodynamic and Delft Dashboard cyclone models were used to calculate inundation levels in efforts to build long-term adaptation plans (Rezaie & Haque, 2022). Sebastian et al. (2014) used the SWAN and ADCIRC hydrodynamic models to develop synthetic storm surge scenarios along the Texas coast and the results were incorporated into flood mitigation studies. The ADCIRC hydrodynamic model was also adopted by Pringle et al. (2021) in global storm tide modelling. Similarly, the MIKE21 and delft3d-flow numerical models have been used by Fadillah et al. (2020) in Indonesia which presents a comparison between the two models for tidal modelling.

In South Africa, Rautenbach et al. (2020) coupled hydrodynamic models, namely delft3d and SWAN, to provide an experimental physical description of South African storm surges for six coastal locations using wind, atmospheric pressure, and waves as the physical drivers. Mather & Stretch (2012) applied a more practical approach to the Durban coastline to address the

information gap on the likely effects of a combination of severe sea storms and future sea level rise on the shoreline using the Carter and Bruun models. The results indicate that storm surges and associated sea level rise along the sandy southern African coastline will have far reaching effects extending beyond just inundation and coastal erosion, suggesting that a lack of information creating a barrier for decision-making, and the lack of funds for coastal protection infrastructure places an increased burden for future disaster management.

Limited studies on storm surges were conducted in South Africa. A possible reason for this is described in Wahl (2016: ii), “Many scholars have essentially ruled out the possibility of large storm surges along the South African coast on the bias that winds are too moderate to agitate significant wind setup. As a result, storm surge heights for the South African coast, specifically, has never been thoroughly researched or documented.” Mather & Stretch (2012) similarly noted that research is lacking in terms of the likely effects of sea storms and future sea level rise, given the increase in coastal storms in Southern Africa. Their study used GIS and high-resolution aerial imagery to identify hazard zones in response to sea level rise and storm surges along the Durban coastline. Based on the Bruun Rule, the results describe and maps current and future risk of flooding and erosion to infrastructure and the natural environment.

The modelling of extreme weather events such as storm surges are primarily centered around hurricane-induced models that are based on empirical studies considering parameters such as wind, atmospheric pressure, waves, geomorphology of the coastline, geology, and bathymetry (Balstrom & Kirby, 2022). In lieu of this, Balstrom & Kirby (2022) presented a similar but simpler application for modelling storm surges where predictions are based on digital elevation data while assuming steady state terrain conditions. Using Model Builder in ArcGIS Pro, the DHyMSea model goes a step further to reveal water entry locations at various storm surge levels and propose mitigation actions such as the proposition of dikes as a coastal defense, which according to Balstrom & Kirby (2022), numerical models do not have that capability.

2.5 Natural coastal processes

Most of the world’s coastlines are eroding (Bird, 1985; Pilkey & Cooper, 2004; Smith et al., 2010). The drivers of coastal erosion are often complex and related to site specific conditions such as sediment transport patterns, sediment availability, human activity such as port construction, sea level rise, and other geomorphological factors. Understanding the role of a particular driver of coastal erosion is important for coastal planning and intervention.

Schoonees &Theron (2002) define longshore sediment transport as the process whereby sediment is moved parallel to the coastline by waves and ocean currents (Fig. 2.4). The sediment is stirred up by wave action and, as it becomes suspended, longshore currents (generated by wind, tidal variation, or waves approaching the coastline obliquely) transport it alongshore. The longshore transport rate, also known as littoral drift, is the rate at which sediment is moved parallel to the coast in the littoral zone (Schoonees & Theron, 2002; Palalane, 2016). Various numerical models are used to calculate longshore drift. These models can predict the movement of sediment over time and space, considering factors such as wave refraction and tidal currents (Schoonees & Theron, 2002; van Rijn, 2014; Palalane, 2016). As such, the design of port breakwaters and their dredging requirements need a thorough knowledge and understanding of the local longshore sediment transport rates and patterns.

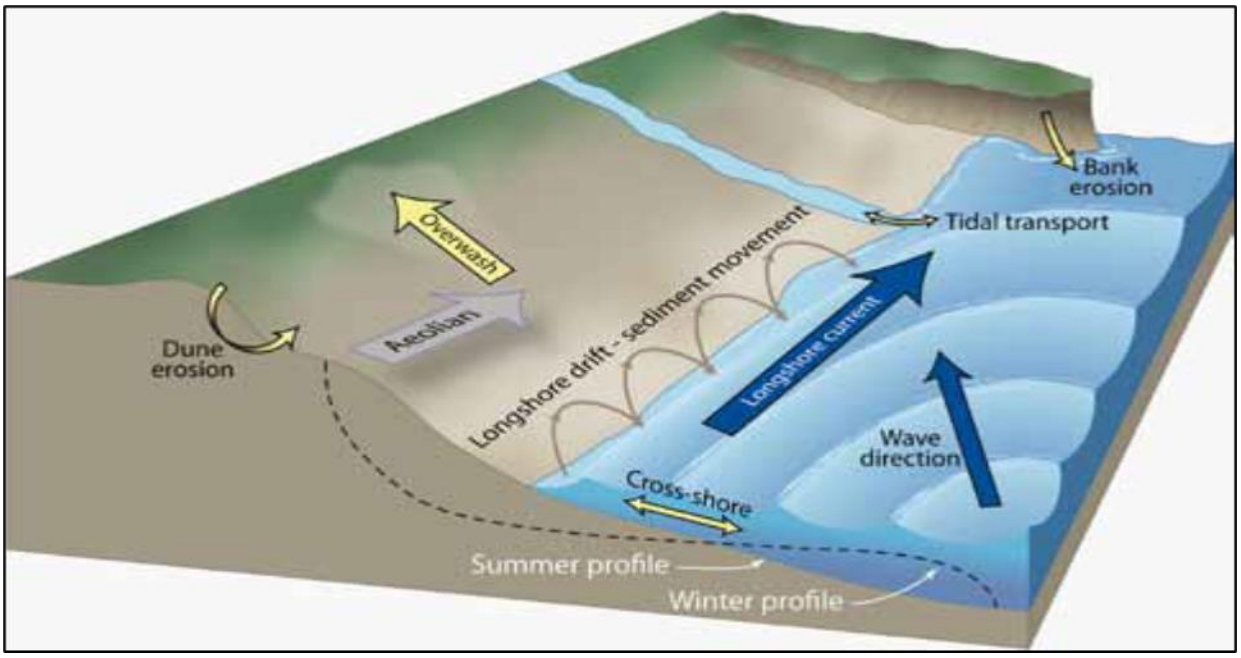

Figure 2.4: Diagrammatic representation of longshore sediment transport among other coastal processes (Source: WHSGP, 2011).

A study was undertaken by de Waal et al. (2007) to determine whether a significant physical impact on the shoreline of Richards Bay might result from the dredging of sand in the harbour. Approximately 1.3 million cubic metres of sand was required to fill behind a quay wall of a berth as part of the expansion to the Richards Bay Coal Terminal situated at the port. The study concluded that dredging sand can cause either erosion or accretion or both to the shoreline,

depending on the sand regime (i.e. longshore sediment pattern). The literature indicates that port infrastructure development can have an impact on natural coastal processes.

The main sediment source of the beaches in the study area comes from the Thukela River located approximately 75 km south of the study area with smaller rivers such as the uMhlathuze, and Mlalazi also contributing towards the sediment supply (Simmonis, 2016). When the Thukela River is in flood, sediment is pushed out to sea approximately 20 to 30 km from the beach at a rate of approximately 679 x 10 m^3 per year (Bosman et al., 2007). The longshore drift carries this sediment northwards where it is deposited onto beaches including the coast of Richards Bay. The creation of dams upstream (Esterhuizen, 2019) and illegal sand mining (Breetzke et al., 2016) impede delivery of sand to the coast resulting in increased erosion and the reduced capability of a beach to recover after a storm event.

2.6 Natural coastal defenses

In our efforts to quantify erosion rates for coastal management, natural solutions are to be highlighted and put forward as viable strategies. Knight (2023) demonstrates that coastal landforms can be considered as “green infrastructure” which can provide significant coastal protection. The study highlighted the critical role that coastal landforms such as dunes, rocky outcrops, and mangrove swamps play as a defense strategy and that effective management of these landforms can lead to positive impacts for coastal communities. Indeed, the move toward “green infrastructure” is gaining traction. For example, dune construction, where dunes are replicated, offer sustainable approaches to coastal erosion and consequent flooding. These nature-based solutions have increased significantly in the last decade (Singhvi et al., 2022). Recent advances in coastal engineering have benefited from the use of hybrid systems where traditional structures such as sea dikes are covered with layers of sand in an attempt to mimic dunes (D’Alessandro et al., 2022). Singhvi et al. (2022) conducted an integrated literature review on the “grey” versus “green” coastal protection infrastructure and found that combining the two were most beneficial. They also found that dikes and dune construction take up a wider portion of the grey-green spectrum.

In addition to the importance of coastal dunes as a land-sea barrier, mangrove swamps also play a role in coastal protection. Mangroves buffer coastal erosion and sea level rise and therefore can also be considered a coastal ‘landform’ where “the roots stabilize the substrate and encourage sediment aggradation” (Knight, 2023: 8). It is to be noted that the study area contains

the largest coverage of mangroves in South Africa (KZN EDTEA, 2023). This extensive coverage of mangroves, together with its significant dune formations, make it an important area to implement the concept of nature-based solutions to coastal erosion. However, more studies are required to substantiate this statement, i.e a more thorough knowledge of the coastal area, including natural beach fluctuations, and beach-dune dynamics needs to be understood and analysed.

Anthropogenic attempts to control the position of the shoreline can be seen in almost all coastal systems. The exploitation of the coast for tourism activities results in ‘coastal squeeze’, reducing the area available for natural coastal processes to prevail and making the management of coastal erosion a challenging task. However, we are not left empty handed. Technological advances have enabled us to simulate coastal behavior which can be used as a tool for predicting impacts and implementing mitigation measures. Although the overall problem of erosion cannot be stopped completely, it is imperative to understand the vital role that natural features such as dunes and mangroves play in coastal protection.

Chapter 3: Study area and methodology

3.1 Study area

3.1.1 Location

Richards Bay is a coastal town in northern Kwa-Zulu Natal and is situated within the uMhlathuze Local Municipality (Fig. 3.1). Hosting the country's largest and deepest Port, as well as one of the largest coal export terminals in Africa, the town has seen immense growth since the port was developed in the late 1970's. The municipality is bordered by 48 km of coastline of which 80% is still in its natural state and characterised by sandy beaches backed by well-established dune formations (uMhlathuze SDF, 2022). The subtropical climate, warm ocean, abundant wetlands, high biodiversity coupled with an extensive and high coastal dune system, makes it an ideal eco-tourism destination.

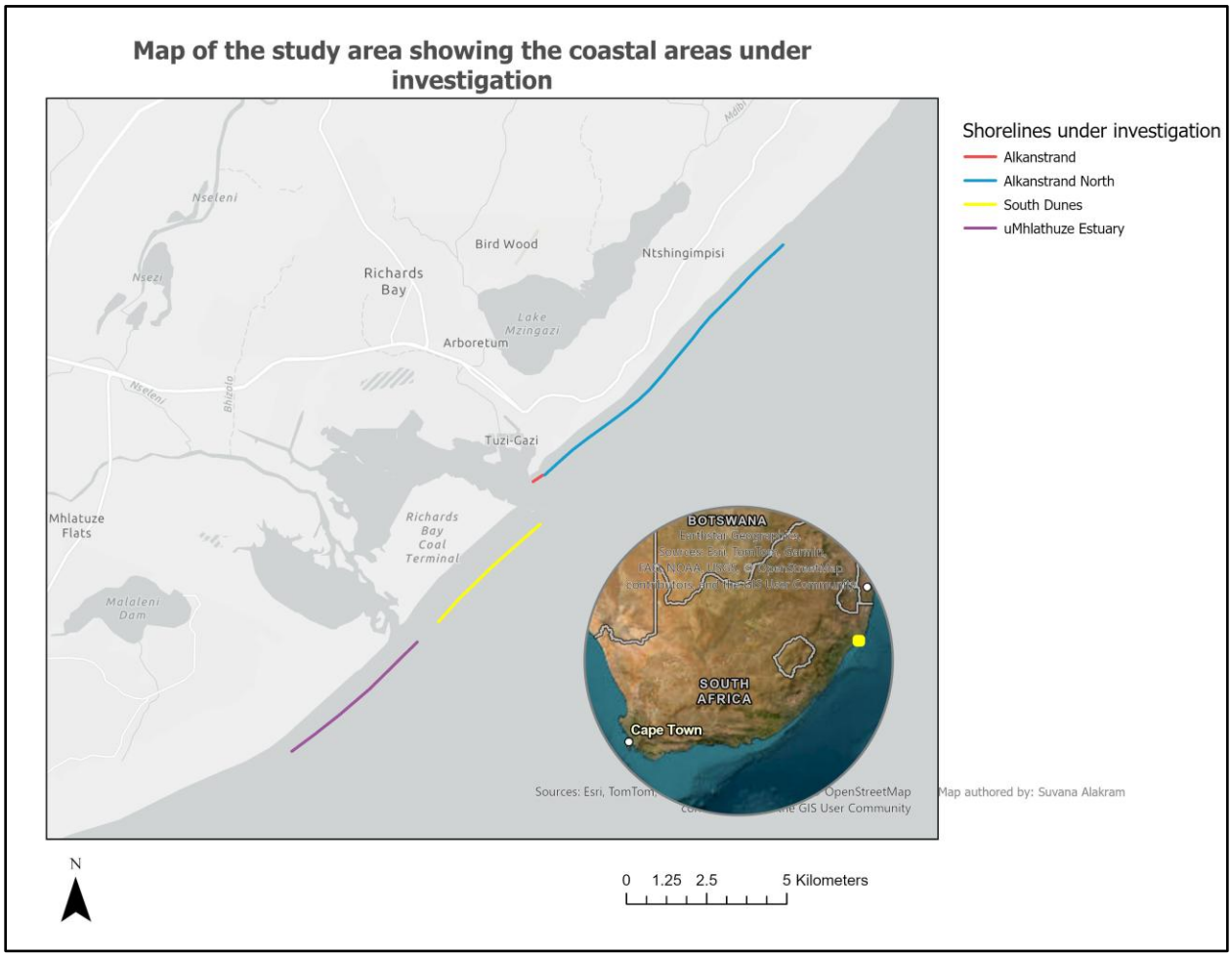

Figure 3.1: Location of the study area on the north-east coast of South Africa.

The coastline in the study area is described as a dune fringed coast. The dunes sit on top of semi-consolidated rock known as the Port Dunford Formation. The Formation is some 20 to 25 m thick and consists of “mammalian remains, marine fossils, crustacean burrows and wood debris, separated by a persistent lignite bed averaging 1.3 m thick from an upper cross-bedded Arenaceous Member up to 15 m thick” (Hobday & Orme, 1974: 1). This Pleistocene Port Dunford Formation is exposed in eroding sea cliffs along the Zululand coastline (Fig. 3.2), more specifically in the study area (Fig. 3.3).

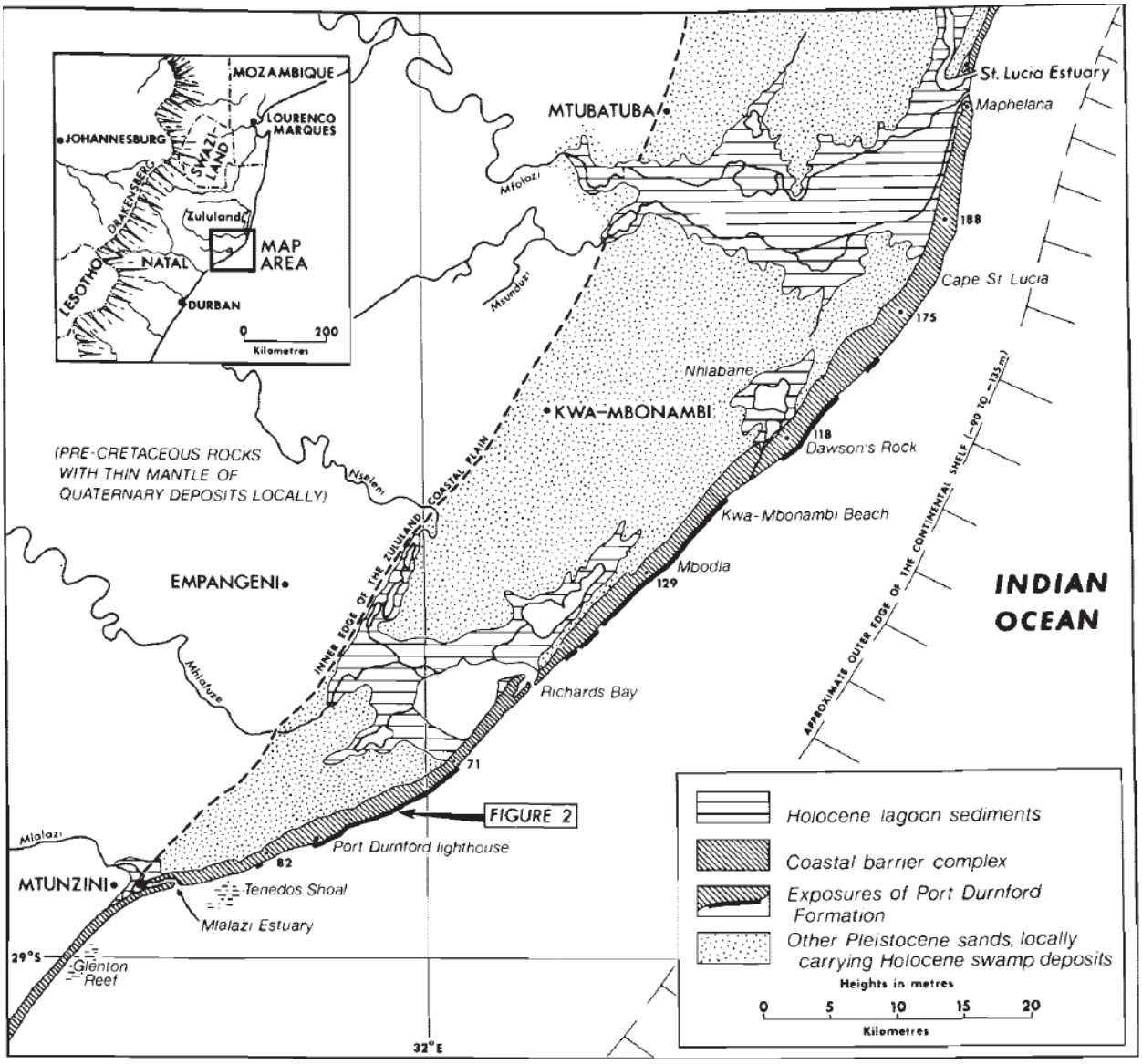

Figure 3.2. The coastal plain of Southern Zululand, showing the location of the Port Dunford Formation and associated features (Hobday & Orme, 1974).

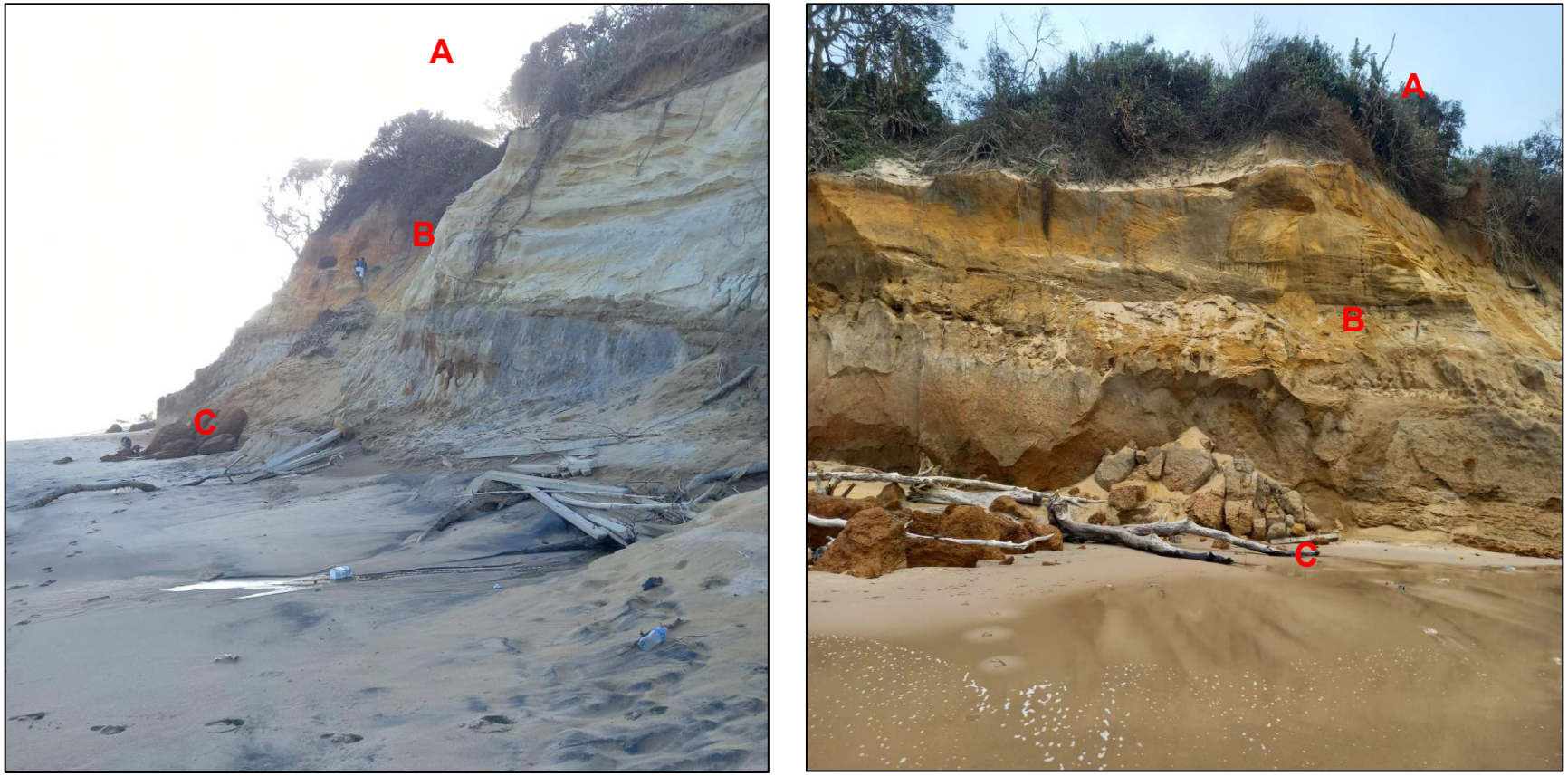

Figure 3.3. Eroding sea cliffs exposing the Port Dunford Formation: A: Vegetated dunes, B: Port Dunford Formation, C: Seashore (Alakram, 2022).

3.1.2 Topography and climate

Richards Bay is generally flat and situated on a coastal plain (Fig. 3.4). The terrain can be described as low relief towards the coast and characterized by an undulating surface of old dune ridges supporting shrubland and forest, swampy drainage lines, and lake systems (Naicker & Teurlings, 2013; uMhlathuze SDF, 2022). The dune ridges were formed in an alternating sequence to the present coastline by a receding Pleistocene sea at the onset of the Würm glaciation (Tinley, 1985). The Zululand Coastal Plain has a surface area of roughly 7000 km² and is underlain by the largest primary coastal aquifer in South Africa (Meyer et al., 2001). It is an environmentally sensitive region and extends from Mtunzini in the South to the Mozambique border (250 km) in the North but stretches a further 1000 km northward into Mozambique (Rawlings, 1991). Landwards of the study area, the topography is characterized by hills and steeply incised valleys with altitudes increasing to 900 m above sea level (KCDM Draft IDP, 2024-2025). The low level coastal floodplain is subject to natural flooding but sea level rise associated with climate change will increase flood risks over time (uMhlathuze SDF, 2022).

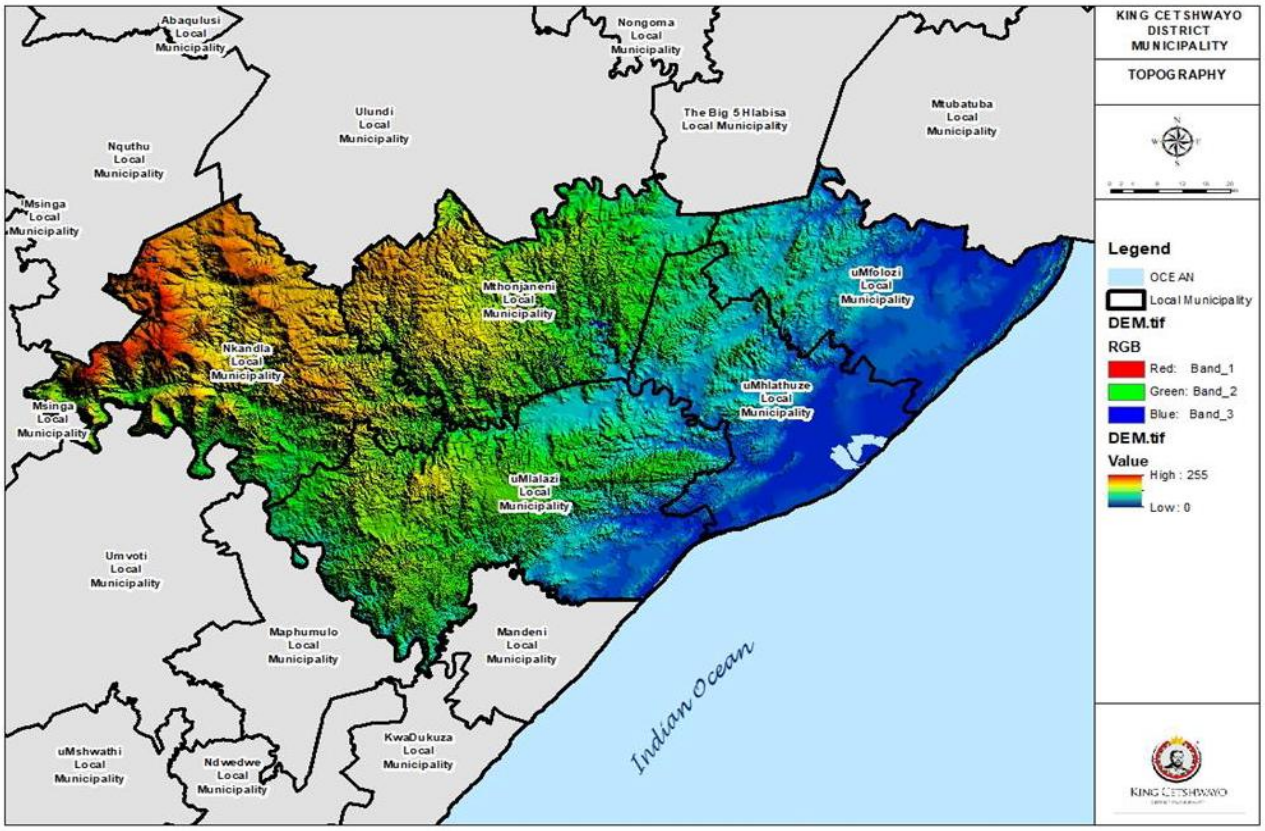

Figure 3.4: Topography DEM of the broader study area (KCDM, 2024-2025).

Richards Bay has a humid, subtropical climate comprising warm to hot summers with a relatively low diurnal temperature range (Weerts, 2002). The Mean Annual Precipitation (MAP) is 1288 mm with early summer rainfall being derived from mainly deep, convective showers and thunderstorms with occasional hailstorms (Weerts, 2002; Naicker & Teurlings, 2014). Precipitation occurs mainly in summer from October to March, with the peak being February-March. The dry season experiences an average of 45 mm of rain per month (Esterhuizen, 2019). Extreme rainfall does occur when occasional tropical cyclones from the Indian Ocean make landfall over the area during their regular migration southwards (Kelbe, 2010).

3.1.3 History of severe storms on the KZN coast

The KZN coast has a history of severe storms and associated flooding. The northern parts of KwaZulu-Natal are especially affected because of its close proximity to the Mozambique Channel. A historical record of severe storms on the KZN north coast is provided below:

- Cyclone Astrid (December 1957 – January 1958) – Struck Mozambique and brought up to 500mm of torrential rain to northern KZN. (Esterhuizen, 2019)
- Cyclone Claude (December 1965-January 1966) – Started on 24 December 1965 and ended on 10 January 1966 bringing largscale destruction. (Esterhuizen, 2019)
- Cyclone Caroline (February 1972) – Start on 3 February 1971, lasting 12 days. (Esterhuizen, 2019)
- Cyclone Eugenie (21-22 February 1972) – The coastal area experienced approximately 350 mm of rain causing widespread flooding. (Esterhuizen, 2019)
- Cyclone Danae (27 – 31 January 1976) – Cyclone Danae hit the east coast of Mozambique and the South African coast. Danae had a death toll of 50. (Esterhuizen, 2019)
- Cyclone Emilie (6-8 February 1977) – Following shortly after Cyclone Danae's destruction, this time claiming 300 lives. (Esterhuizen, 2019)
- Cyclone Kolia (March 1980) and Cyclone Justine (March 1982) - Cyclone Kolia lasted 18 days. In 1982, Cyclone Justine developed north of Madagascar and eventually moved in the direction of the north-eastern coast of South Africa. (Esterhuizen, 2019)
- Cyclone Domoina and Cyclone Imboa (29-31 January 1984) – Cyclone Domoina was the fourth cyclone to hit the KZN coast in the summer of 1983/1984. The death toll rose to 242 and destroyed crops, infrastructure, homes, and livelihoods. (Esterhuizen, 2019)
- Floods of September 1987 - September 1987 brought one of the greatest flood disasters in KZN, even more than cyclone Domoina. (Esterhuizen, 2019)

- Storm swell of March 2007 – On 19 and 20 March 2007 a storm swell that coincided with a spring high tide struck the KZN coast causing significant coastal erosion and damage to coastal property. The high water line retreated by 30 m. (Smith *et al*., 2007)
- April 2022 floods – A slow-moving storm named Issa brough record breaking rainfall to the coastal zone resulting in over 430 deaths. (Bopape *et al*., 2025)

These storms are often linked to cut-off low systems and tropical cyclones that bring rainfall and can exacerbate coastal erosion. (Bopape et al., 2025).

3.1.4 Hydrological regime

Historically, Richards Bay qualified as one of three estuarine bays in South Africa, along with Durban Bay and the Knysna estuary. In the South African context, estuaries have been defined by Day (1980) as partially enclosed bodies of water which are either permanently or periodically open to the sea, and within which there is a measurable variation of salinity due to the mixture of seawater with freshwater derived from land drainage. After the development of the Port of Richards Bay in 1976, activities associated with normal port development resulted in a change in the hydrological regime (Fig. 3.5). The original bay had five rivers flowing into it (the uMhalthuze, Bhizolo, Mzingazi, Mtantatweni, and Manzinyama rivers) (Weerts, 2002; Dladla et al., 2021). During the development of the port, a berm was constructed that divided the bay into two independent systems with two separate mouths to the sea. Now functioning as two independent water bodies, the Port of Richards Bay and the uMhlathuze Estuary still offer the complete range of habitats found in the tidal reaches of estuaries, including intertidal and subtidal mudflats, sandbanks, mangroves and seagrass beds (DFFE, 2019).

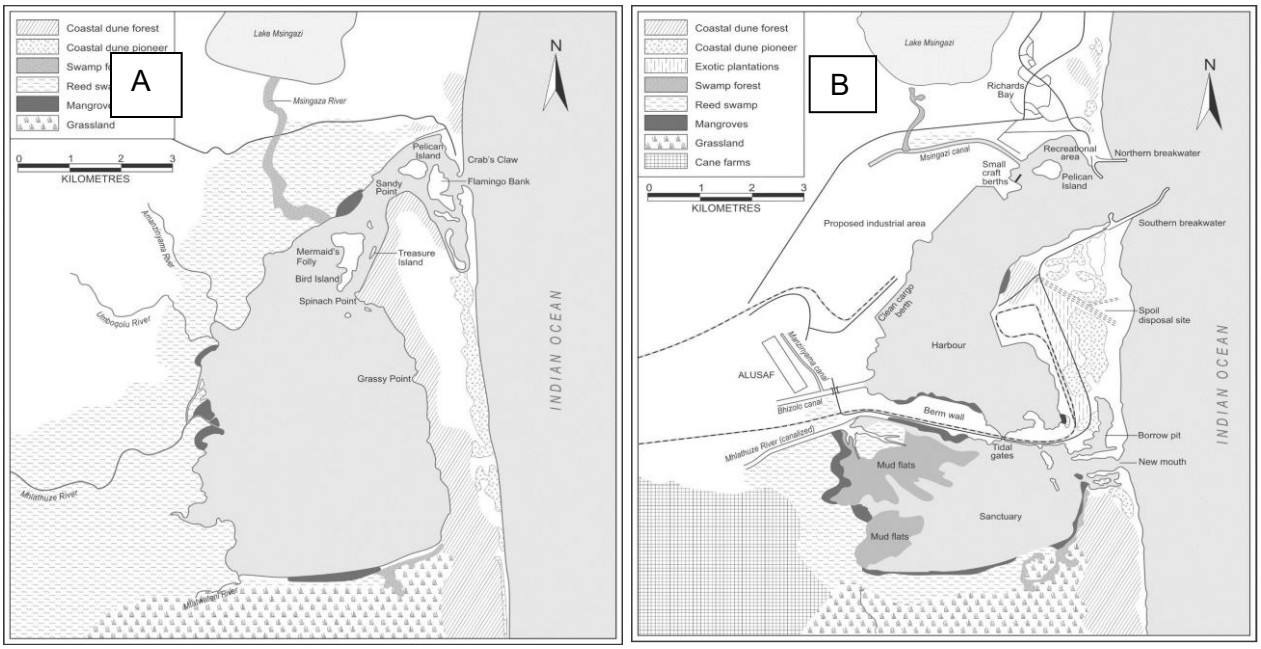

Figure 3.5: a) Map of the Port of Richards Bay in its natural state (1964), b) following construction of the harbour in 1976 (Elliott et al., 2016).

The uMhlathuze estuary and the Richards Bay harbour estuary falls within the Usutu-uMhlathuze Water Management Area. The uMhlathuze River drains a catchment area of 4209 km² with a Mean Annual Runoff (MAR) to the uMhlathuze estuarine system estimated at 560 to 645 x 10^6 m^3 (Weerts, 2002). The catchment area of the Richards Bay harbour estuary covers an area of 183 km^2, with its MAR yet to be determined (DFFE, 2019). There are several rivers, streams, canals and diffuse seepage zones that drain towards the estuary and harbour (Fig. 3.6). These are all linked hydrologically and ecologically to a large number of lakes, swamps and wetlands that form important ecological systems (Kelbe, 2010). The importance of the groundwater and its strong hydrological linkages to the surface water bodies were highlighted by many authors (Meyer et al., 2001; Weerts, 2002; Taylor et al., 2006; Elliot et al., 2016; Dladla et al., 2021). A significant feature of the study area is that the groundwater is the main flow component into and out of these surface water bodies and as a result has been known to provide important ecological functions for sustaining coastal wetlands (Taylor et al., 2006).

The northern Kwa-Zulu Natal coastal plain is dominated by semi-diurnal tides. Richards Bay has an average tidal range of 1.84 m with a maximum tidal height of 2.47 m (Smith et al., 2010). The coastline can thus be described as being micro-tidal, i.e. where the tidal range is less than 2 m (Ware, 2001). The coast of Richards Bay is classified as a dissipative beach (Simmonis, 2016), characterised by gentle slopes, fine, sandy sediment, and steep waves. The waves strike

the shore obliquely from a southeast direction, resulting in a dominant northerly flow of the longshore drift. (Ware, 2001). These characteristics renders the shoreline more susceptible to erosion and inundation. Offshore, the middle to outer shelf is dominated by the Agulhas Current, a swift-flowing western boundary current that can reach speeds of up to 2 m/s (Dladla et al., 2021).

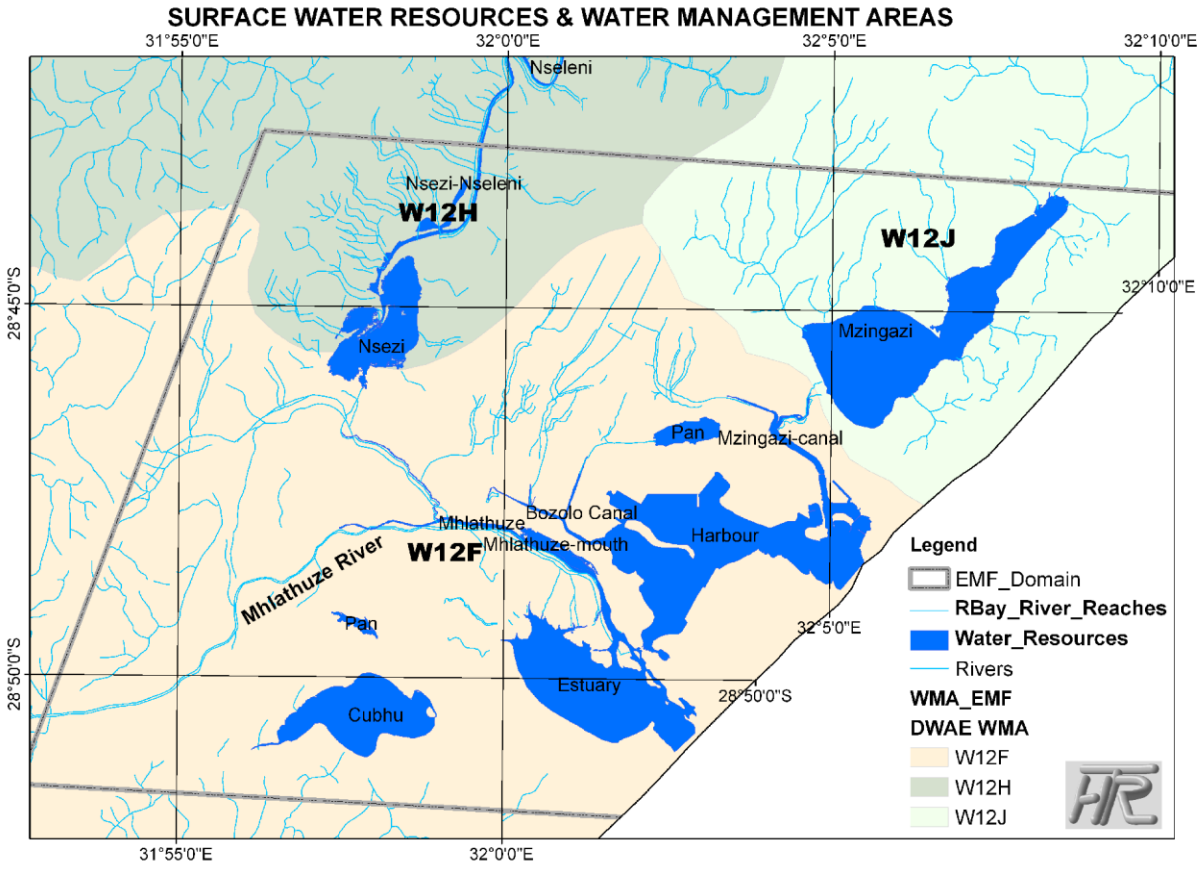

Figure 3.6: The main water resources in the study area (Kelbe, 2010).

3.1.5 Geology and geomorphology

The continental shelf along the KwaZulu-Natal coast is very narrow, ranging from a few kilometres to 47 kilometres in some areas (Cooper & Smith, 2014). The coastal plain in the study area is made up almost entirely of Quaternary (or Pleistocene period) sediments, mainly sand, deposited as beaches and dunes during the periods of rising and falling sea levels (Mol, 2013; Cooper & Smith, 2014). Kelbe (2010) noted that the physical geological foundation of the study area controls the occurrence, distribution, and type of water resources in the area, including groundwater.

The geomorphological features surrounding the study area have predominantly been formed by erosion from alluvial and aeolian forces (Kelbe, 2010). The main landscape feature is the coastline, with its stunning frontal dune formations, some of which are the highest in the world (Ware, 2001; Cooper & Smith, 2014). Inland of the coastal plain, the landscape is generally formed by the rivers and their tributaries.

The sand dunes of northern KwaZulu-Natal are rich in heavy minerals such as ilmenite, zircon, and rutile. Richards Bay Minerals (RBM), owned by the global mining giant Rio Tinto, has been extracting heavy minerals from the sand dunes since 1976. Rehabilitation takes place after mining by means of restoring the coastal dune forests by initiating ecological succession (Fig. 3.7) (Goble & Oellerman, 2022).

Figure 3.7: Sand dune mining in Richards Bay (Goble & Oellerman, 2022).

3.1.6 Terrestrial biodiversity

From a conservation perspective, the Mhlathuze Estuary is ranked in the top ten most important estuaries in South Africa, with the estuary at the Port of Richards Bay coming in at 26th place (DFFE, 2019). Significantly, these two systems contain the largest area of mangroves of all South African estuaries, and are known to have the oldest areas of mangroves in the country (Breetzke et al., 2022). Mangroves serve as an important coastal defence by reducing the ability of waves to erode sand. They are also regarded as a natural defence against climate change,

acting as a carbon sink by absorbing large quantities of carbon dioxide. Mangrove forests in Richards Bay are considered to be critically endangered (TNPA corporate brochure, ND).

The port of Richards Bay and its surrounding landscape also includes other habitats of significant conservation importance. The municipal area falls within the Maputaland-Pondoland-Albany biodiversity hotspot which is recognized as the second richest floristic region in Africa, containing approximately 80% of South Africa's remaining forests, rich birdlife, fisheries, and many supporting a total of 174 IUCN Red List of Threatened Species (uMhlathuze SDF, 2022). Evidently, it can be established that the study area is of local, regional, and national significance.

An indication of the high biodiversity can be seen in the five different terrestrial vegetation types that are present in the study area which is extraordinary; given the small extent of the study area (Forbes et al., 2013). The South African National Biodiversity Institute (SANBI), samples, classifies, describes and maps vegetation from the nine different biomes in South Africa. Forbes et al. (2013) confimed these vegetation units diring a terrestrial and aquatic baseline assessment conducted in Richards Bay as follows:

1. Subtropical Dune Thicket
2. Maputaland Coastal Belt
3. Northern Coastal Belt
4. Subtropical Alluvial Vegetation
5. Subtropical Seashore Vegetation

3.1.7 Land use in the study area

The uMhalthuze Local Municipality has an area of 1233.25 km^2 (uMhlathuze SDF, 2022). The Richards Bay deep water port is pivotal in the spatial development of the area. The National Ports Authority of Transnet owns, operates and controls eight commercial seaports along the South African coastline on behalf of the state in terms of the National Ports Act (Act No 12) of 2005. In 1976, the first phase of the Richards Bay Port was opened. Commodities moving through the port include material and products related to forestry, mining, aluminium, bagged cargo, granite, minimum containers, heavy lifts, ferro alloy, andalusite, chrome, clay, copper concentrate, fertilizer, magnetite, rock phosphate, rutile, titanium slag, woodchips, zircon alumina, cooking coal, salt, sulphuric acid, and chemicals and chemical products. Coal remains the single largest commodity moving through the Richards Bay Port in terms of volume and is the second largest

foreign exchange earner for the South African economy after gold (TNPA corporate brochure, ND).

The port of Richards Bay covers an area of 3.773 ha, but has the potential to expand when required, making it potentially one of the largest ports in the world (TNPA corporate brochure, ND) Currently, the port of Richards Bay is undergoing large-scale expansion (Fig. 3.8). This expansion is being done to consolidate its position as a seaport from which coal and chrome and be transported, while increasing its container handling facilities, as well as increasing its capacity to import and store liquified natural gas (LNG) and liquid fuels. Port authorities have acknowledged the impacts that storm surges, and have announced their plan to refurbish the breakwater dolosse to help cope with the changing conditions (see Port Development Framework, 2022). An estimated R30-billion will be required in the coming 10 years to facilitate these developments (Port Development Framework, 2022). The relocation of the South African Navy base from the port of Durban to the port of Richards Bay also forms part of these developments. As such, this large scale infrastructure development, while increasing economic wealth for the region, will also significantly impact sensitive environmental resources in and around Richards Bay. These impacts are associated with changes to ecosystem function and loss of biodiversity among others.

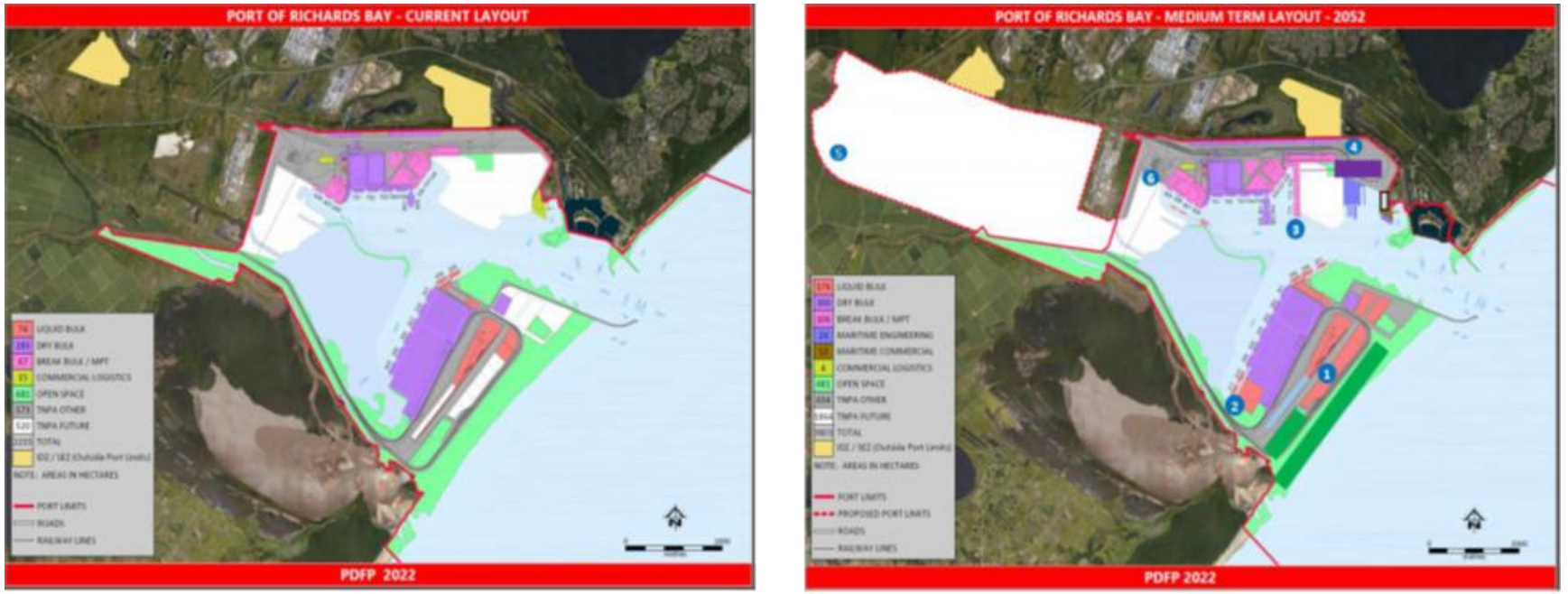

Figure 3.8: Left: Port of Richards Bay current layout, right: medium term layout (Source: Transnet National Ports Authority, 2022)

The municipality also has an airport and a couple of landing strips. The main land uses in the study area are sugarcane farming (34%), human settlement activities (27%), and forests and plantations (23%) (uMhlathuze SDF, 2022). Other activities such as mining and cultivated fields take up a much smaller percentage of land cover (Fig. 3.9).

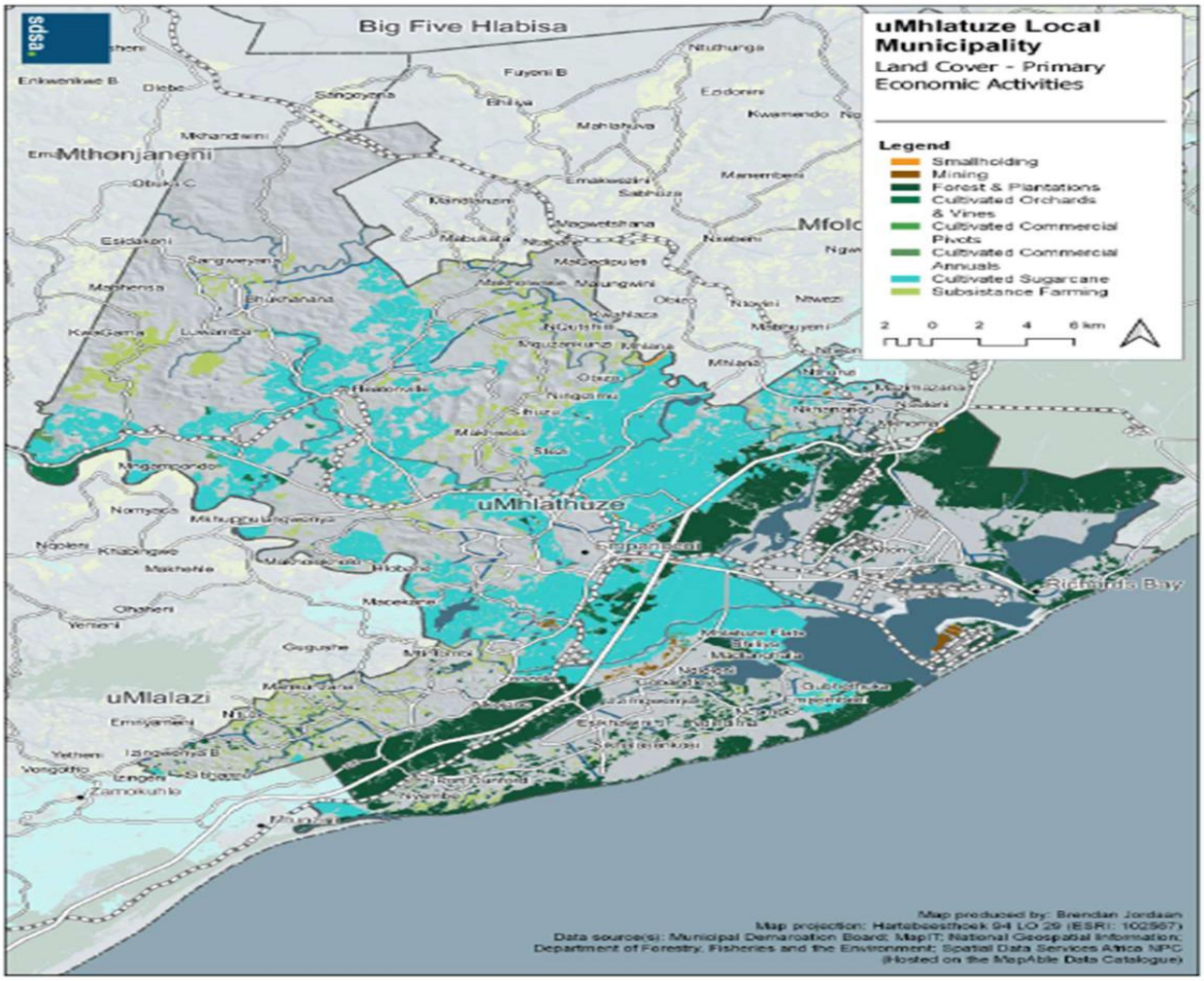

Figure 3.9: Land use in the uMhlathuze Local Municipality (uMhlathuze SDF, 2022).

3.1.8 Historical overview of coastal infrastructure

Since the opening of the Port of Richards Bay in 1976, breakwaters, synonymous with groynes, were constructed to protect the shoreline by dissipating wave energy and to facilitate safe navigation for vessels entering and leaving the port. In addition to this, the dolos breakwater was used to protect the main breakwaters (Fig. 3.10)

Figure 3.10: Dolos breakwaters in Richards Bay (Alakram, 2024).

The dolos, an anchor-shaped concrete block, was invented by South African Eric Merrifield in 1963 for the protection of breakwaters and foreshore banks (Zwambon, 1989). The idea behind the shape was to provide good interlocking capability and consequently higher stability. The dolos has found worldwide application since its inception and won the 1972 South African Design prize bringing worldwide recognition to its inventor (Zwambon, 1989). Richards Bay is seen as the most important local application of the dolos units with the placement of 25 000, each weighing between 5 tons and 30 tons, between 1973 and 1976 (Zwambon, 1989). The dolos units have provided coastal protection from high energy waves, yet the problem of erosion in Richards Bay remains a critical concern. Upgrades to the dolos units by Transnet to cope with the increasing storm surges and associated sea level rise is in the planning phase (Port Development Framework, 2022).

In 2015 geotextile sand bags weighing 3 ton each were placed in a 200 m stretch of coast following concerns over the loss of the lifeguard tower and beach area for bathers (Figure 3.11 A and B). Since then, severe storm surges and wind action have diminished the effectiveness of the bags and shifted its leaving room for sand to be eroded between the bags. In 2023 the uMhlathuze Municipality attempted to use a combination of geotextile sandbags, rocks, and sand replenishment as a mitigation measure on the same stretch of coastline as can be seen in Figure 3.11 C and D. These effects are still being implemented. The uMhlathuze Municipality recognises the challenges faced in the context of climate change and associated sea level rise coupled with the increase in frequency and intensity of storm surges and avers that additional measures are being explored to tackle the problem of coastal erosion within its jurisdiction (uMhlathuze SDF, 2024)

A: 2015: Lifeguard tower in Alkantstrand North beach facing immediate threat from coastal erosion and prior to placement of geotextile sand bags (Source: Zululand Observer, 2015).

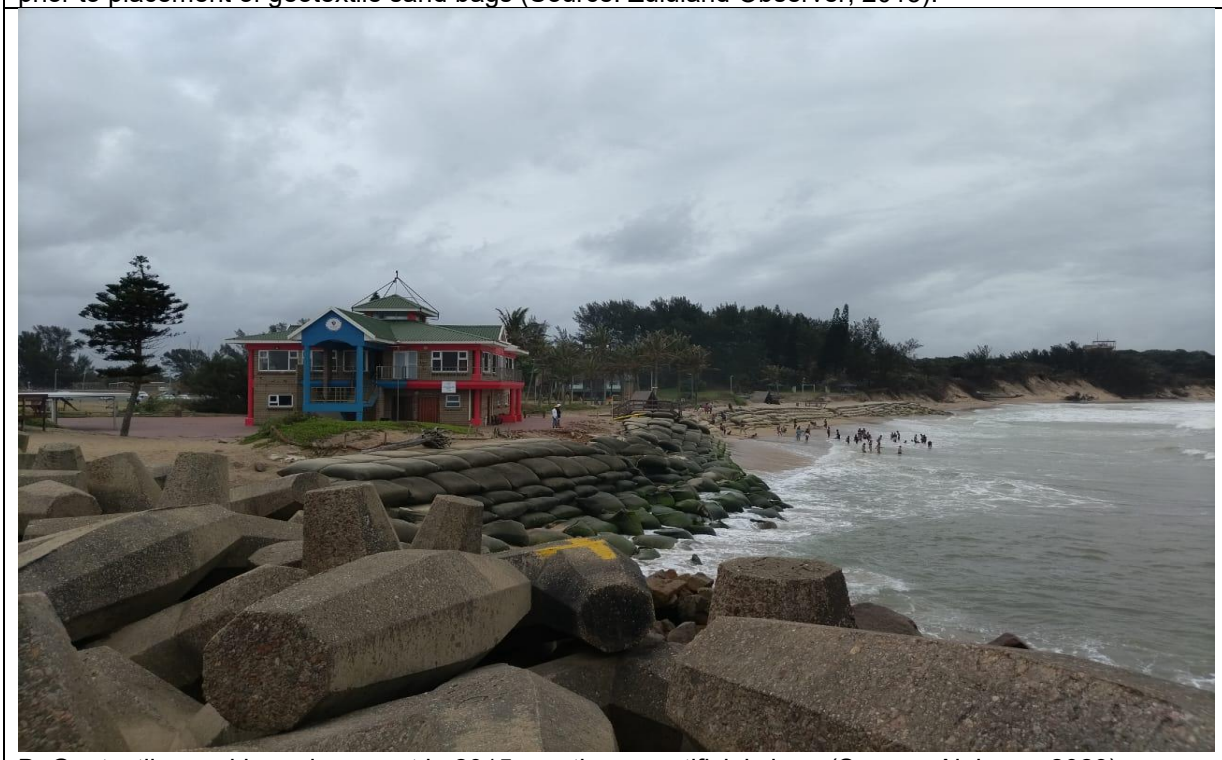

B: Geotextile sand bag placement in 2015 creating an artificial slope (Source: Alakram, 2023).

C: 2024/2025 - Severe storm surges resulting in the shifting of geotextile sand bags causing sand to erode under the bags. Sand replenishment used as a soft engineering approach (Source: Alakram, 2025).

D: 2025 - A combination of geotextile sand bags and rock revetments as a recent strategy. Sand replenishment was undertaken landward of the rocks. (Alakram, 2025).

Figure 3.11: Coastal defences around Richards Bay.

3.1.9 Sediment supply

Beaches get their sand primarily through long term erosion of rocks and geological material, which are broken down by wind and water (Esterhuizen, 2019). These particles travel down rivers and streams, eventually settling on the coast, while ocean waves break down shells,

coral, and volcanic rock. In the study area this occurs in the littoral active zone which drives this sand predominantly from south to north and is comprised of the near shore, beach and the dune system where sand is highly mobile (Ware, 2001). Simmonis (2016) states that although the northerly flow dominates, reversals do occur, especially in summer as a result of the greater number of easterly winds and swells. The sand grains in the study area range in size from 0.05 mm to 2 mm and comprise mainly silica and quartz minerals and shell fragments (Simmonis, 2016). Sand size is important as it determines the beach slope and therefore its susceptibility to erosion. The sand supply to the beaches of the study area predominately originates from the Thukela River during flood conditions (Bosman et al., 2007; Esterhuizen, 2019).

3.2 Methodology

3.2.1 Shoreline change analysis

The Digital Shoreline Analysis System (DSAS) was first released in 1992 and the software program since undergone continuous refinement (Table 3.1). Forming a critical component of the United States Geological Surveys' Coastal Change Hazards programmatic focus, it provides a robust suite of rate of change and distance measurements intended to facilitate the calculation of shoreline change (USGS, 2024). The software is also suitable for any application that calculates positional change over time such as addressing glacier limits in sequential aerial photographs, river edge boundaries, or land-cover change (Himmelstoss et al., 2021). The DSAS has been used worldwide in support of resource management and critical coastal decision-making.

Table 3.1: Releases of the DSAS software.

DSAS software releases	***Associated software***
Version 1.0 (1992)	MapGrafix / ArcInfo GIS
Version 2.0	ArcView 3.X
Version3.X	ArcGIS 9
Version 4.2	ArcGIS 9.2-9.3.X
Version 4.3	ArcGIS 10.4 – 10.5
Version 5.0 – 5.1	ArcGIS10.4 – 10.X
Version 6 (2024)	Stand-alone, can be used in any GIS

This study makes use of Version 6 of the DSAS to estimate how rapidly the shorelines in the study area eroded or accreted in the past. In order to do this, DSAS computes a range of statistical methods that can be used to measure changes between shoreline positions through time. These rate of changes statistics and measurement changes are discussed in detail in Chapters Four and Five.

3.2.2.1 Data

The main source of data used for the study is aerial imagery captured between 1977 and 2022 spanning 45 years (Table 2). The aerial photographs were obtained from the National Geospatial Information (NGI), a division of the Department of Agriculture, Land Reform and Rural Development (DALRRD), that is responsible for the collection, compilation, and preservation of South Africa's geospatial information. The photographs from 1977, 1984, and 1992 were scanned black-and-white images with their associated metadata. These were rectified and georeferenced to align with ESRI's ArcGIS Pro imagery basemap (2019) and projected to WGS 1984 UTM Zone 36S.

The time series for this dataset was primarily chosen based on the development of the harbour in 1976. Historical aerial photographs prior to 1977 were obtained from the NGI (1954 and 1969) but due to the dramatic change in landscape features before and after the harbour construction, it was not possible to to create ground control points to georeference the image in ArcGIS Pro.

Ground control points were identified in each of the 40 photographs to link to the basemap layer used as the reference image and transformed using a first order polynomial transformation. This transformation method is commonly used to reference imagery because it transforms the image without deforming it (ArcGIS tutorial, 2024). It can shift or move the image, scale it horizontally, scale it vertically and rotate it. Google Earth images from 2004 and 2022 were georeferenced in the same way. The NGI provided georectified high resolution images for 2009, 2013, and 2016, respectively (Table 3.2). The georeferenced images were then combined using the mosaic tool thereby creating a single raster dataset for each year respectively. A total of eight shorelines from different years were analysed for rates of shoreline change (Table 3.2).

Table 3.2: Summary of the historical aerial photographs data.

Shoreline No	*Year*	*Source*	*Scale/Resolution*	*No of photographs*
1	1977	NGI	1:30 000	4
2	1984	NGI	1:20 000	7
3	1992	NGI	1:50 000	3
4	2004	Google Earth	1:10 000	5
5	2009	NGI	0.5m georectified	5
6	2013	NGI	0.5m georectified	5
7	2016	NGI	0.5m georectified	6
8	2022	Google Earth	1:10 000	5

The study area covers a 21 km stretch of coastline in Richards Bay which have been divided into four beach areas under investigation as illustrated in Figure 3.12. These beaches are seperated by breakwater dolosse and a river mouth and thus could not be analysed as a single stretch of coastline in the DSAS system. The beaches south of the harbour are uMhlathuze Estuary measuring 6.8 km and South Dunes measuring 4.3 km in length and the beaches north of the harbour are Alkanstrand, a relatively small beach measuring 0.4 km and Alkanstrand North measuring 10.4 km in length. Both Alkanstrand and Alkanstrand North constitute the main recreational beach areas whereas South Dunes is by permit access only and uMhlathuze Estuary is not typically accessed by the public. Erosional trends have been occurring at Alkandstrand North and will be the focal point of the analysis in terms of erosion.

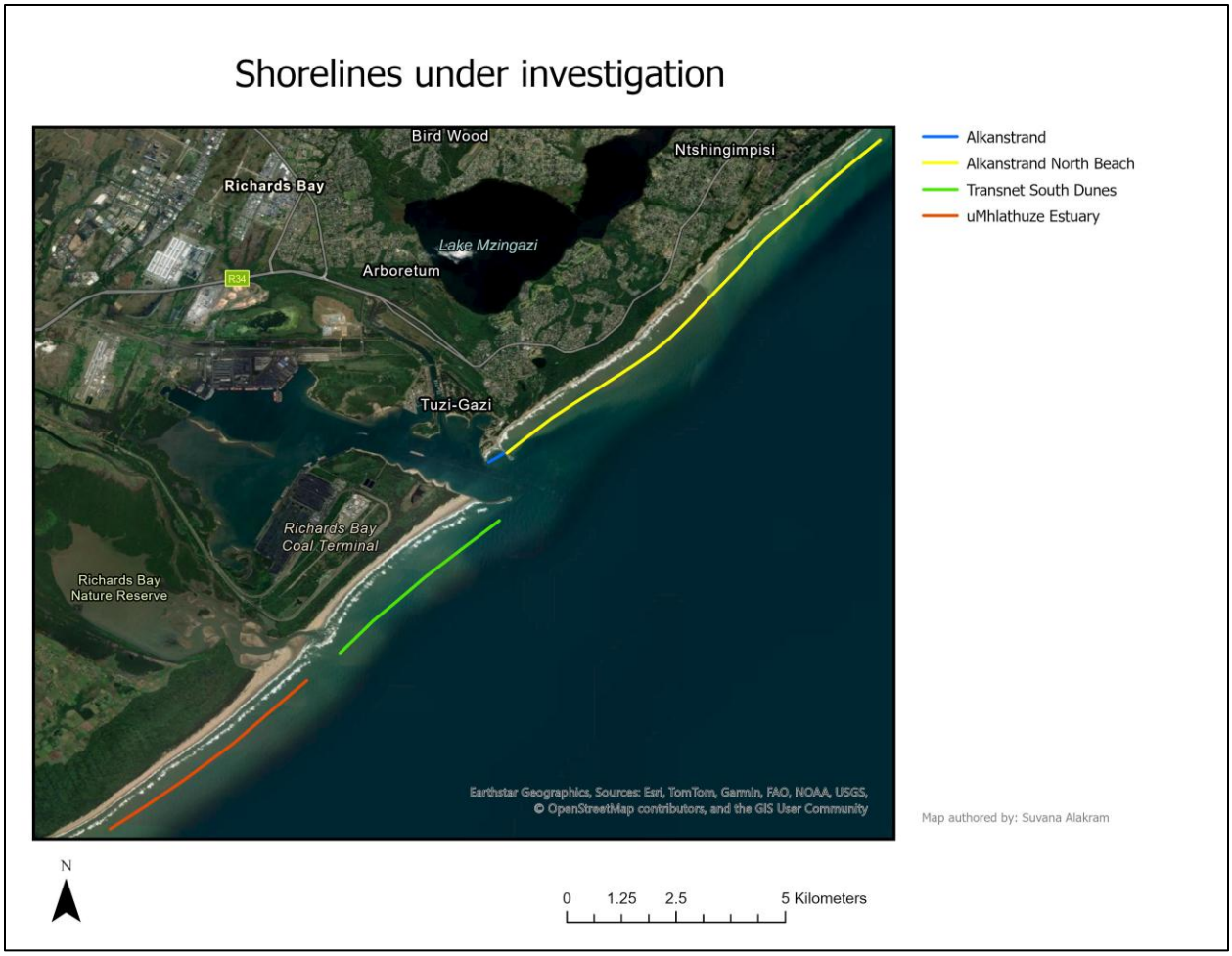

Figure 3.12: Google Earth image showing coastal areas under investigation.

3.2.1.2 Georeferencing errors

Scanned, historical aerial photographs are digital images with no associated spatial reference. In order to use these photographs in a GIS system, they would first need to be georeferenced, i.e. linked to a spatial reference system that allows it to be positioned in the real world. One of the key tasks in georeferencing is the creation of control points. Control points are known locations on the Earth that can be accurately identified in the historical image and linked the same point in the reference image. Georeferencing and removing distortions from maps and aerial photographs will always result in an associated error or uncertainty in its position (Murray et al., 2023). These errors can be attributed to human error by choosing inaccurate control points, applying inaccurate transformation methods, or image resolution or scale (Morton & Miller, 2005, Murray et al., 2023).

The resultant residual error is the distance between two points (historical image, x, and reference image, y) and is based on the Pythagorean formula:

Square Root (Residual x^2 + Residual y^2)

For this study, the georeferencing errors were noted as being between 5 and 10 m. These values are input into the DSAS software as it uses these values as uncertainty values when computing shoreline change rates.

3.2.1.3 Delineation of the shoreline

Different proxies for shoreline positions are used to validate shoreline change rates. Morton & Miller (2005) utilise the High-Water Line (HWL), Wet-Dry Line (WDL), vegetation line, dune toe or crest, toe of the beach, cliff base or top, and the line of Mean High Water (MHWL). The choice of which proxy to reference depends on coastal geomorphology, image resolution, and scientific preference (Morton & Miller, 2005). In this study, the HWL is used as a reference to digitize the shorelines. The HWL for this study can be described as a point that represents the maximum rise of a body of water over land. The eight shorelines were manually digitized and stored as a feature class with its associated errors. It was then converted to a .geojson format to be analysed in the DSAS system.

3.2.1.4 DSAS analysis

Following the preparation of the input data in ArcGIS Pro, the DSAS software is used to conduct the shoreline change analysis. DSAS uses a measurement baseline method to calculate rate-of-change statistics. A baseline was created parallel to the shore. The baseline serves as a starting point for all transects cast. Figure 3.12 below provides a graphic representation on how the baseline and shorelines are projected in relation to how the transects are cast by DSAS. Transects intersect each shoreline to create a measurement point, and these measurement points are used to calculate shoreline change rates (Himmelstoss et al., 2021). Figure 3.13 provides a summary of the basic workflow required to conduct the shoreline analysis.

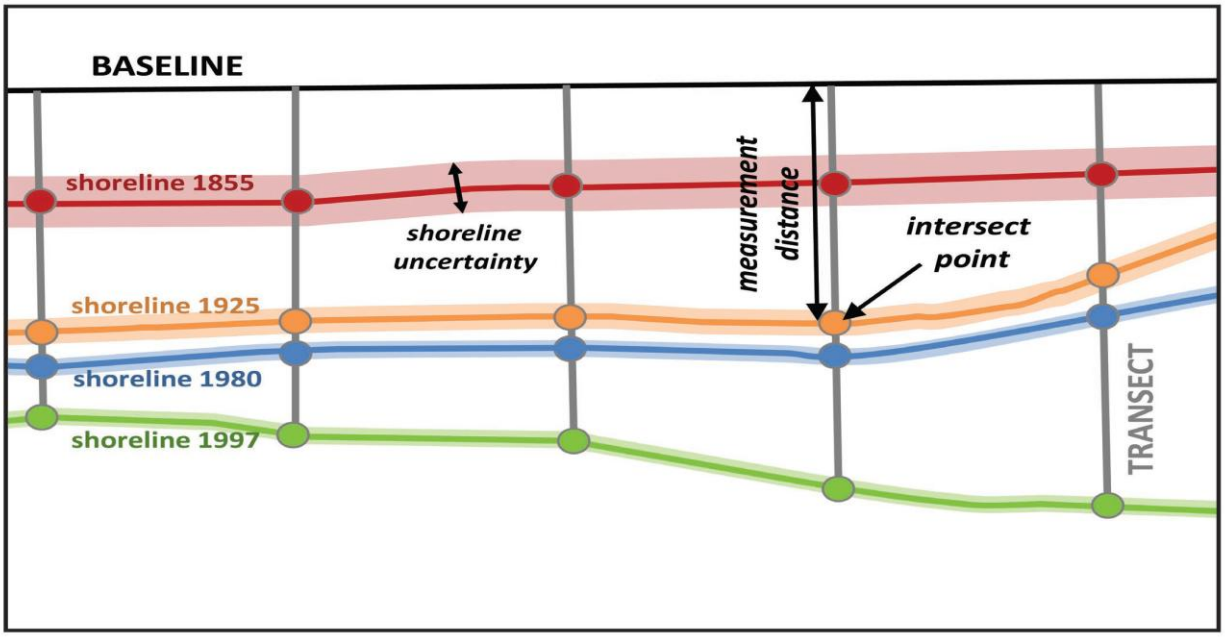

Figure 3.13: Example of baseline and shoreline shapefiles with DSAS generated transects.

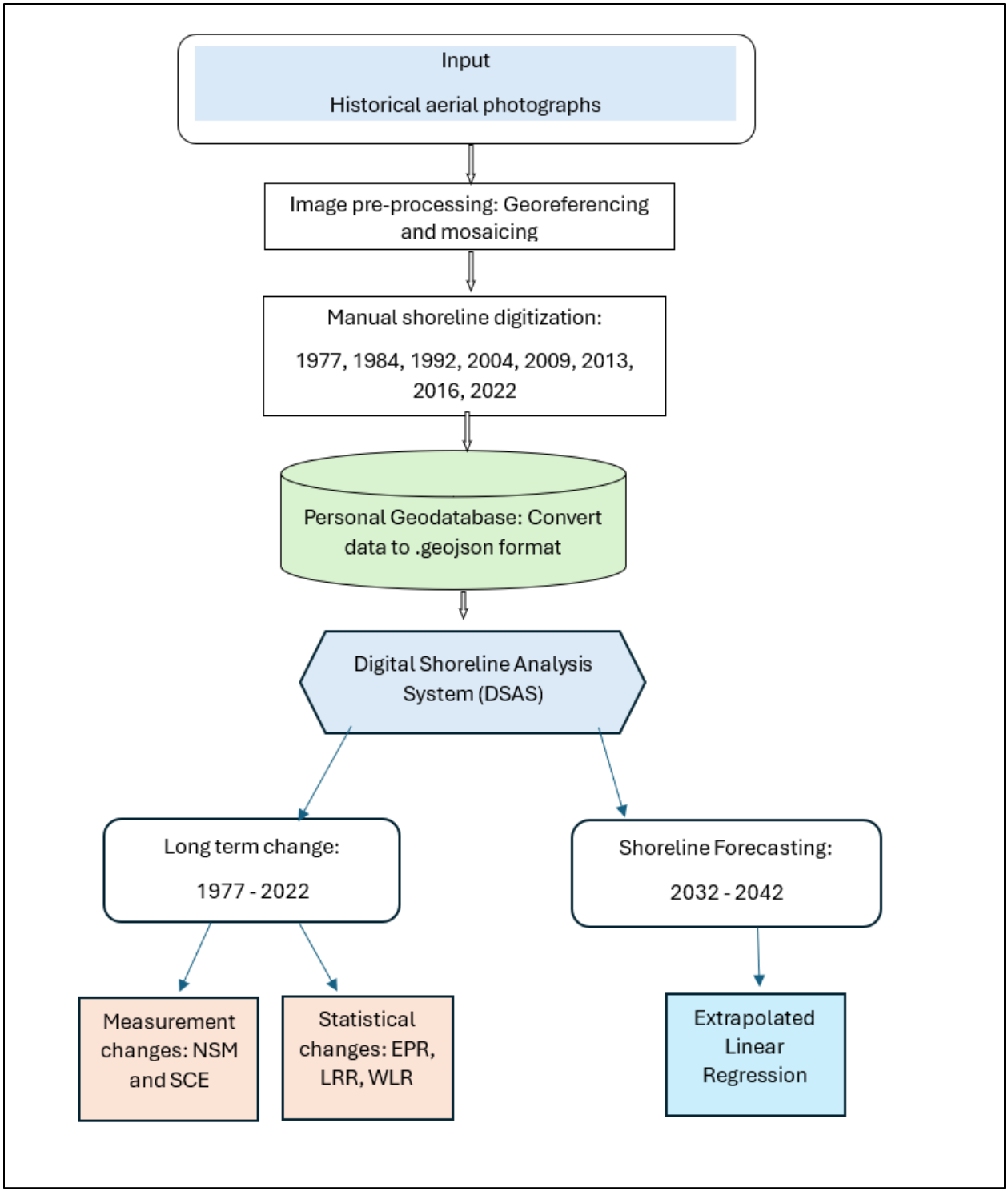

Figure 3.14: Basic workflow methodology for conducting shoreline change analysis.

3.2.2 Shoreline forecasting

Shoreline forecasting predicts the expected range of recession of the current coastline to aid in decision-making around coastal risk reduction (e.g. to develop set-back lines to determine how far inland to plan new developments). To do this, a linear regression of the available number of shorelines is performed to calculate a rate of change. This rate of change is then used to "extrapolate a linear regression into the future." (Farris et al., 2023: 1). In this study, the Extrapolated Linear Regression (ELR) method is utilized to predict shoreline positions 10 and 20 years into the future (i.e. 2032 and 2042). ELR method is a statistical technique used to predict values outside the range of observed data (refer to Fig. 3.14). It assumes that the relationship between two variables remains constant and linear even beyond the observed range. Thus, the predicted shoreline position (Y_f) given by Farris et al. (2023) is:

$$Y_f = m \cdot X_s + b$$

Where:

m – the rate of shoreline change

X_s – date of the latest shoreline

B – y-intercept

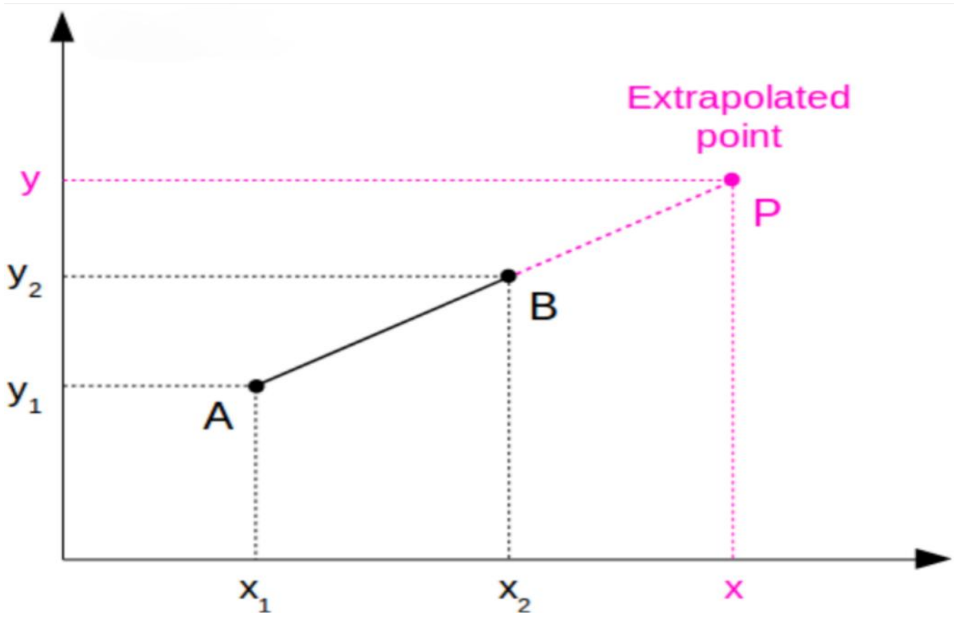

Figure 3.14: The ELR method is used to predict values outside the range of observed data where the slope is used to estimate future shoreline positions.

For the m value, the Linear Regression Rate (LRR) will be taken from the results of the DSAS analysis for the shoreline change analysis along with its associated uncertainties. The year is expressed as a decimal year. The formulas will be computed in Microsoft Excel to extrapolate future shoreline positions 10 and 20 years into the future. The formula will be used to calculate future shoreline positions for all four shorelines in the study area.

An estimation for future shoreline positions is important for coastal risk reduction as erosion control is increasingly being seen as a critical component in Integrated Coastal Zone Management (Hoosein et al., 2022; KZN EDTEA, 2023). The KZN Coastal Management Programme, drafted by the KZN Department of Economic Development, Tourism and Environmental Affairs (KZN EDTEA) in 2023 has placed the KZN coast at significant risk of erosion due to climate change, sea level rise, intensification of tropical and extra-tropical cyclones, and increased flooding and wash-over events. Thus, shoreline forecasting can prove useful in the planning of mitigation strategies and identify coastal sections at risk. Several types of infrastructure in the study area have already been lost to the sea due to erosion (Fig. 3.15) with many more at imminent risk.

Figure 3.15: The Richards Bay Lighthouse was demolished due to its imminent collapse. Built in 1979, standing 200 m from the edge of the cliff, it was demolished in 2018, standing a mere 5m from the sea cliff edge (Zululand Observer Newspaper, 2017).

3.2.3 Storm surge analysis

In the context of climate change, it is useful to identify the coastal areas that are in danger of becoming permanently inundated due to sea level rise and storm surges. During March 2007 severe storms impacted the coast which was compounded by above average spring tides. Storm surges resulted in inundations of coastal areas particularly in the study area where seawater surged 2 km into the harbour (Smith et al., 2010). This GIS-based screening workflow provides an overview of storm surge consequences and for identifying possible remedies to inundations.

3.2.3.1 Input data

To run the inundation workflow, the most important input data required is a Digital Elevation Model (DEM). The DEM was provided by the Centre for Geographical Analysis (CGA), Stellenbosch University with a resolution of 5 m from 2019. Created through interpolation from contour lines and spot heights, it offers the accuracy required for the analysis. The spatial reference used is Hartebeesthoek 1994 based on the WGS 1984 ellipsoid.

The next step is to hydro-condition the DEM. It is crucial to hydro-condition the DEM before the analysis because it makes provision for the flow paths to represent water flowing under bridges, roads etc (Fig. 3.16). This is done using the following steps in ArcGIS Pro 3.4:

- Create an empty line feature class and name it ‘HydroAdaptations’.
- Digitize the desired hydro-adaptations located in the study area extent and store them in the feature class.
- Burn all hydro-adaptations stored in the HydroAdaptations layer onto the DEM using the ‘Burn Flowlines onto DTM’ tool created by Balstrom & Kirby (2021).

The hydro-conditioned DEM, called the DyMSea layer, will then be used to identify floodable areas using ModelBuilder in ArcGIS Pro.

Figure 3.17: The elevation of the bridge (in red) is higher than the elevation of the water passing under the bridge (in yellow) (Adapted from Bastrom & Kirby, 2021).

3.2.3.2 Modelling

The model used in the inundation screening workflow (Fig. 3.17) was created by Thomas Balstrom at the University of Copenhagen in Denmark (Kirby & Balstrom, 2021). It is executed in Model-builder in ArcGIS Pro. In ArcGIS Pro, Model-builder is used to create, edit and manage geoprocessing models.

- Create Inundation Model – models how water propagates starting from a source. Inputs used is the 5 m DEM, a source line feature, and desired storm surge levels.

The model generates a series of maps based on the storm surge level input into the model. These maps will then be used to identify areas that are vulnerable to storm surges and associated sea-level rise.

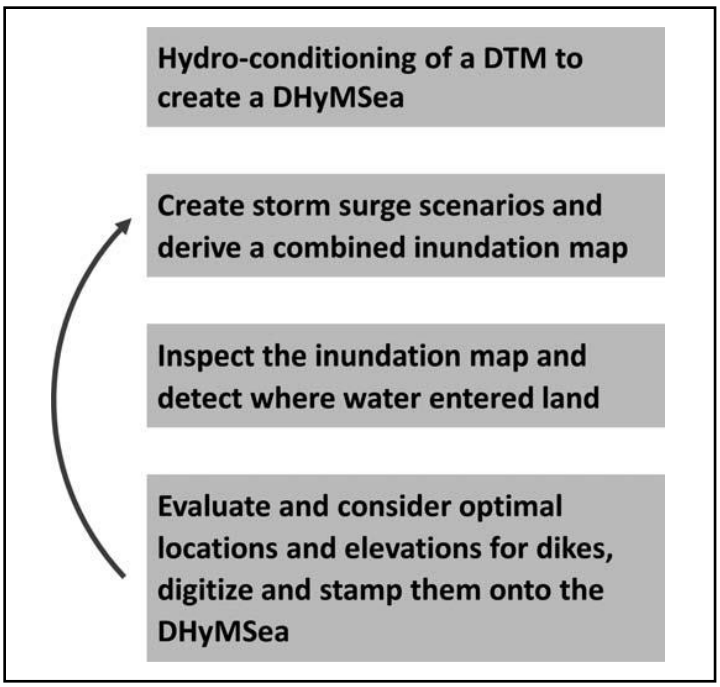

Figure 3.18: Overview of the major steps in the storm surge analysis (Adapted from Bastrom & Kirby, 2021).

Chapter 4: Results

4.1 Shoreline change results

The results of the shoreline change analysis, shoreline forecasting, and the inundation modelling (storm surge) are presented in this chapter. Shoreline rates of change for the study area were calculated by digitizing shoreline positions from eight different time periods from 1977 to 2022, spanning 45 years. After preparing the data in ArcGIS Pro, it was converted to a format accepted by DSAS version 6 (i.e. geojson format). The Digital Shoreline Analysis System (DSAS) was then used to calculate various rates of change based on measured differences between shoreline positions through time along with its relative uncertainty. The morphology of the four shorelines in the study area is shown in Fig. 4.1 and Table 4.1 describes the characteristics of the study area. Fig. 4.2 depicts the extensive erosion around Alkanstrand within the study area.

Figure 4.1: Morphology of the shorelines studied: uMhlathuze Estuary, South Dunes, Alkanstrand and Alkanstrand North (Source: Google Earth).

Figure 4.2: Close up of Alkanstrand (top) and Alkanstrand North (bottom) showing eroding sea cliffs (Alakram, 2024).

Table 4.1: Study area characteristics and shoreline information.

	uMhlathuze Estuary	South Dunes	Alkanstrand	Alkanstrand North
Length of shoreline	6.8 km	4.3 km	0.4 km	10.4 km
Tidal conditions	Micro-tidal	Micro-tidal	Micro-tidal	Micro-tidal
Morphology	Sandy beach backed by well-established, high vegetated dunes (Fig. 4.1)	Sandy beach backed by vegetated dunes (Fig. 4.1)	Steeply inclined sandy beach backed by small dunes (mostly eroded) (Fig. 4.1 & 4.2)	Sea cliffs – dunes on top of semi-consolidated sediment (Fig. 4.1 & 4.2)
Infrastructure	Natural state	Mostly natural, breakwater dolosse towards the North.	Breakwater dolosse on either side	Breakwater dolosse towards the South, natural going North. Receives sand nourishment on an irregular basis.
No-of shorelines used in analysis	8	8	8	8
Shoreline dates	1977, 1984, 1992, 2004, 2009, 2013, 2016, 2022	1977, 1984, 1992, 2004, 2009, 2013, 2016, 2022	1977, 1984, 1992, 2004, 2009, 2013, 2016, 2022	1977, 1984, 1992, 2004, 2009, 2013, 2016, 2022

Table 4.2 below provides a definition of the rate of change statistics and distance measurement provided by DSAS and a summary of the results map from the DSAS is presented in Figure 4.3 below.

Figure 4.3: Summary of the results map from DSAS showing erosion in **red**, accretion in **blue** and no change in **yellow**.

The DSAS generates transects that are cast perpendicular to the reference baseline at a spacing of 50 m (Fig. 4.4). It then measures the distance between the baseline and each shoreline intersection along a transect, combines date information, and positional uncertainty to generate the change statistics and distance measurements:

It is noteworthy that, the Linear Regression Rate (LRR) uses all the shoreline dates to calculate linear trends over time, while the Weighted Linear Regression (WLR) multiplies all shoreline transect values by the square inverse of their respective uncertainty values (Murray et al., 2023). Since the images from 1977, 1984 and 1992 have larger uncertainty values (±10 m), the WLR can be considered a more accurate representation of shoreline change.

Table 4.2: Definitions of the rate of change statistics and distance measurements from DSAS.

Rate of Change Statistics	**Description**
Linear Regression Rate (LRR)	An ordinary least square regression of shoreline change over time. The LRR can be determined by fitting a least-squares regression line to all shoreline points for a transect; units: metres per year.
Weighted Linear Regression (WLR)	The linear regression rate through all the data weighted by shoreline uncertainty; units: metres per year
End Point Rate (EPR)	Is calculated by dividing the distance of shoreline movement by the time elapsed between the oldest and most recent shoreline.
Distance Measurements	**Description**
Net Shoreline Movement (NSM)	The distance between the oldest and the youngest shorelines for each transect, expressed in metres
Shoreline Change Envelope (SCE)	The distance between the most landward and most seaward shorelines, expressed in metres. SCE is always a positive value as it a distance measurement.

The reported rates are presented in metres. Negative values represent erosion while positive values represent accretion. Tables 4.3 - 4.8 provide summaries of the rate of change statistics and distance measurements provided by the DSAS.

Table 4.3: Summary of the Linear Regression Rate.

Linear Regression Rate (m/yr)						
Shoreline	Average erosion rate	Percentage of erosional transects	Maximum value erosion	Average accretion rate	Percentage of accretional transects	Maximum value accretion
uMhlathuze Estuary	-0.13	3.25%	-0.17	2.33	96.75%	5.46
South Dunes	-3.25	61.54%	-4.84	1.32	38.46%	2.17
Alkanstrand	-3.25	100%	-3.48	0	0.0%	0
Alkanstrand North	-2.28	100%	-4.73	0	0.0%	0

Table 4.4: Summary of the Weighted Linear Regression.

Weighted Linear Regression (m/yr)						
Shoreline	Average erosion rate	Percentage of erosional transects	Maximum value erosion	Average accretion rate	Percentage of accretional transects	Maximum value accretion
uMhlathuze Estuary	-0.33	16.26%	-0.67	2.44	83.74%	4.86
South Dunes	-2.35	56.41%	-3.50	1.74	43.59%	2.92
Alkanstrand	-2.93	100%	-3.03	0	0.0%	0
Alkanstrand North	-2.22	100%	-5.37	0	0.0%	0

Table 4.5: Summary of the End Point Rate.

End Point Rate (m/yr)						
Shoreline	Average erosion rate	Erosional transects (%)	Maximum value erosion	Average accretion rate	Accretional transects (%)	Maximum value accretion
uMhlathuze Estuary	-0.04	1.63%	-0.06	2.10	98.37%	4.09
South Dunes	-5.18	58.97%	-7.75	2.09	41.03	3.51
Alkanstrand	-3.73	100%	-3.91	0	0.0%	0
Alkanstrand North	-2.18	100%	-4.86	0	0.0%	0

Table 4.6: Summary of the Net Shoreline Movement (NSM), with landward movement as negative and seaward movement as positive.

Net Shoreline Movement (m)					
Shoreline	Average distance	Net Erosion (%)	Maximum erosion	Net accretion (%)	Maximum accretion
uMhlathuze Estuary	93.06	1.63%	-2.65	98.37%	183.97
South Dunes	98.90	58.97%	-348.84	41.03%	157.87
Alkanstrand	-167.80	100%	-176.09	0.0%	0
Alkanstrand North	-98.20	100%	-218.80	0.0%	0

Table 4.7: Summary of the Shoreline Change Envelope (SCE), positive in either direction.

Shoreline	Average distance	Maximum distance	Minimum distance
uMhlathuze Estuary	136.98	302.33	57.50
South Dunes	193.10	363.06	45.48
Alkanstrand	169.74	184.52	149.73
Alkanstrand North	123.88	218.80	70.77

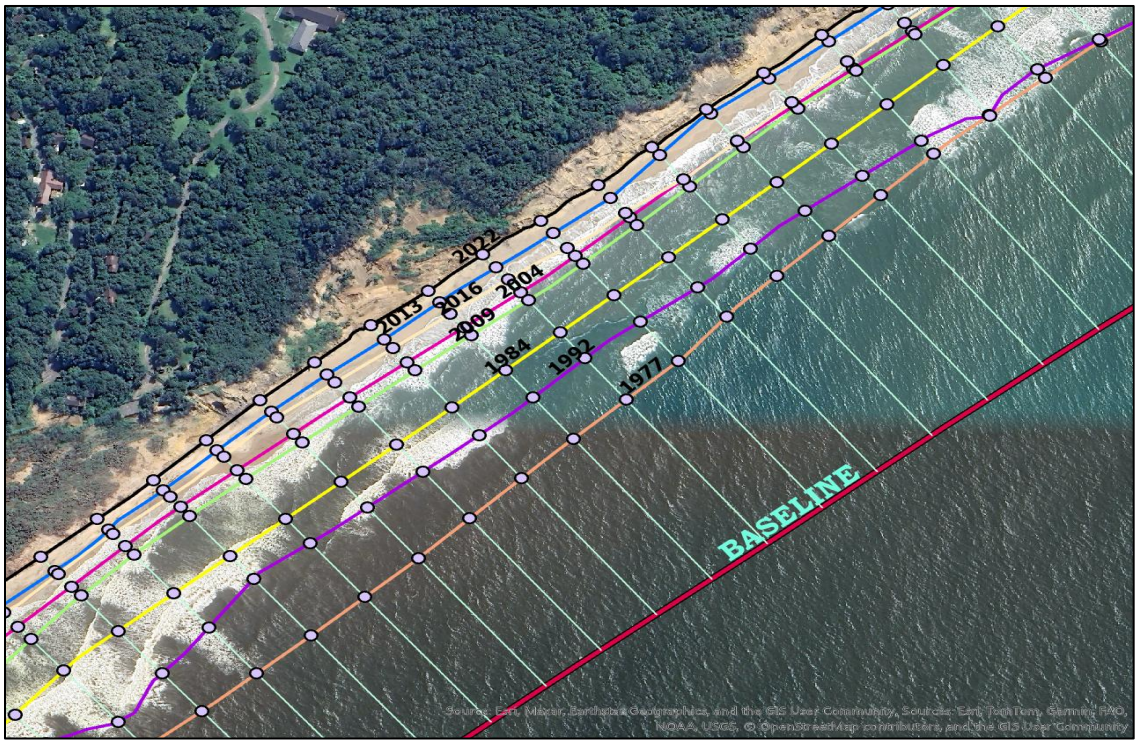

Figure 4.4: A section of digitized shorelines of Alkanstrand North showing DSAS-generated transects (spaced 50 m apart) with reference baseline (red) and historical shoreline positions (multiple colours). The measurement distance from the baseline to each intersect point is used in conjunction with the corresponding shoreline date to compute rate of change statistics.

4.1.1 Digitized shorelines

4.1.1.1 uMhlathuze Estuary beach

Situated to the South of the Port of Richards Bay (Fig. 4.5), the uMhlathuze Estuary stretch of beach experienced a net accretion of 98.37%, and a net erosion of 1.63% (Table 4.6). A total of 123 transects were used to calculate the shoreline change statistics (Fig. 4.4). The position of eight shorelines over time were digitized in ArcGIS Pro (3.4).

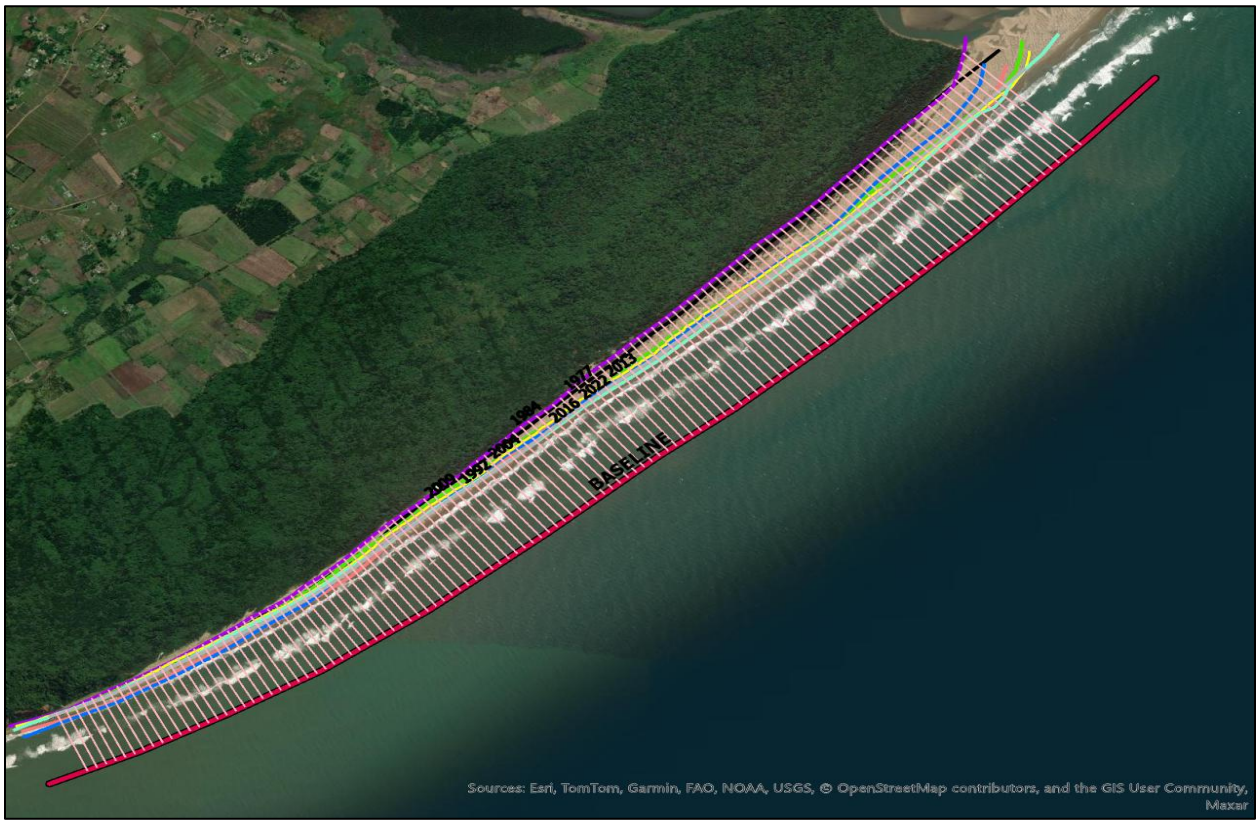

Figure 4.5: The 6.8 km stretch of beach known as uMhlathuze Estuary showing 123 transects spaced 50 m apart, the reference baseline (red), with digitized historical shoreline positions (multicolour).

4.1.1.2 South Dunes beach

The South Dunes beach is a private beach owned by Transnet National Ports Authority (TNPA). It is restricted to the public and only be accessed with a permit. The Richards Bay Coal Terminal is located in close proximity to this beach and is separated from the uMhlathuze beach by a natural mouth and to the South separated from the Alkanstrand beach by the breakwater comprising dolos units and main port entrance. This shoreline experienced a net accretion of 41.03% and a net erosion of 58.97%. A total of 78 transects were used to calculate the shoreline change statistics (Fig. 4.6). The position of eight shorelines over time were digitized in ArcGIS Pro (3.4).

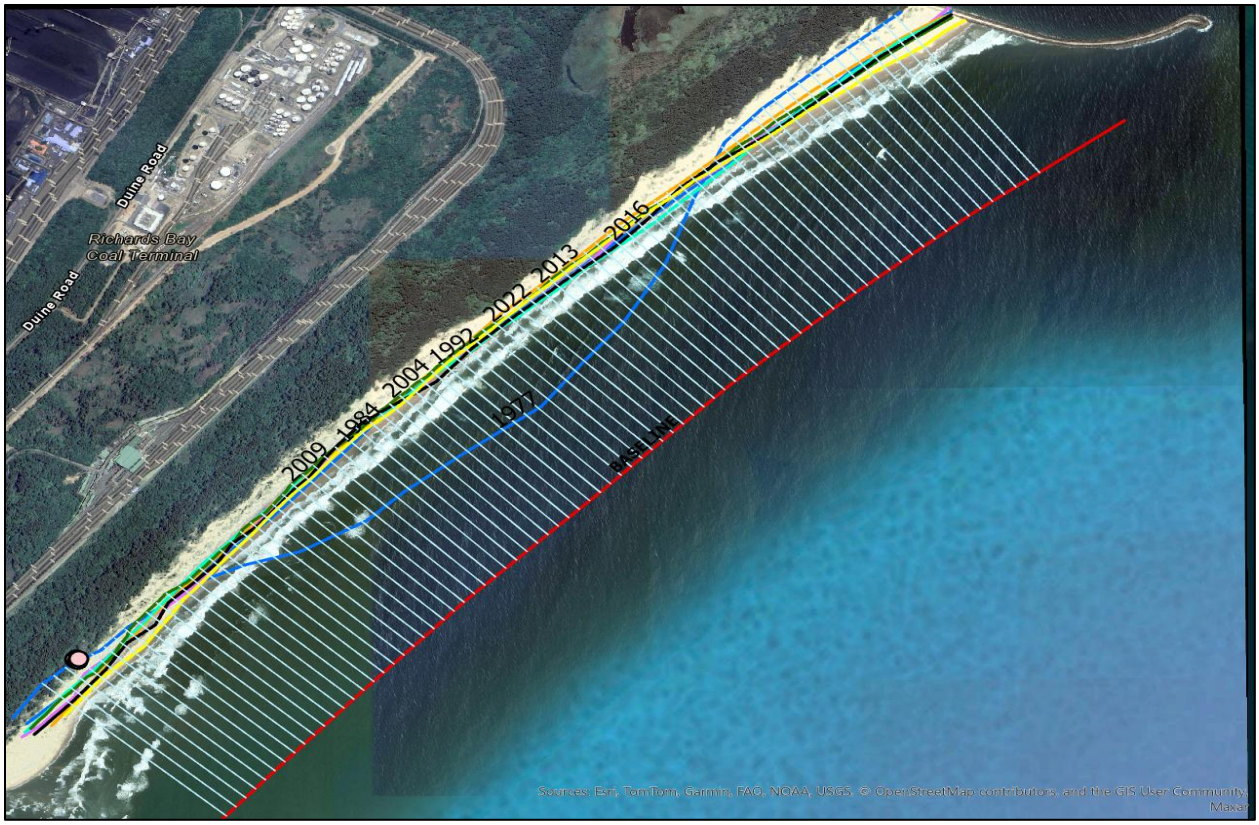

Figure 4.6: The 4.3 km stretch of beach known as South Dunes showing 78 transects spaced 50 m apart, the reference baseline (red), with digitized historical shoreline positions (multicolour).

4.1.1.3 Alkanstrand beach

This small stretch of beach (0.4 km) situated between two breakwaters has experienced 100% net erosion over the time period of the analysis. The analysis revealed that the shoreline moved 176.09 m landward during the 45 year period (Fig. 4.7).

Figure 4.7: The 0.4 km stretch of beach known as Alkanstrand showing 6 transects spaced 50 m apart, the reference baseline (red), with digitized historical shoreline positions (multicolour).

4.1.1.4 Alkanstrand North beach

Situated North of the breakwater of dolos units and the Port of Richards Bay, this stretch of beach has seen significant amounts of erosion in the 45 year period of analysis. With 100% net erosion and a net shoreline movement of 218.80 landward (Fig. 4.8), it is evident that more planning and adaptation strategies are required for this stretch of coastline. This will be discussed in Chapter 5.

Figure 4.8: The 10.4 km stretch of beach known as Alkanstrand North showing 203 transects spaced 50 m apart, the reference baseline (red), with digitized historical shoreline positions (multicolour).

4.2 Shoreline forecasting

Shoreline Forecasting was predicted for 10 and 20 years (i.e. 2032 and 2042) into the future, based on the Extrapolated Linear Regression method (ELR). Each transect has a unique historical rate associated with it. The full list of the total number of transects and their associated rates calculated by DSAS for each of the four shorelines in the study area is given in Appendix 2. The linear regression rate was used to calculate the ELR, using a chosen transect (Fig. 4.9 - 4.12).

4.2.1 uMhlathuze Estuary

Fig 4.9 (A) below shows the graphical representation of the linear regression rate for the uMhlathuze Estuary with the x-value representing the historical years from 1977 to 2022 and the y-value representing the distance from baseline, which will be discussed in Chapter 5. This data was used to extrapolate the future shoreline positons for 2032 and 2042 (Fig 4.9 (B) using the following formula adapted from Farris et al. (2023), and known as the ELR formula:

$$Y_f = m \cdot X_s + b$$

Where:

m – the rate of shoreline change

X_s – date of the latest shoreline

B – y-intercept

The m vlaue represents the slope of the data and is calculated using the SLOPE formula in excel. The y-intercept was calculated using the INTERCEPT formula in excel. The results of the forecasted positions will be discussed in Chapter 5. The same equation was used for all four shorelines analysed.

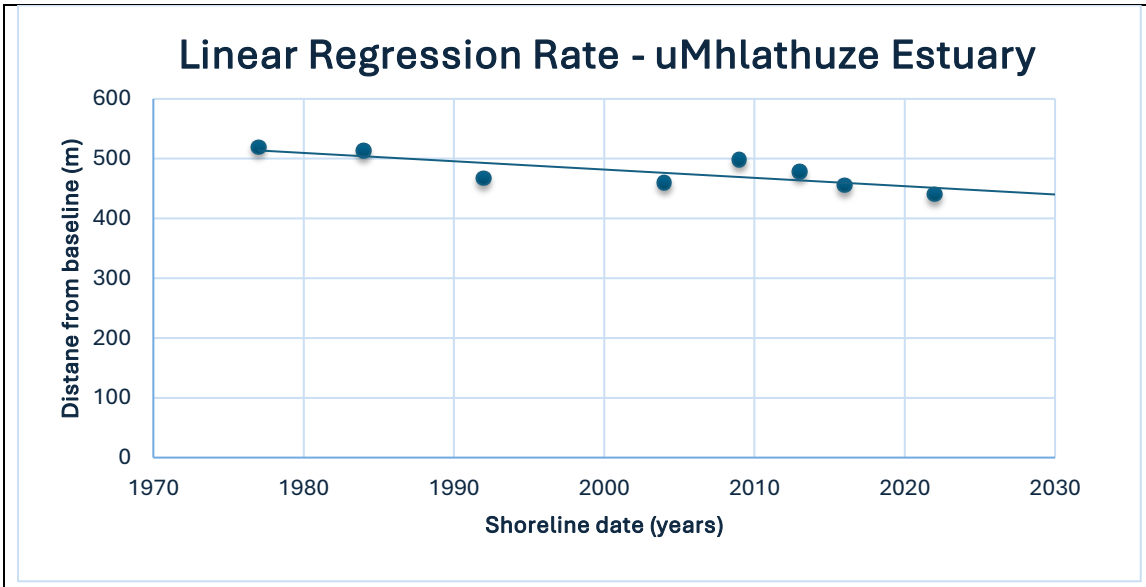

A: Linear regression rate

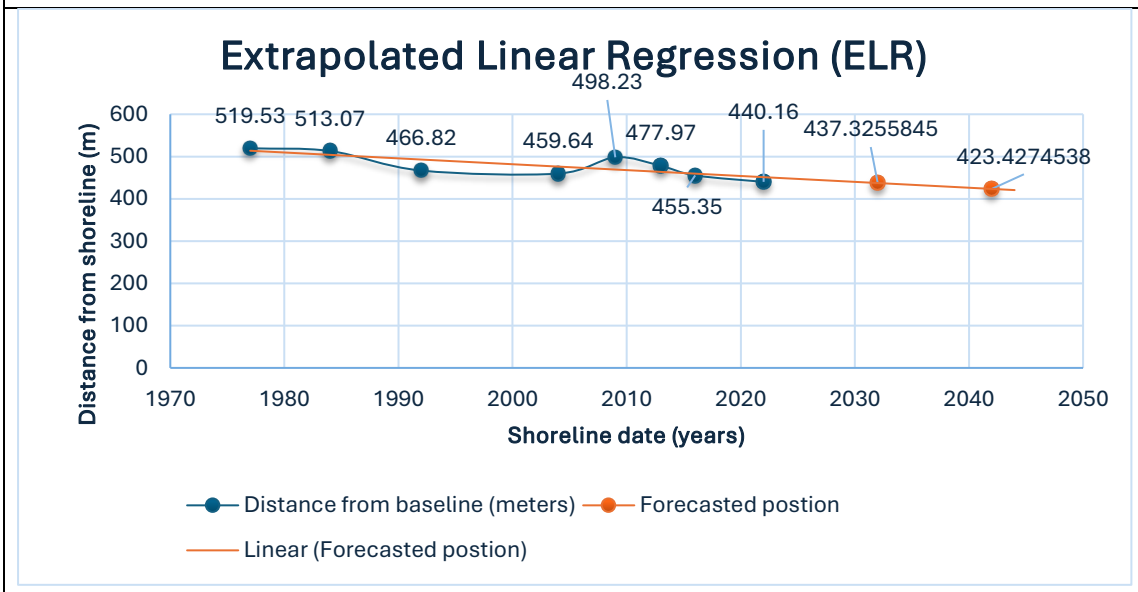

B: Extrapolated linear regression

Figure 4.9: Transect no.53 was chosen to calculate the ELR.

4.2.2 South Dunes

Fig 4.10 (A) below shows the graphical representation of the linear regression rate for South Dunes with the x-value representing the historical years from 1977 to 2022 and the y-value representing the distance from baseline, which will be discussed in Chapter 5. This data was used to extrapolate the future shoreline positons for 2032 and 2042 (Fig 4.10 (B)) using the ELR formula.

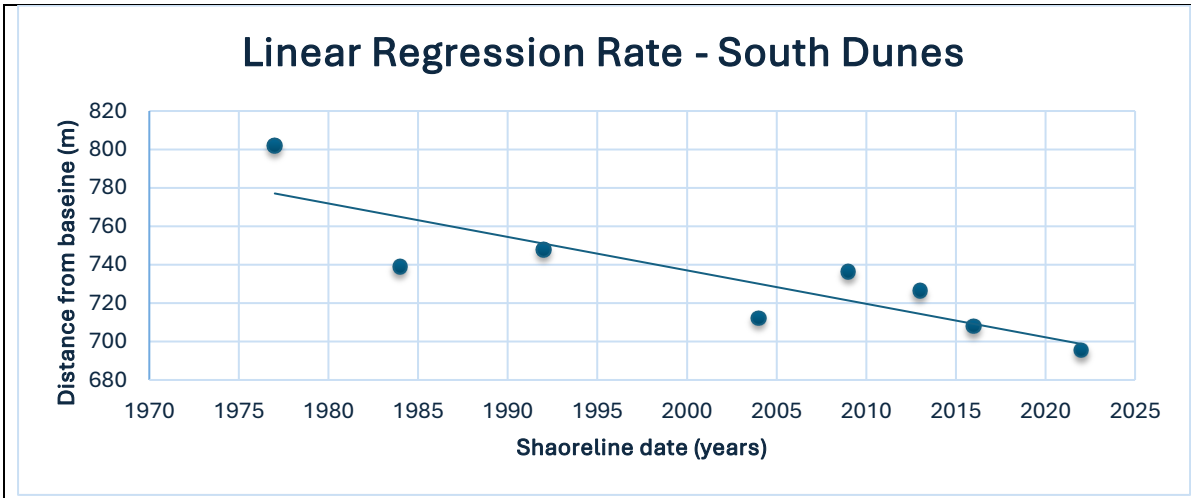

A: Linear regression rate

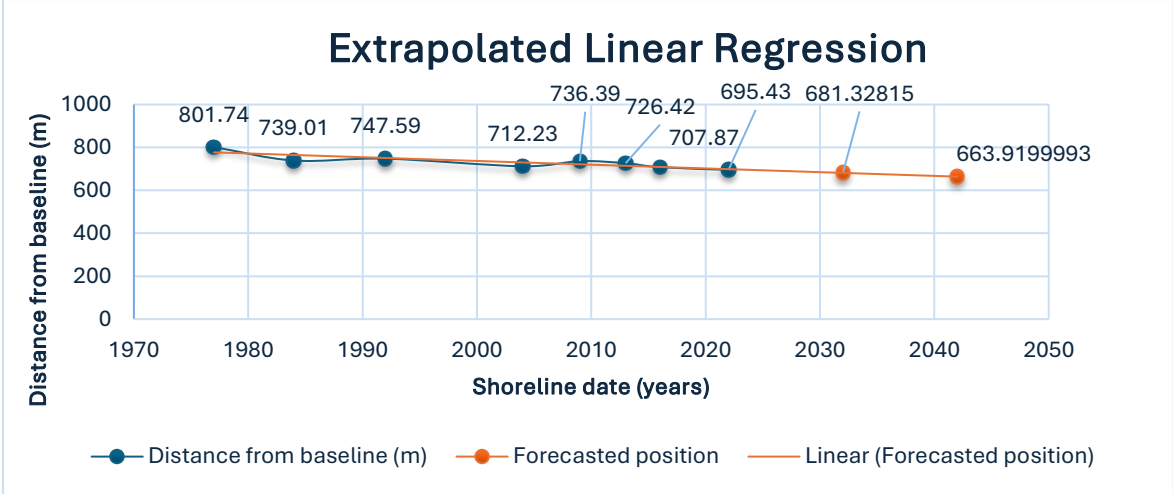

B: Extrapolated linear regression

Figure 4.10: Transect no. 4 was chosen to calculate the ELR.

4.2.3 Alkanstrand

Fig 4.11 (A) below shows the graphical representation of the linear regression rate for Alkanstrand with the x-value representing the historical years from 1977 to 2022 and the y-value representing the distance from baseline, which will be discussed in Chapter 5. This data was used to extrapolate the future shoreline positons for 2032 and 2042 (Fig 4.11 (B)) using the ELR formula.

A: Linear regression rate

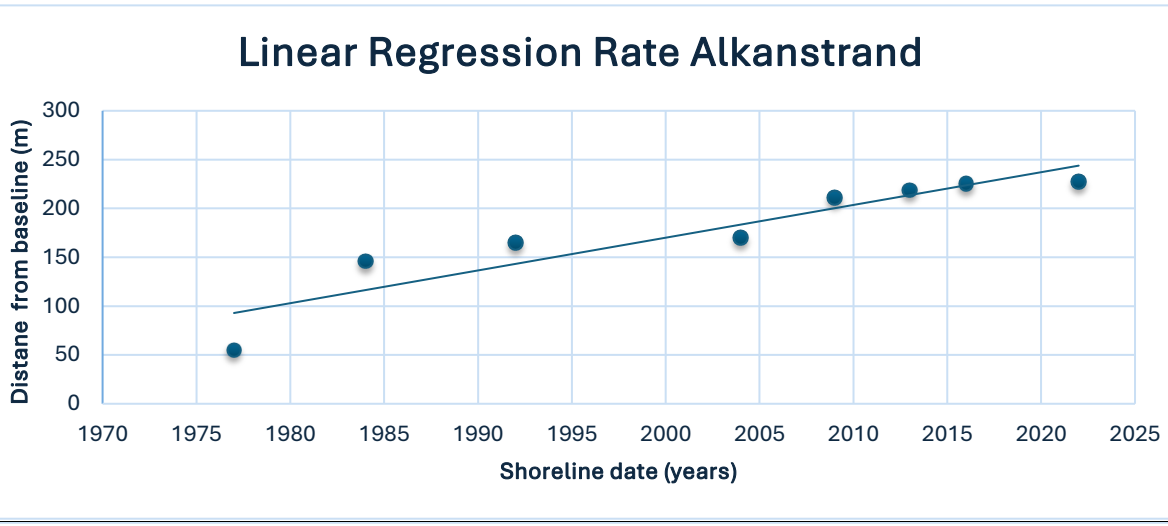

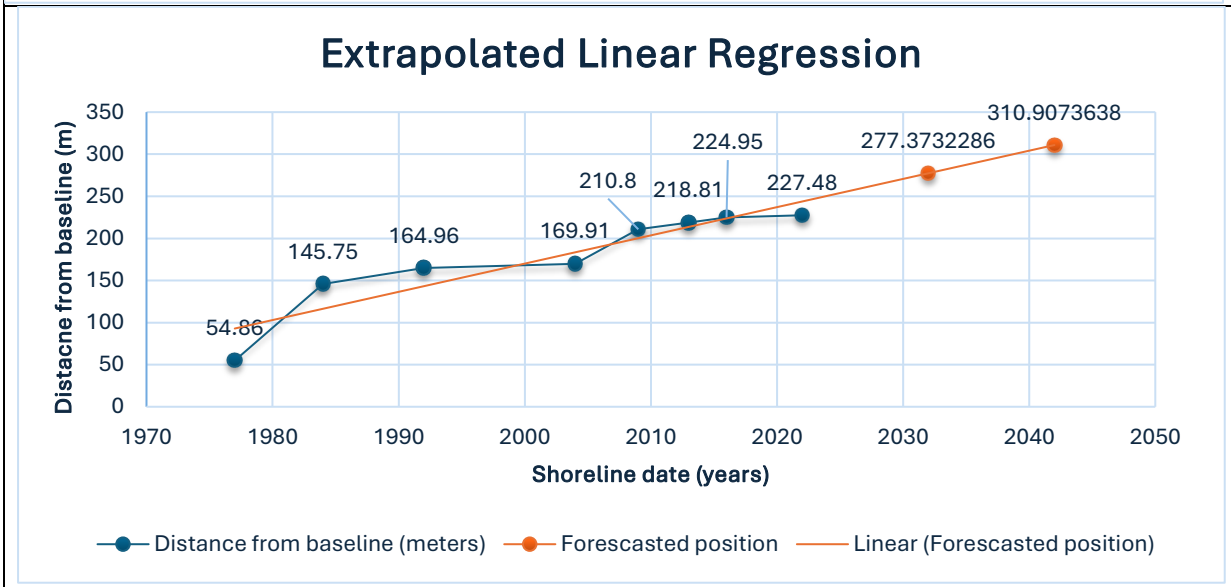

B: Extrapolated linear regression

Figure 4.11: Transect no. 3 was chosen to calculate the ELR.

4.2.4 Alkanstrand North

Fig 4.12 (A) below shows the graphical representation of the linear regression rate for Alkanstrand North with the x-value representing the historical years from 1977 to 2022 and the y-value representing the distance from baseline, which will be discussed in Chapter 5. This data was used to extrapolate the future shoreline positons for 2032 and 2042 (Fig 4.12 (B)) using the ELR formula.

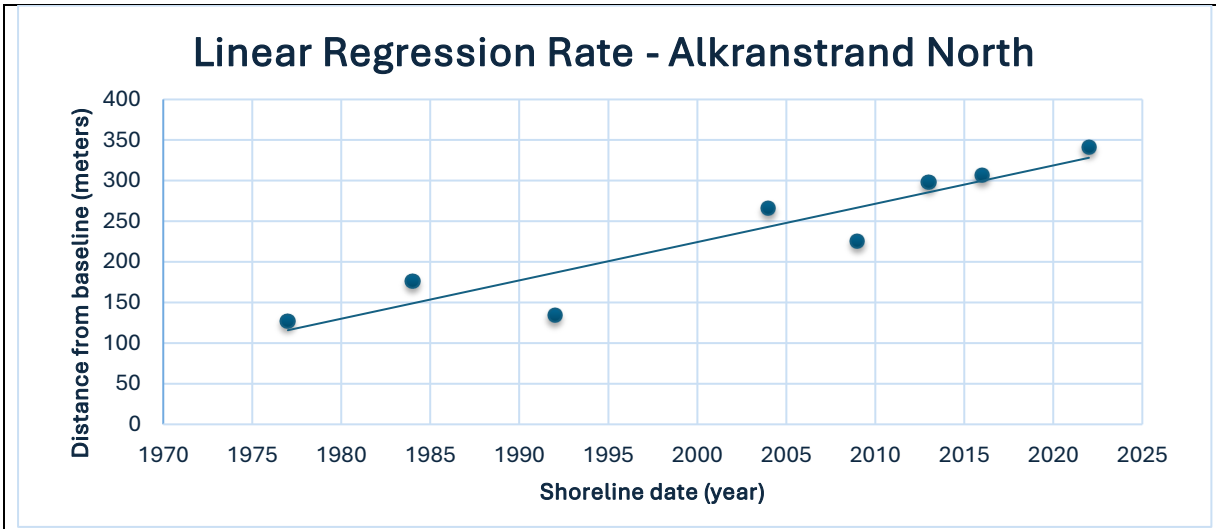

A: Linear regression rate

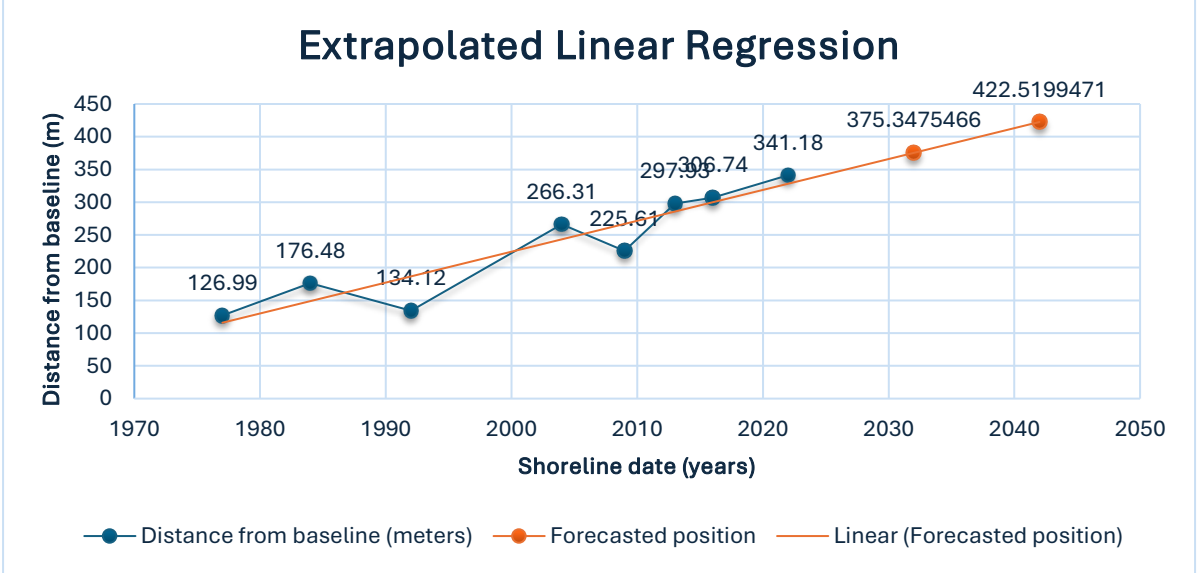

B: Extrapolate linear regression

Figure 4.12: Transect no. 6 was chosen to calculate the ELR.

4.3 Storm surge results

Four different levels of storm surges were analysed to determine the potential impact of storm surges on the coastal region of Richards Bay. The chosen surge levels of 7, 8, 9 and 10 m were used in the analysis to emulate the data previously recorded. Smith et al. (2010) indicated that large swells of maximum 8-10 m are commonly recorded during mid-winter storms in the KwaZulu Natal Bight. The first step in the process was to hydro-condition the DEM to allow flow paths from bridges, canals, or underpasses. This process involves the identification of these types of infrastructure in the area of interest. These were then stamped onto the DEM creating a new layer called the DhyMSea layer (Fig. 4.13)

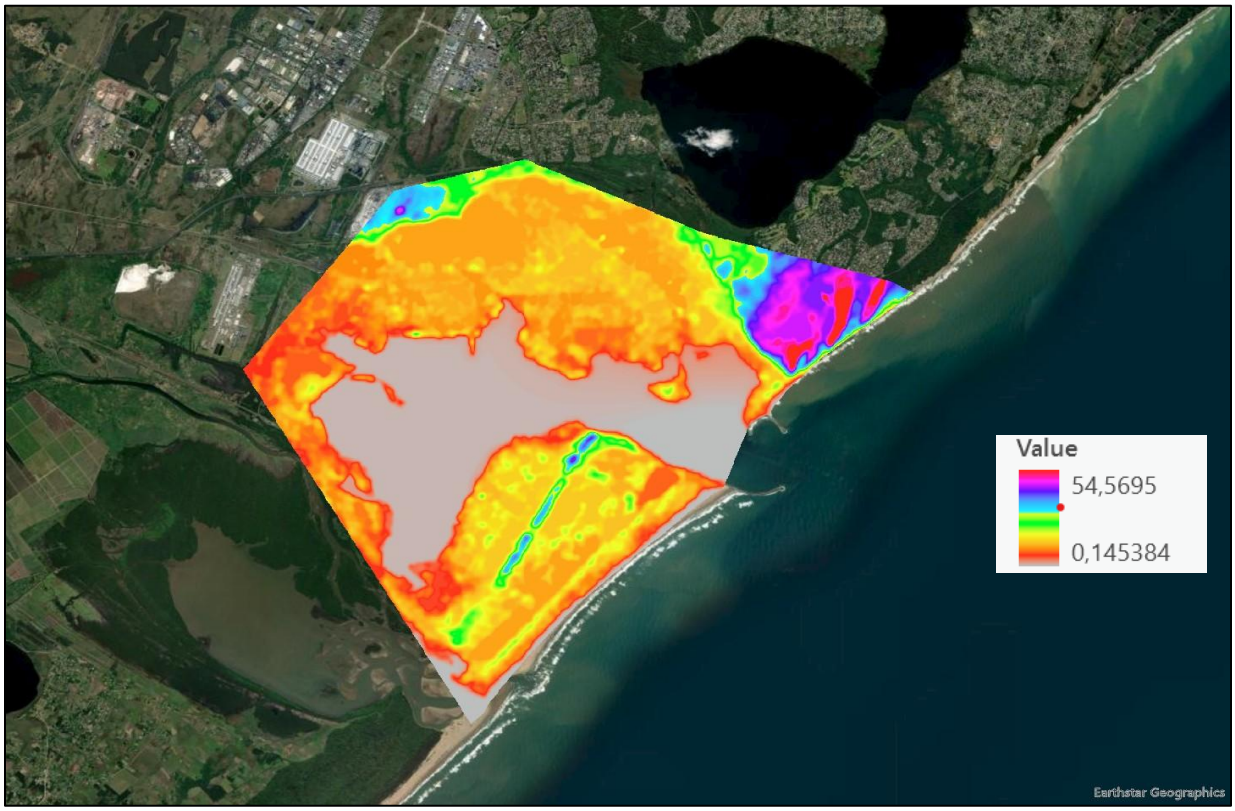

Figure 4.13: Overview of the elevation layer: The hydro-conditioned DEM known as the DhyMSea layer.

A 5 m DEM was used to create the DhyMSea layer which is a hydro-conditioned version of the DEM. The 5 m DEM means that each cell represents a square on the ground of 5 m by 5 m. Importantly, each raster cell represents the elevation above mean sea level in metres. The elevation varies from about 0.1 m to 54.5 m some areas. The higher elevation areas represent the magnificent frontal dune systems of the study area. Fig. 4.14 below represents all the layers used as input files in the model used to generate the inundation scenarios caused by different levels of storm surges.

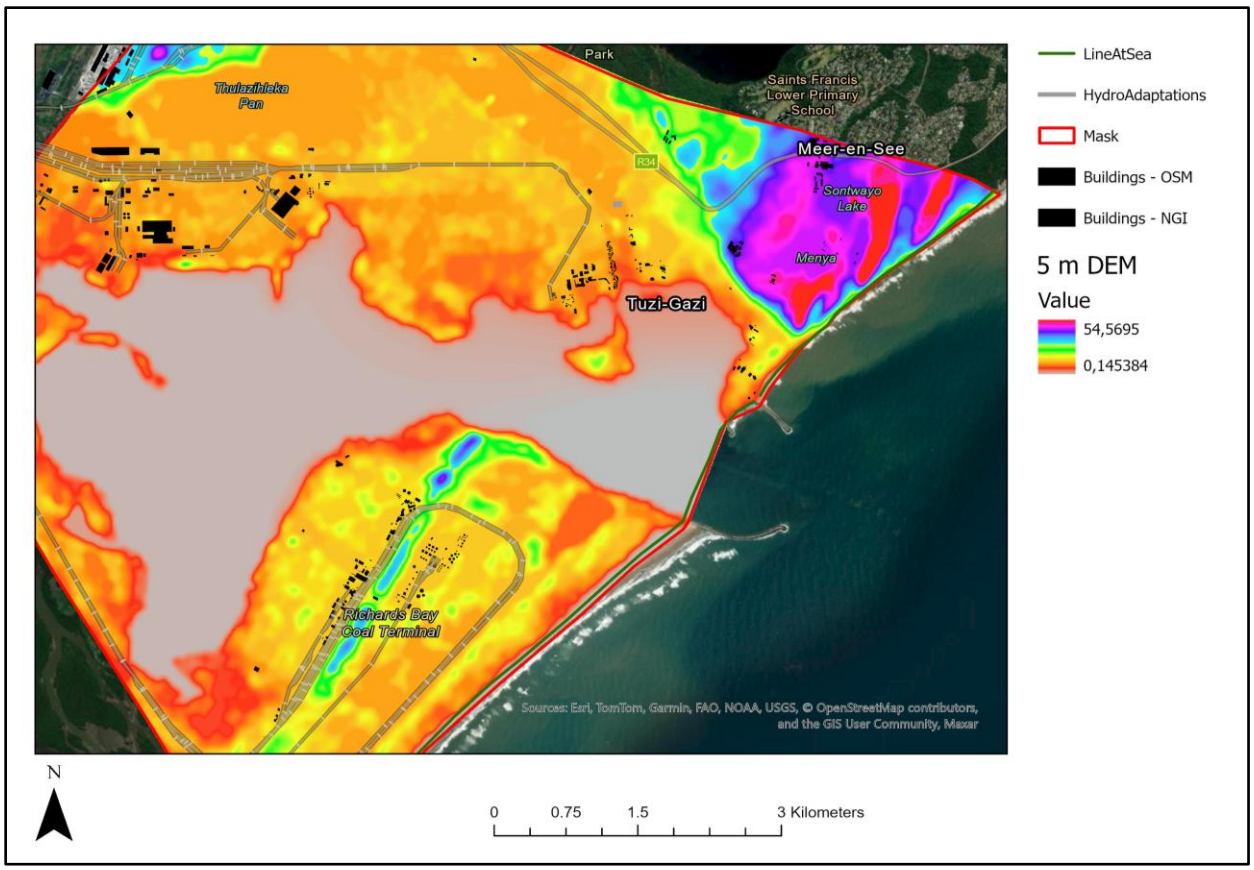

Figure 4.14: Data used as inputs in modelling storm surges in ArcGIS Pro.

The LineAtSea feature class represents the sea line from where the storm surge will come in the analysis. The hydro-adaptations feature class represents all the line features such as bridges that were hydro-conditioned (i.e. to add the missing flow paths to the DEM). To do this, the 'Burn Flowlines onto DEM' tool was used. For each hydro-adaptation line feature, the model locates the lines' endpoints, assigns them elevation values extracted from the DEM and averages them. This mean elevation (Z) value is then automatically assigned to relevant DEM raster cells along the flow using the Polyline to Raster and Raster Calculator tools. As a result, the water flows are enabled through one-cell-wide hydrologic flow paths. The land mask polygon is used to limit certain results to land areas. The buildings polygon feature class represents the study area in 2017, provided by ESRI and the NGI. The buildings layer was added to the analysis to visualize which buildings will be affected by different levels of storm surge. The following maps were generated from the results of the storm surge inundation exercise at levels of 7, 8, 9, and 10 m.

Figure 4.15: Inundation Model depicting the floodable areas of the study site when experiencing a storm surge level of 7 m.

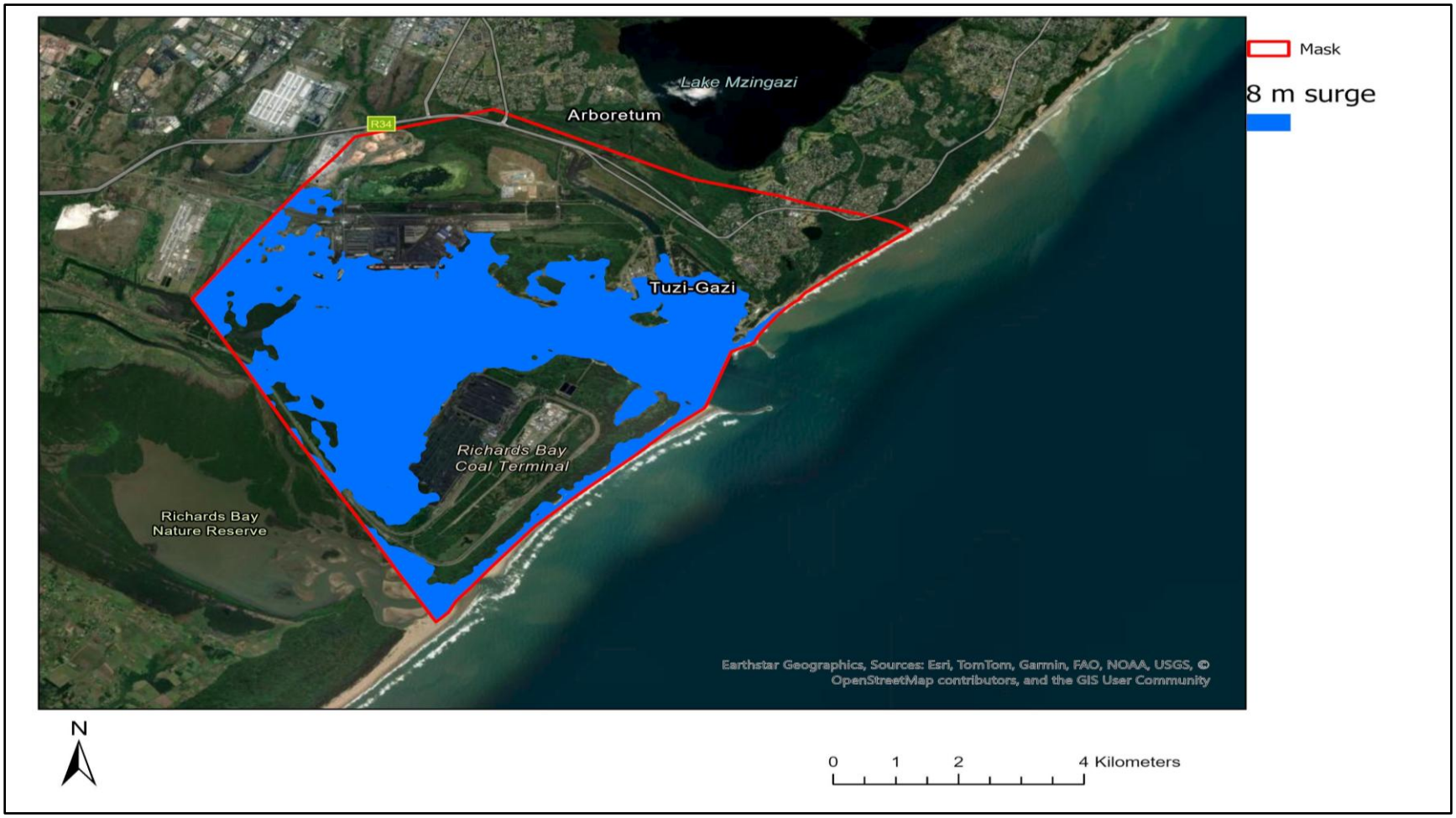

Figure 4.16: Inundation Model depicting the floodable areas of the study site when experiencing a storm surge level of 8 m.

Figure 4.17: Inundation Model depicting the floodable areas of the study site when experiencing a storm surge level of 9 m.

Figure 4.18: Inundation Model depicting the floodable areas of the study site when experiencing a storm surge level of 10 m.

The storm surge analysis model clearly depicts the spatial extent and which areas of the study site will be inundated with water during certain storm surge scenarios. To provide a quantifiable measure of this, the spatial extent (area) of the affected area is calculated for the study area (Table 4.8).

Table 4.8: Analysis of the spatial extent of impact from storm surges in the study area.

Storm Surge Height	**Area (%) of the study area that will be affected**	**Expansion of the water extent (%)**	**Area (%) of the study area that will not be affected**
7 m	39.7%	5.2%	60.3%
8 m	44.1%	17%	55.9%
9 m	60.6%	60%	39.5%
10 m	68.8%	82%	31.2%

Chapter 5: Discussion

5.1 Introduction

This chapter presents a discussion of the results of the shoreline change analysis for a 45-year period between 1977 and 2022, as well as the storm surge inundation screening exercise. The findings of the DSAS analysis on shoreline change rates reveal that accretion is consistent South of the harbour and erosion towards the North. The discussion on the results of the storm surge analysis showed that the inundation consequences of 9 m and 10 m surges are significantly higher than the 7 m and 8 m. Longshore sediment drift, impacts of climate change, and sand mining are discussed as possible contributors to the problem of erosion along the coastline around the Port of Richards Bay.

5.2 Shoreline change discussion

5.2.1 Net Shoreline Movement (NSM)

The Net Shoreline Movement (NSM) represents the distance between the oldest and the most recent shorelines. uMhlathuze Estuary and South Dunes, situated South of the Port of Richards Bay experienced 98.37% and 41.03% accretion, with an average seaward expansion of 93.06 m and 98.90 m, respectively. While Alkanstrand and Alkanstrand North, situated North of the Port of Richards Bay experienced 100% erosion, with an average landward retraction of -167.80 m and -98.20 m respectively. A visual representation of the data are represented in figures 4.4 – 4.7 above. Figures 5.1 – 5.4 below further illustrates the NSM for all four shorelines. The oldest shoreline being 1977 and the most recent being 2022.

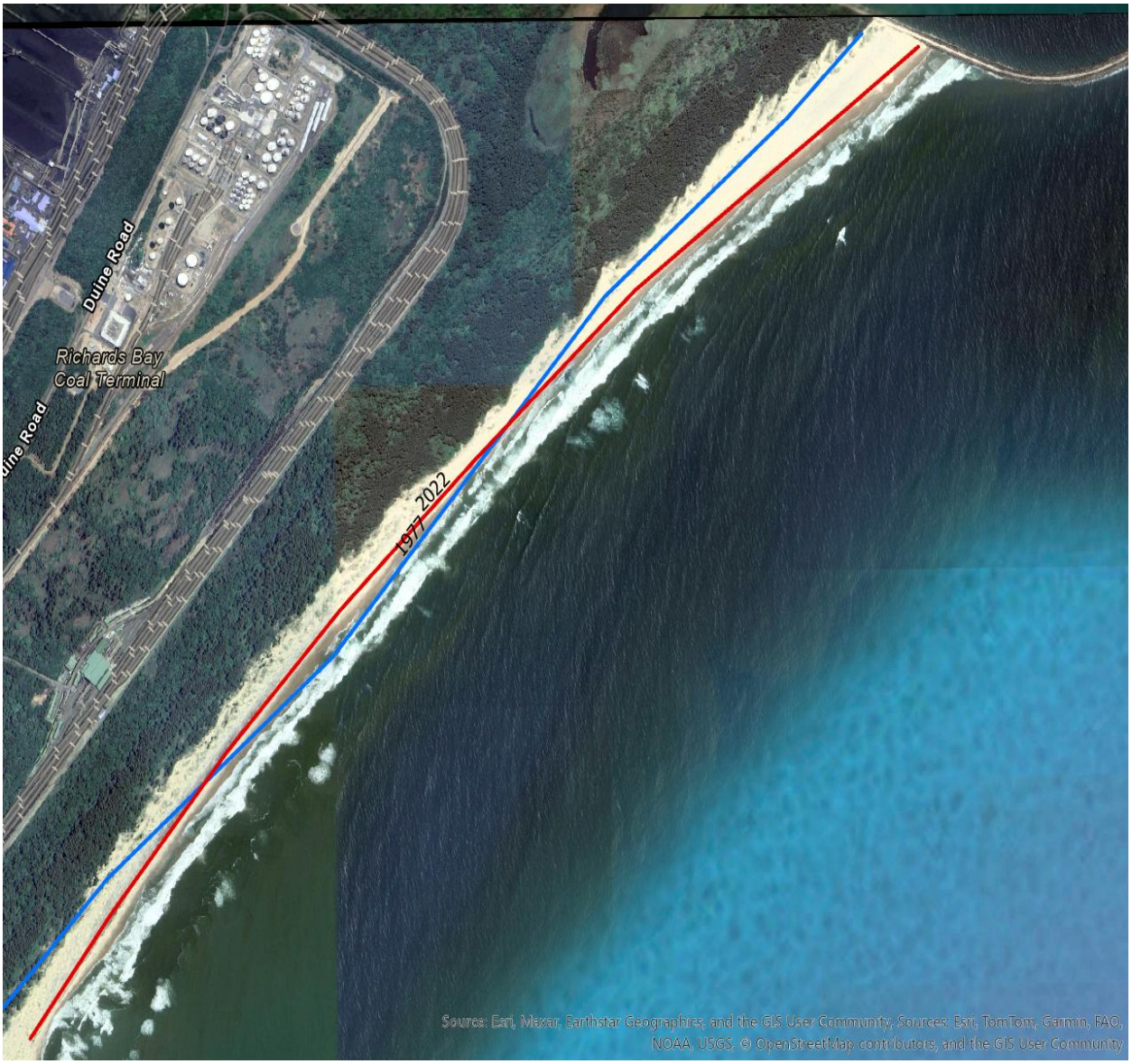

Figure 5.1: The Net Shoreline Movement for South Dunes between 1977 and 2022 was 98.90 m in a seaward direction (accretion) according to the DSAS calculations.

Figure 5.2: The Net Shoreline Movement for uMhlathuze Estuary between 1077 and 2022 was 93.06 m in a seaward direction (accretion) according to the DSAS calculations.

Figure 5.3: The Net Shoreline Movement for Alkantstrand between 1977 and 2022 was 167.8 m in a landward direction (erosion) according to the DSAS calculations.

Figure 5.4: The Net Shoreline Movement for Alkantstrand North between 1977 and 2022 was 98.20 m in a landward direction (erosion) according to the DSAS calculations.

Figure 5.5: A comparison from 2004 and 2022, South of the harbour, with the 2004 shoreline being noticeably narrower than the 2022 shoreline, validating the results of the DSAS analysis (Source Google Earth).

Figure 5.6: A comparison of 2009 and 2022 aerial photographs of the area North of the harbour (Alkandstrand and Alkanstrand North), with the 2009 shoreline showing a wider beach area validating the results of the DSAS analysis (Source: NGI (2009) and Google Earth (2022)).

5.2.2 Shoreline Change Envelope (SCE)

The Shoreline Change Envelope (SCE) value represents the greatest distance among all the shorelines that intersect a given transect regardless of date or direction (i.e. the distance between the most landward and most seaward shorelines). For the uMhlathuze shoreline, all 123 transects cast differed from that of the NSM value. This means that the position of the shoreline has shifted back and forth or had significant changes in different directions over time, resulting in a wider range of movement captured by the SCE than the NSM. Figure 5.7 shows the uMhlathuze digitized historical shorelines. The most landward shoreline is not the earliest shoreline, therefore the SCE provides a broader perspective on shoreline variability.

Figure 5.7: uMhlathuze Estuary showing variability between SCE and NSM.

The results for South Dunes showed that 28% of the 78 transects cast matched the NSM values (Fig. 5.8), while Alkanstrand showed very similar values for all 6 transects cast (Fig. 5.9). At Alkanstrand North beach, the longest stretch of coastline in the study area, the results showed that 31% of all 203 transects cast were the same as the NSM value (Fig. 5.10).

Figure 5.8: South Dunes showing variability between SCE and NSM. The year 1977 differs greatly due to the construction of the harbour.

Figure 5.9: Alkanstrand beach showing little variability between SCE and NSM.

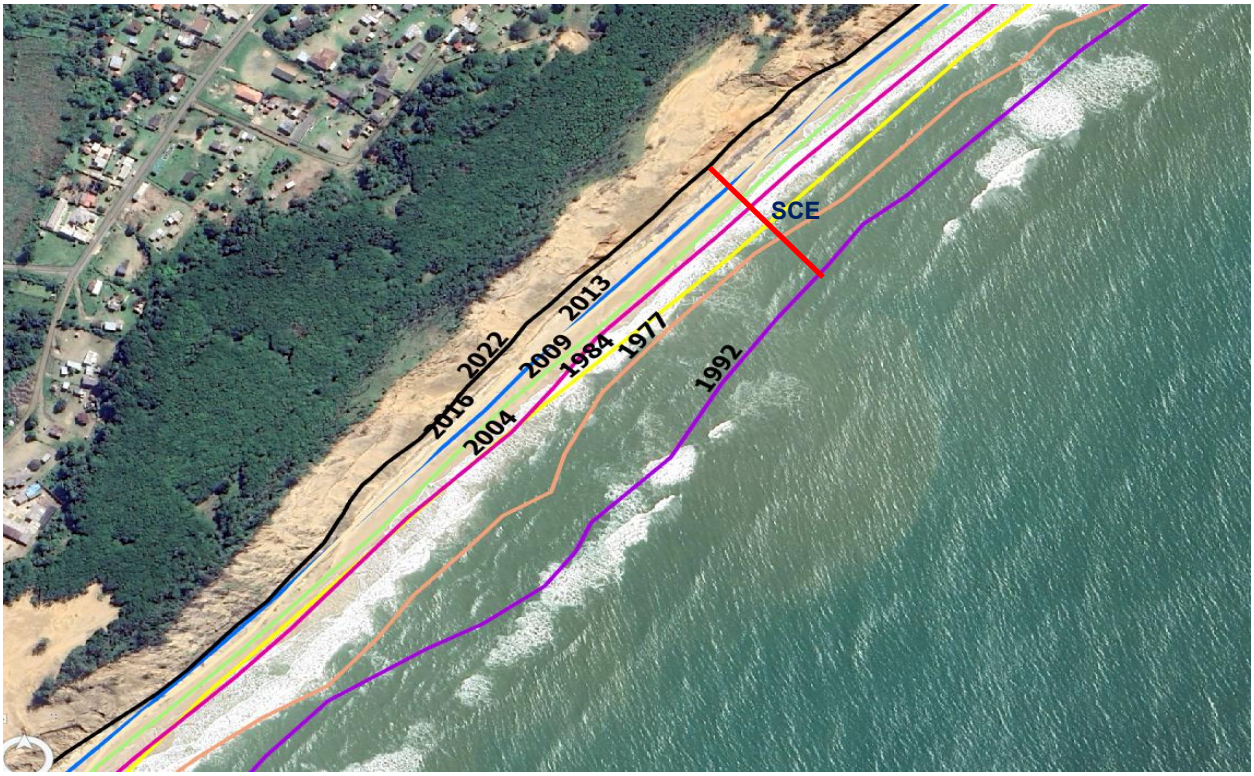

Figure 5.10: A portion of Alkanstrand North beach showing the difference in SCE and NSM.

A discrepancy between NSM and SCE highlights the importance of considering the complete history of shoreline movement, and not just the net change. For example, for uMhlathuze Estuary, the shoreline experienced erosion between 1977 and 1984, and then drastically accreted between and 1984 and 1992 (Fig. 5.7), before following a linear trend of accretion. Understanding this dynamic behaviour is crucial for effective coastal management, as it can influence decisions about infrastructure, development, and hazard mitigation strategies.

5.2.3 Linear Regression Rate (LRR) and Weighted Linear Regression (WLR)

The Linear Rate Regression (LRR) uses all the shoreline dates to calculate linear trends over time based on the Least Sum of Squares method. The LRR is therefore the slope of the line as shown in Figures 4.7 – 4.10 (Chapter 4) for the four shorelines in the study area. The LRR for Alkanstrand and Alkanstrand North revealed 100% erosional transects in the 45 year period of analysis, with an average erosion rate of -3.25 and -2.28 m per year, respectively. In contrast, uMhlathuze Estuary had 96.75% accretional transects with an average erosion rate of 0.13 m per year, while South Dunes showed an average erosion rate of -3.25 m per year.

Murray et al. (2023) assert that even though a 95% Confidence Interval (CI) was assigned to their results of the LRR, it does not consider the uncertainty values in the calculations. To address this, DSAS calculates a weighted linear regression, “which multiplies all shoreline transect values by the squared inverse of their respective uncertainty values.” (Murray et al., 2023: 11). The Weighted Linear Regression (WLR) assigns different weights to data points based on their uncertainty values. Uncertainty in shoreline positions can be affected by various factors including digitizing errors, the quality of the data, georeferencing errors, and other uncertainties. WLR is generally considered more reliable over LRR because it accounts for the uncertainty in the data, thus providing a more robust estimate of the shoreline change rate. The WLR for the four shorelines revealed a decreased average erosional rate compared to the LRR.

5.2.4 End Point Rate (EPR)

The End Point Rate (EPR) is another statistical method the DSAS uses to calculate shoreline change. It is calculated by dividing the total distance of shoreline movement by the time elapsed between the oldest and most recent shoreline, giving a rate in metres per year. Positive values indicate accretion while negative values are associated with erosion. The results of the EPR was similar to the LRR, where an average erosion rate of -3.73 m and -2.18 m per year was calculated for Alkanstrand and Alkanstrand North respectively. Similarly, uMhlathuze and South Dunes reported an average accretion rate of 2.44 m and 1.74 m per year, respectively.

From the statistical and distance measurements calculated by the DSAS, as well as observed historical aerial photographs of erosion and accretion (Fig. 5.5 and 5.6), it can be deduced that an erosional trend is consistent with the beaches North of the harbour, while an accretional trend is consistent with the beaches South of the harbour. A discussion of possible reasons for these trends will be discussed later in this chapter.

5.3 Shoreline forecasting

From the results of the shoreline change rate statistics, it was determined that the beaches north of the harbour, Alkanstrand and Alkanstrand North, experienced 100% erosion during the 45 year analysis period, while the beaches south of the harbour, South Dunes and uMhlathuze Estuary have experienced mostly accretion, with a small portion of South Dunes showing some erosion and areas of no change as indicated by the DSAS results map in Figure 4.3.

Forecasted shoreline positions 10 and 20 years into the future (i.e. 2032 and 2042) have been computed and the results show that for Alkanstrand North the shoreline will erode by a further 10% by 2032 and 23% by 2042 when compared to the most recent shoreline (2022). These results assume that the linear trend continues. In line with the erosion trend, the 400 m stretch of Alkanstrand beach shows a percentage increase of 21% by 2032 and 36% by 2042 when compared to the most recent shoreline (2022). The analysis does not consider the future effects of seal level rise, climate change induced weather events such as storm surges and high intensity sea storms, or other geomorphological events. Therefore it is assumed that these figures are under-estimates and might be higher than predicted.

Contrarily, the results for South Dunes revealed a slight 2% increase in accretion by 2032 and 4% by 2042, assuming the linear trend in accretion continues. Forecasting for uMhlathuze Estuary by 2032 shows a predicted seaward movement of the shoreline of 0.6% and 1.7% by 2042. It is noticeable that the rate of erosion is much higher to the North of the Port of Richards Bay than the rate of accretion to the South. The predicted shorelines for 2032 and 2042 are visualised below (Fig. 5.10).

Figure 5.11: Predicted shorelines positions for 2032 (green) and 2042 (blue) with 2022 (red) as a reference.

5.4 Storm surge discussion

The results of the storm surge analysis reveal that for a 7 m and 8 m storm surge, the study area is minimally affected with a 5.2% and 17% expansion of water extent, respectively. However, when experiencing a surge level of 9 m and 10 m, a significant portion of the study area modelled is inundated (i.e. 60% and 82%, respectively). During these modelled surge levels, most of the buildings and infrastructure are affected, with the exception of a few pockets of higher elevation areas. This can be an important source of information for flood risk analysis within the Port of Richards Bay and can be used as a guide to design mitigation measures aimed at limiting affected buildings and infrastructure from becoming inundated with floodwaters. Such measures can include the strengthening or refurbishment of the current breakwaters to better cope with the changing conditions under climate change. Information about the inundations due to storm surges can also be useful in rescue and damage assessments (Balstrom & Kirby, 2021).

Evidence indicates that the coastline around Richards Bay will become more vulnerable to tropical storms and cyclones (Nathaniel & Baxter, 2025). Temperatures in South Africa are expected to increase as high as 4°C by the year 2100 (Fitchett at al., 2016). In addition to this, changes in wind direction and speed, severity of precipitation events and rising sea levels are also expected (Fitchett et al., 2016). Sea level rise additionally results in an increased risk of storm surges for low-lying areas. Thus, the likelihood of the study area experiencing a 9 m or 10 m storm surge level or more is increased. Although data of recent storm surge levels in the area are limited or not available, Mather & Stretch (2012) indicated that a surge level of 8.5 m was recorded in Richards Bay during severe storms in March 2007. Storm surges create a temporary rise in sea levels leading to destruction of the environment, infrastructure, and poses a threat to human lives. In the context of climate change, sea level rise, and increased frequency of storm surges, an inundation screening of this nature was essential for the study area.

5.5 Longshore sediment transport

For the KZN coastline, the longshore sediment generally flows from South to North, driven by prevailing wave climate (Cooper, 1991; Smith et al., 2016; Simmonis, 2016). Simmonis (2016) states that coastal engineering such as the breakwater dolosse in Richards Bay along with the frequent requirement to dredge the harbour bed has resulted in the interruption of the longshore drift, causing accretion on the updrift side (South), and erosion on the downdrift (North). Similarly studies by Smith et al. (2016: 8) found that “the Durban and Richards Bay breakwaters are interfering with longshore drift and consequently the worst erosion is down longshore drift of these

inlets. Sand nourishment schemes are in place but are inadequate". Wells (2015: ii) used Richards Bay as a case study to "model and compare alternative sand nourishment schemes to alleviate the problem of erosion due to the disruption of the longshore sediment supply".

The evidence is clear that severe, consistent coastal erosion occurring in areas with a high anthropogenic influence, is linked to the longshore sediment transport, where erosion on one stretch of coast is likely to result in accretion elsewhere. This is especially true for Richards Bay and has been verified from the results of this study. As Smith et al. (2016: 8) state, with reference to the KZN province, "Outside of urban areas or human-influenced areas, there have been no reports of ongoing coastal erosion". The movement of sand along the beach is a natural process, and, when interrupted, can lead to the loss of its natural coastal defence. The study area has lost a significant amount of natural dunes that provided a natural barrier to the effects of coastal erosion and flooding, due to the interruption of the longshore sediment from port developments, as well as storm surges. This, coupled with the onset of global climate change and associated sea level rise, the consequences of coastal erosion could become increasingly severe.

5.6 Other contributing factors leading to coastal erosion

5.6.1 Climate change and associated sea level rise

Climate change in the coastal zone is associated with sea level rise and increased frequency of storm surge events. The literature agrees that sea levels are rising as a consequence of climate change (Mather & Stretch, 2012; Smith et al., 2016; Nathaniel & Baxter, 2025). According to Luck-Vogel et al. (2019), sea levels are expected to be about 0.35 m and 1.0 m higher along the South African coastline by the year 2100. This statistic alone places the study area at a greater risk due to its location in a coastal plain. Moreover, climate predictions for the eastern and south-eastern coasts of South Africa forecasts a higher frequency and intensity of storms (Luck-Vogel et al., 2019). These predictions increase the risk and vulnerability of the coastline to flooding and erosion. The goal, therefore, is to reduce this risk by implementing mitigation and adaptation strategies that are specifically suited to the area. These strategies are discussed later in this Chapter.

5.6.2 Sand mining

A critical aspect exacerbating the problem of erosion in the study area and in KZN at large is the reduction in the supply of sediment to the beaches. It is estimated that approximately 80% of sand in the coastal zone are supplied by rivers (GESAMP, 1994) but sand mining and the

impoundment of rivers is preventing sediment from reaching the coastal region. The reduction in sediment budgets to the coastal zone are likely due to anthropogenic impacts such as river impoundments, changes in land use, and sand mining (Smith et al., 2016; Leuci et al., 2022).

Sand mining, where sand is mined from riverbeds, estuaries, etc, in the KZN region is increasing as a result of the increase in demand for river sand in the building and construction industry in South Africa (Breetkze et al., 2016). Most of these sand mining activities are taking places illegally, i.e. without a permit from the Department of Mineral and Petroleum Resources (DMPR), and at an unsustainable rate leading to a reduction in sediment supply to the coast (KZN EDTEA, 2023).

A study undertaken by the Council for Scientific and Industrial Research (CSIR) on the KZN beaches, specifically beaches in the eThewkini region revealed that the impact of both dams and sand mining could result in an average erosion rate of 1 m per year (Breetzke et al., 2016). The same study found that the total mined volume for the 18 rivers in the eThekwini region in 2008 amounted to an estimated 400 000 m^3 a year, which equates to a staggering 66% reduction in natural sand yield (Breetzke et al., 2016). These statistics reveal the unsustainable rate of sand mining and its negative impact to the coastal zone.

5.7 Limitations to the study and reliability of the results

5.7.1 Calculated rates of shoreline change

Morton & Miller (2005) suggest three possible reasons that limits the reliability of the results for the calculated rates of shoreline change as follows:

1. Measurement errors that determine the accuracy of each shoreline position.
2. Sampling errors that account for the variability of shoreline position; and
3. Statistical errors (variability) associated with compiling and comparing shoreline positions.

Typical measurement errors are related to the mapping and digitizing of the historical shoreline positions. Positional errors when digitizing errors are attributed to scales and inaccuracies in the original survey (aerial imagery). Human error when digitizing, and the lack of availability of high resolution remote sensing data can be seen as the main limitations to achieving accurate results. Furthermore, the DSAS primarily focuses on quantifying shoreline change rates. It does not consider underlying processes driving these changes, such as wave and wind

dynamics, sediment transport, or human-induced changes. It assumes a steady state terrain which will not accommodate changes in future climate.

5.7.2 Storm surge analysis

The inundation screening is based on digital elevation data while assuming steady state terrain conditions, i.e. geomorphological conditions during the event are not considered. For instance, they do not consider that a water barrier may collapse during a storm surge. In addition, they do not account for all the complexity of real-life coastal inundation dynamics (Balstrom & Kirby, 2021).

The resolution of the DEM is a critical factor in obtaining realistic results. The higher the resolution, the more accurate the results. An ideal resolution for this type of analysis would be a 0.4 m as utilized by Balstrom & Kirby (2021) in the surge analysis of Denmark in 2020. However, this level of spatial resolution is not available for the study area. Thus, a 5 m DEM was used for the analysis. A third limitation relates to errors in a DEM. Errors in the DEM may not be accounted for, such as a thin wall whose elevation is not represented.

5.8 Recommendations

The study revealed that the main driver of coastal erosion in Richards Bay is due to the disruption of the longshore sediment transport caused by the construction of the breakwaters around the port. This disruption of the natural flow of sediment moving northward results in an accumulation of sand updrift of the harbour and accretion on the downdrift side (north) (Wells, 2015., Simmonis, 2016). A sand bypassing scheme, where sand is dredged from the accumulation zone and used to nourish the eroded section of the beach (Figure 5.12), has been a coastal defence strategy over the years. However, erosion still persists due to the lack of consistency in nourishing the beaches (Wells, 2015).

Figure 5.12: Left: The hopper dredger docked inside the harbour and connected to the discharge pipeline. Right: Sand is pumped onto Alkanstrand beach via the discharge pipeline. Adapted from Wells (2015).

Other contributing factors leading to coastal erosion along the coastline of Richards Bay is linked to activities in the hinterland such as sand mining in rivers, river impoundment, and climate-related impacts such as sea level rise and the increase and intensity of storm surges (Luck-Vogel et al., 2019; KZN EDTEA, 2023). Should the erosion rates and extreme weather events continue, the shoreline will keep retreating leading to further loss of natural habitat, coastal dunes and associated vegetation, and infrastructure.

As a major port in South Africa, TNPA has a vested interest in coastal protection and actively manages its own infrastructure and contributes to broader coastal management efforts within the port area. The uMhlathuze Municipality also plays a role in coastal management by allocating resources for the planning and development of coastal protection infrastructure (uMhlathuze SDF, 2024). At a broader scale, the Provincial Coastal Management Programme (PCMP) driven by the KZN EDTEA is an integrative planning and policy instrument guiding coastal management in KZN under the directive of the Integrated Coastal Management Act (ICMA) (Act No 28 of 2008) as amended. The ICMA promotes the conservation of the coastal environment in South Africa, and ensuring sustainable and equitable use of coastal resources. It also contains tools to ensure the coastal zone is managed cooperatively, and the development of PCMPs is key to this (KZN EDTEA, 2017).

Coastal protection infrastructure on many coastlines involves the implementation of hard engineering structures such as breakwaters, dolosse, dikes, sea walls, rock revetments, artificial reefs, jetties and groynes (e.g. Morton & Miller, 2005; Schoonees et al., 2006; Corbella & Stretch, 2012b; Pranzini & Margeta, 2022). Some of these structures are known to cause a sediment imbalance as deduced from this study. Some of the drawbacks associated with hard engineering structures are the cost implications (the construction and implementation is expensive), and while they help prevent erosion, some structures can also prevent sand movement along the beach (Angnuureng et al., 2023).

In response to the mounting impacts of climate change, Nature-Based Solutions (NBS) are increasingly being proposed as a sustainable approach (Singhvi et al., 2022; O'Leary et al., 2023). O'Leary et al. (2023: 2) describes NBS as "systematic actions that work with and enhance nature to provide environmental, social and economic benefits that simultaneously address multiple challenges." In the context of this study, NBS as a defence mechanism for coastal erosion and flooding involve sand nourishment to beaches via a sand bypassing scheme, dune construction/stabilization, and the use of geotextile sand bags. These are also known as soft engineering solutions.

This section explores possible pathways to coastal resilience and proposes strategies to mitigate coastal erosion and flooding in a changing environment. The proposed strategies are based on the findings of the study, and a review of the literature on coastal protection infrastructure.

5.8.1 Sand nourishment

Sand bypassing schemes (Fig. 5.12) are a method of beach nourishment where the sand is dredged from the accumulation section of the coast and pumped onto the eroded section of the beach (Morton & Miller, 2005; Wells, 2015). TNPA has been pumping sand onto the beaches of Richards Bay to mitigate against coastal erosion, however, this system is not being implemented on an ongoing basis (Observation; Simmonis, 2016; uMhlathuze SDF, 2017). In the absence of this system, the uMhlathuze Municipality has implemented soft engineering solutions such as the placement of geotextile sand bags and rock revetements (discussed in Chapter 2) to maintain a recreational beach (uMhlathuze SDF, 2017).

A relevant study was conducted by Wells (2015) in the same study area as this research, modelled three different nourishments schemes to assess their effectiveness. The results of the study are summarised in the Table 5.1 below (Wells, 2015: 50).

Table 5.1 Results of the sand bypassing schemes modelled by Wells (2015).

Sand bypassing scheme	**Model result**
Continuous nourishment – entails dumping 2 740 m^3 per day of sand continuously for the entire year.	The results show the mimicking of the natural drift of sand north of the harbour and an expansion of the entire beach area which represents an ideal situation.
Bulk nourishment – entails dumping all the budgeted sand (1000 000 m^3) onto the beach rapidly at a rate of 10 000 m^3 per day amounting to 100 days.	Results revealed significant differences to the other two nourishing schemes. Although the main recreational beach remained in a nourishd state, the beaches to the far north went back to experiencing significant erosion.
Bi-monthly – entails pumping approximately 166 500 m^3 every two months at a rate of 10 000 m^3 per day.	This result was similar to the continuous nourishment scheme.
*The sediment budget for each case was 1 000 000 m^3 for the year	

Wells (2015: 2), emphasises the importance of a well-executed sand bypassing scheme for the study area and as such has stated that “Implemented correctly, sand nourishment schemes can be a cost-effective solution to coastal vulnerability with environmental and economic benefits while reducing storm damage.” Another benefit of beach nourishment via a sand bypassing scheme is that the sediment collected and deposited are of the same grade and no foreign material is introduced into the marine system which has an added environmental incentive.

In 2019, TNPA announced its unique sand bypassing scheme implementation in its Port of Ngqura (Gqeberha), being the first port in the world to have a fixed jet pump sand bypassing system mimicking the natural longshore drift of sand (TNPA, 2019). Should this system prove economically viable in the Port of Richards Bay, it would stabilise the shoreline, promote the recovery of environmentally sensitive dunes and their vegetation, and help the beaches cope with the impact of storm surges.

5.8.2 The development of risk set-back lines

The role of risk setback lines is outlined in the ICM (Act No 28 of 2008) as amended. The ICM Act identifies a setback line as a line “seawards of which development can be prohibited or controlled.” (Goble & MacKay, 2013: 2125). In South Africa, there is no legislative requirement on how setback lines are delineated or undertaken. As such, this research makes use of the 2032 and 2042 predicted shoreline positions as calculated by DSAS and the ELR method to demarcated risk setback lines for the study area (Fig. 5.10).

The indicated 2032 and 2042 shoreline positions can be regarded as buffer zones where no development should take place. The establishment of these set-back lines can prove useful in coastal development planning and in a disaster management planning context. Farris et al. (2023) notes that some states in the Unites States primarily uses set-back lines associated with 30-year erosion rates extrapolated into the future as a basis for regulations.

5.8.3 Geotextile sand bags and rock revetments

These methods have already been undertaken in the study area to stabilise the shoreline since 2015. Rock revetment (Fig. 5.13) has been implemented in 2024 (observation). It has been noted from observation and documented in the local newspapers that the geotextile sand bags were not a lasting erosion protection measure. Intense storm surges bringing high energy waves and wind result in the shifting of the bags and erode the sand beneath them.

Figure 5.13: Rock revetments as a coastal protection strategy in Richards Bay (Alakram, 2024).

However, Corbella & Stretch (2012a) note that the geotextile sandbags have proven to be successful in Durban, South Africa, and Australia. Since the bags are placed at a slope to achieve maximum benefit, Corbella & Stretch (2012a: 62) demonstrate that “in order for the bags to be stable the frictional force must be equal to or greater than the active soil force behind the bags.” (Fig. 5.14). Some of the advantages of the geotextile sandbags include its cost effectiveness, ability to be applied in emergency situations, and it can be easily cut and removed if required (Corbella & Stretch, 2012a).

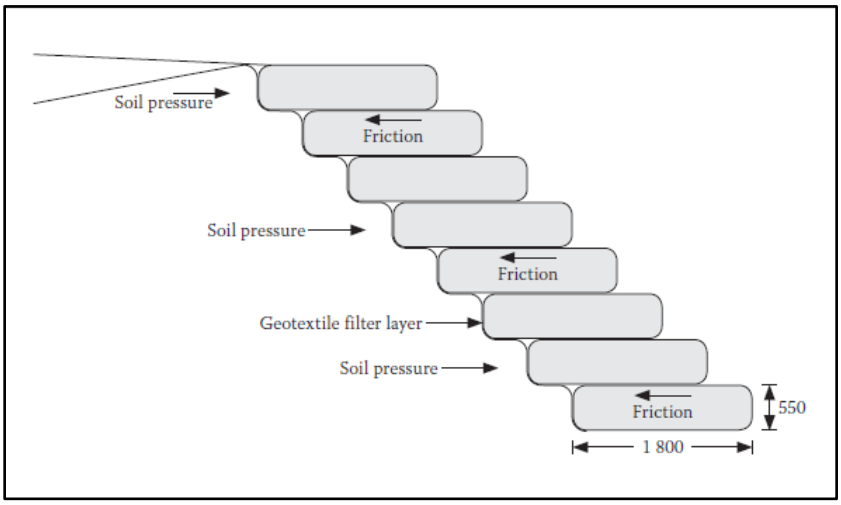

Figure 5.14: A demonstration of bag placement for maximum benefit (Corbella & Stretch, 2012a).

Rock revetments have also been successfully installed in Durban (Corbella & Stretch, 2012a). These structures were installed in the study area in 2024 and its success it yet to be documented (Fig 5.13).

5.8.4 Addition of breakwater dolosse towards the northern beaches

Since breakwaters typically result in an eroding beach downdrift of the structure, a series of groynes acting together as a system will produce a domino effect leading to a stabilised beach (Pranzini & Margeta, 2022). This approach is proposed to be most effective when conducted together with a sand bypassing scheme (Fig. 5.15).

Figure 5.15: A series of breakwaters in Croatia (Pranzini & Margeta, 2022).

5.8.5 Retreat

Retreat can be seen an adaptation strategy where it consists of the relocation of existing structures to less vulnerable areas (Corbella & Stretch, 2012a). In the study area, the process is already taking place, with the relocation of the Richards Bay Lighthouse in 2018 due to its location being 5 m away from the current sea cliff edge where it once stood 200 m away when it was constructed in 1979 (Zululand Observer, 2017).

In order to remain adaptable and sustainable, coastal areas facing challenges with erosion, flooding and the impacts of climate change need robust coastal protection strategies that will yield positive and enduring results. While an eroding shoreline cannot be stopped completely, studies have found that a combination of hard and soft engineering solutions are most effective in reducing the severity (Morton & Miller, 2005; Corbella & Stetch, 2012a; Singhvi et al., 2022).

Sea walls and dikes are not proposed as viable mitigation measures for the shoreline protection in the study area as most of the eroding sections of the shoreline do not have enough beach width to implement these strategies. In addition, Morton & Miller (2005) found that engineering structures like these will have little effect on an eroding beach due to the beach width being further reduced and it also prevents dunes from growing.

The results of this study indicate that dune construction/stabilization will also not be a viable mitigation measure to propose as the current rate of erosion and wave overtopping indicates that sand building will be washed away with the next storm surge. It is, however, possible that dune stabilization can occur once other strategies prove successful in increasing the beach width leaving enough room for dunes to stabilize and grow.

Chapter 6: Conclusion

It can be simply stated that the coast will erode and eventually the shoreline will recede, but we need to know the quantity of the eroded volume and the range of expected recession to prepare a sustainable solution for coastal risk reduction. The study found that large-scale erosion is taking place north of the harbour due to disruption of the longshore sediment pattern (Shoonees & Theron, 2002; Wells, 2015; Simmonis, 2016), lack of sediment supply (Breetzke, 2016; Esterhuizen, 2019), and severe weather events (Smith et al., 2010).

Coastal dunes act as a natural barrier against storm surges and coastal inundation. They play a key role in stabilising the coast, acting as an essential sediment reserve for beaches (Flor-Blanco et al., 2021). Rising sea levels induced by climate change and uncertaintly over increased storminess necessitates the need for beach and dune erosion to be actively monitored.

6.1 Summary

The purpose of this research was to monitor historical shoreline changes along the coastline of Richards Bay and to predict its future position using remote sensing and GIS technologies. The DSAS software was utilized to calculate the shoreline change rate statistics over a period of 45 years (1977-2022). This data was used to predict its position 10 and 20 years into the future using the ELR statistical method. In response to the increase in frequency and intensity of storm surges in recent years, a storm surge indundation screening exercise was conducted that modellled the flow paths of water when experiencing surge levels of 7, 8, 9 and 10 m. The results are expected to aid in disaster risk planning and management in the coastal zone.

Eight (8) shorelines from different years ranging between 1977 and 2022 were analysed by the DSAS software using a 95% Confidence Interval (CI) and computing the statistical methods of End Point Rate (EPR), Linear Regression Rate (LRR), and Weighted Linear Regression (WLR). In addition, two distance measurements, Net Shoreline Movement (NSM) and Shoreline Change Envelope (SCE) were computed by the DSAS. The shoreline change rate statistics and distance measurements provide an indication of the evolution of the shoreline in the study area which is vital information to inform decisions around coastal zone management and planning, assessing vulnerability, and disaster risk management.

Four (4) shorelines/beaches within the study area were chosen and analysed separately and the results were as follows:

- For the LRR, the average erosion rates for uMhlathuze Estuary, South Dunes, Alkanstrand, and Alkanstrand North were 0.1, 3.3, 3.3, and 2.3 m, respectively, while average accretion rates were recorded for uMhlathuze Estuary (2.33 m) and South Dunes (1.32 m).
- The WLR for the assessed sections varied slightly to the LRR due to the inclusion of the uncertainty values considered in the calcuations.
- The EPR, which is calculated by dividing the distance of shoreline movement by the time elapsed between the oldest and newest shoreline, reported average erosion rates of 0.04, 5.2, 3.7 and 2.2 m for uMhlathuze Estuary, South Dunes, Alkanstrand, and Alkanstrand North, respectively, while average accretion rates of 2.1 m were recorded for both uMhlathuze Estuary and South Dunes.
- The NSM calculated an average shoreline movement of +93.1, +98.9, -167.8, and -98.2 m for uMhlathuze Estuary, South Dunes, Alkanstrand, and Alkanstrand North beaches respectively. Negative figures denote erosion and positive figures denote accretion.
- The SCE, which calculates the distance between the most landward and most seaward shorelines, revealed an average distance of 136.9, 193.1, 169.7, and 123.9 m for uMhlathuze Estuary, South Dunes, Alkanstrand, and Alkanstrand North, respectively.

The results of the DSAS analysis was used to predict future shoreline positions 10 and 20 years into the future, i.e. 2032 and 2042 using the Extrapolated Linear Regression (ELR) method and the formula given by Farris.et al (2023). The data from the LRR was utlised to calculate the LRR. Based on the linear trend of the data, uMhlathuze Estuary and South Dunes shows consistent accretion, while Alkanstrand and Alkanstrand North shows consistent erosion. The storm surge analysis utilized four (4) different levels of storm surges (7, 8, 9, and 10m) to determine the potential impact of storm surges in the study area using models in ArcGIS Pro.

The main discussion points on the shoreline change rates, shoreline forecasting, and storm surge analysis reveal the following:

- The 45-year analysis indicates that beaches south of the harbour experienced net accretion while the beaches north of the harbour experienced net erosion.
- Erosion rates are much higher than the accretion rates.

- Through a literature review it was determined that the trend of erosion towards the north and accretion towards the south is linked to the disruption of the longshore sediment transport pattern owing to the construction of the port breakwaters.
- Other notable contributing factors leading to coastal erosion in the study area include the impacts of climate change leading to an increase in frequency and intensity of storm surges as well as seal-level rise, as well as sand mining and river impoundment in the hinterland which limit the delivery of sediment to the ocean.
- The findings of the shoreline forecasting reveal that for the year 2032 the shoreline will erode a further 10% for Alkanstrand North, and 21% for Alkanstrand while for uMhlathuze Estuary and South Dunes it will accrete at a rate of 2% and 0.6% from the 2022 position.
- For the year 2042, the shoreline will erode a further 23% for Alkanstrand North, and 36% for Alkanstrand while for uMhlathuze Estuary and South Dunes will accrete at a rate of 4% and 1.7% respectively from the 2022 positon.
- The storm surge analysis concluded that the study area is minimally affected when experiencing a surge level of 7 and 8 m (5.2% and 17% expansion of water area, respectively), however when experiencing a surge level of 9 and 10 m, a significant portion of the study area will be inundated (60% and 82% expansion of water area, respectively).
- These findings serve as a vital source of information for flood risk analysis, disaster management, and the designing of flood protection infrastructure in the study area.
- Evidence suggests that the likelihood of a 9 and 10 m storm surge is increased due to the onset of climate change.
- Unmanaged coastal erosion can lead to the loss of habitat, destruction of environmentally sensitive sand dunes and increase vulnerability to storm surges and flooding.

Recommendations were proposed to help mitigate against coastal erosion in the study area. These site-specific strategies are based on the results of the study and geomorphological features of the landscape. Although the problem of erosion cannot be stopped completely, it can be significantly reduced by the implementation of the proposed mitigation measures. It can be simply stated that the coast will erode and consequently the shoreline will recede, but we need to know what the eroded volume will be, and the range of expected recession to inform our decisions around different coastal protection interventions, planning for future, mitigation and adaptation.

6.2 Recommendations for future research

In order to execute the recommendation proposed in section 5.8.4 which requires the addition of breakwater dolosse in a sequential pattern, more detailed studies need to be conducted pertaining to the modelling of sediment transport patterns in the study area to consider the new arrangement. Studies on natural beach fluctuations in terms of local geomorphological processes and ecological functioning and the effects of additional breakwaters on the shorelines further north and south are also recommended.

The storm surge analysis could benefit from the use of a higher resolution digital elevation model that more accurately depicts the water flow paths during storm surges. Studies on the effects of storm surges in the study area are limited and therefore more studies are needed to build a stronger knowledge baseon the potential impacts and mitigation measures.

References

Aagaard, T. and Sorenson, P., 2012: Coastal profile response to sea-level rise: A process-based approach. *Earth Surface Processes and Landforms*, 37, 354-362.

Abd-Elhamid, H.F., Zelenakova, M., Baranczut, J., Gergelova, M.B. and Mahdy, M., 2023: Historical trend analysis and forecasting of shoreline change at the Nile Delta using RS data and GIS with the DSAS tool. *Remote Sensing*, 15(7), #1737.

Anderson, T.R., Fletcher, C.H., Barbee, M.M., Frazer, L.N. and Romine, B.M., 2015: Doubling of coastal erosion under rising sea level by mid-century in Hawaii. *Natural Hazards,* 28, 75-103.

Andrews, B., Gares, P.A. and Colby, J.D., 2002: Techniques for GIS modelling of coastal dunes. *Geomorphology*, 48, 289-308.

Angnuureng, B.B., Adade, R., Chuk, E.O., Dzanter, S., Brempong, E.K., Agbeko, P., and Mattah, D., 2023: Effects of coastal protection structures in controlling erosion and livelihoods. *Heliyon*, 9(2023), #20633.

Apostolopoulos, D.N., Auramidis, P. and Nikolakpoloulas, K., 2022: Estimating quantitative morphometric parameters and spatio-temporal evolution of the Prokos Lagoon using remote sensing techniques, *Journal of Marine Science and Engineering,* 10(7), #931.

ArcGIS Tutorial, 2024: Georeferencing historical aerial imagery in ArcGIS Pro. Available from: Georeference historical imagery in ArcGIS Pro | Documentation [Accessed 01 Nov 2024]

Baig, M.R.I., Ahmad, I.A., Shahfahad, Tayyab, M. and Rahman, A., 2020: Analysis of shoreline changes in Vishakhapatnum coastal tract of Andhra Pradesh, India: An application of Digital Shoreline Analysis System (DSAS). *Annals of GIS*, 26(4), 361-376.

Balstrom, T. and Kirby, J., 2022: A GIS-based screening workflow for coastal storm surge impact assessments and mitigation action consideration. *Journal of Coastal Research*, 38(4), 712-724.

Barbaro, G., Foti, G.C. and Frega, F., 2022: Beach and dune erosion: Causes and interventions, case study: Kaulon archaeological site. *Journal of Marine Science and Engineering*, 10(14), 1-20.

Bhardwaj, R.K., 2009: Application of GIS technology for coastal zone management: A hydrographer's perspective, A Geospatial World. Available from: Application of GIS technology for Coastal Zone Management: A hydrographer perspective - Geospatial World [Accessed 20 July 2023]

Bheeroo, R.A., Chandrasekar, N., Kaliraj, S., and Mayesh, N.S., 2016: Shoreline change rate and erosion risk assessment along the Trou Aux Biches-Mont Choisy Beach on the northwest coast of Mauritius using GIS-DSAS technique. *Environmental Earth Sciences,* 75, #444.

Bird, E.C.F., 1985: Coastal changes: A global review. John Wiley & Sons, Chichester. ISBN 0-471-90646-8

Boppape, M.M., Keebine, G., Ndarana, T., Mbokodo, I.L., Hlahane, K., Motshegwa, T., Amha, Y., Ogega, O.M., Mfopa, C., Mahlobo, D.D., Engelbrecht, F.A., and Chikoore, H., 2025: Weather related disasters in South Africa from 1980 to 2023. *Environmental Development*, 56, #101254.

Bosman, C., Uken, R., Leuci, R., Smith, A. M., and Sinclair, D., 2007: Shelf sediments off the Thukela

River mouth: Complex interaction between fluvial and oceanographic processes. *South African Journal Science*, 103, 490-492.

Bozzeda, F., Ortega, L., Coasta, L.L., Fanini, L; Barboza, C.A.M., McLachlan, A., and Omar, D., 2023: Global patterns in sandy beach erosion: unravelling the roles of anthropogenic, climatic and morphodynamic factors. *Frontiers in Marine Science*, 10, #1270490.

Breetzke, T., Meyer, C., Clark, B., Rees, A., and Bovim, L., 2022: Gas to power project: Coastal and marine impact assessment report for the port of Richards Bay. Report prepared for Triplo4 Sustainable Solutions (Pty) Ltd. KwaZulu-Natal.

Breetzke, T., Moore, L., and Celliers, L., 2016: Environmental Outlook: A report on the state of the environment chapter 9. *Department of Environment, Forestry and Fisheries*. Pretoria

Bruun, P., 1954: Coast erosion and the development of beach profiles, *Beach Erosion Board Technical Memorandum 44 US Army Corps of Engineers*, Washington DC, 79 pp.

Bruun, P., 1962: Sea level rise as a cause of shore erosion. *Journal of Waterways and Harbors Division, ASCE 88*, 117–130.

Bruun, P., 1988: The Bruun Rule of erosion by sea level rise: A discussion on large-scale two- and three-dimensional usages. *Journal of Coastal Research*, 4, 627–648.

Calkoen, F., Luijendijk, A., Rivero, C.R., Kras, E. and Baart, F., 2021: Traditional vs. machine-learning methods for forecasting sandy shoreline evolution using historic satellite-derived shorelines. *Remote Sensing,* 13, #934.

Camelo, J., Mayo, T.L., and Gutmann, E.D., 2020: Projected climate change impacts on hurricane storm surge inundation in the coastal Unites States. *Frontiers in Built Environment,* 6, #588049.

Carter, R.W.G. and Woodroffe, C.D., 1997: *Coastal evolution: An introduction*. Cambridge University Press, London.

Ciritci, D. and Turk, T., 2020: Assessment of Kalman Filter-based future shoreline prediction method. *International Journal of Environmental Science and Technology,* 17, 3801-3816.

Cooper, J.A.G. and Pilkey, O.H., 2004: Sea-level rise and shoreline retreat: Time to abandon the Bruun Rule. *Global and Planetary Change*, 43, 157-171.

Cooper. J.A.G., 1991: Shoreline changes on the Natal coast: Tugela River mouth to Cape St. Lucia. *Natal Town and Regional Planning Commission Report 76,* Pietermaritzburg,

Cooper, A. and Smith, A., 2014: Geology and geomorphology, Ugu Lwethu – Our coast – A profile of coastal KwaZulu-Natal. KwaZulu-Natal Department of Agriculture and Environmental Affairs and the Oceanographic Research Institute, Cedara, 17-19.

Corbella, S. and Stretch, D.D., 2012(a): Predicting coastal erosion using non-stationary statistics and process-based models. *Coastal Engineering*, 70, 40-49.

Corbella, S. and Stretch, D.D., 2012(b): Decadal trends in beach morphology on the east coast of South Africa and likely causative factors. *Natural Hazards and Earth System Science*, 12, 2515-2527.

D'Alessandro, F., Tomasicchio, G.R., Frega, F., Leone, E., Francone, A., Pantusa, D., Barbaro, G., and Foti, G., 2022: Beach-dune system morphodynamics. *Journal of Marine Science and Engineering*, 10, 1-14.

Day, J.H., 1980: What is an estuary? *South African Journal of Science*, 76, 198.

Dean, R.G. and Houston, J.R., 2016: Determining shoreline response to sea-level rise. *Coastal Engineering*, 114, 1-8.

Department of Forestry Fisheries and the Environment (DFFE): Oceans and Coasts, 2019: *Draft Umhlathuze/Richards Bay Estuarine Management Plan*. Cape Town.

Department of Forestry Fisheries and the Environment (DFFE): Operation Phakisa, 2020: Six year review (2014-2020).

De Waal, L., Schoonees, K., van Tonder, A., Hurt, G., and Antoni, M., 2007: Effect of borrow pit dredging on shoreline stability at Richards Bay. *Civil Engineering: Magazine of the South African Institution of Civil Engineering,* 15 (5), 59-60.

Dissanayake, P., Brown, J., Wisse, P., and Karunarathna, H., 2015: Comparison of storm cluster vs isolated event impacts on beach/dune morphodynamics. *Estuarine, Coastal and Shelf Science,* 165, 301-312.

Dladla, N.N., Green, A.N., Cooper, J.AG., Mehlhorn, P., and Haberzettl, T., 2021: Bayhead delta evolution in the context of late Quaternary and Holocene sea-level change, Richards Bay, South Africa. *Marine Geology,* 441, #106608.

Du Pont, S.C., 2015: Dune morphodynamics. *Competus Rendus Physique*, 16, 118-138.

Elliot, M., Mander, L., Mazik, K., Simenstad C., Valenski, F., Whitfield, A., and Wolanski, E., 2016: Ecoengineering with ecohydrology: Successes and failures in estuarine restoration.

Enrique, A.R., Marcos, M., Falques, A. and Roelvink, D., 2019: Assessing beach and dune erosion and vulnerability under sea level rise: A case study in the Mediterranean Sea. *Frontiers in Marine Science*, 6(4), 1-12.

Esterhuizen, J., 2019: Coastline dynamics at Thukela Mouth and the Amatigulu and Umlalazi River estuary areas. Unpublished Masters Dissertation. University of Pretoria, South Africa.

Fadillah, L.N., Widyastuti, M., Sunarto, and Marafai, M.A., 2020: Comparison of tidal model using Mike21 and delft3d-flow in parts of Java Sea, Indonesia. *IOP Confererence Series: Earth and Environmental Science,* 451, #012067.

Farris, A.S., Long, J.W., and Himmelstoss, E.A: 2023: Accuracy of shoreline forecasting using sparse data. *Ocean & Coastal Management*, 239(2023), #106621.

Ferreira, T.A.B., da Silva, A.G.A., Perez, Y.A.R., Stattegger, K., and Vital, H., 2021: Evaluation of decadal shoreline changes along the Parnaiba Delta (NE Brazil) using satellite image and statistical methods. *Ocean & Coastal Management,* 202, #105513.

Fitchett, J.M., Grant, B. and Hoogendoorn, G., 2016: Climate change threats to two low-lying South African coastal towns: Risks and perceptions, *South African Journal of Science*, 112(5-6), #2015-0262.

Flor-Blanco, G., Alcantara-Carrio, J., Jackson, D.W.T., Flor, G., and Flores-Soriano, C., 2021: Coastal erosion in NW Spain: Recent patterns under extreme storm wave events. *Geomorphology,* 387, #107767.

Forbes, A.T., Forbes, N.T., and Bundy, S., 2013: Baseline assessment for the port expansion programme. Report by Marine & Estuarine Research, #7/2013. KwaZulu-Natal.

Gao, J., Kennedy, D.M. and Konlechner, T.M., 2020: Coastal dune mobility over the past century: A global review. *Progress in Physical Geography*, 44(6), 814-836.

GESAMP., 1994: Anthropogenic influences on sediment discharge on the coastal zone and environmental consequences. Joint Group of Experts on the Scientific Aspects of Marine Environmental Protection (GESAMP). GESAMP reports and studies No.52. UNESCO.

Goble, B.J. and MacKay C, F., 2013: Developing risk set-back lines for coastal protection using shoreline change and climate variables. *Journal of Coastal Research*, Special Issue 65(10065), 2125–2130.

Goble, B.J. and Oellermann, L.K., 2022: Coastal Dune Mining: State of the Coast: KwaZulu-Natal - A review of the state of KwaZulu-Natal's coastal zone. KwaZulu-Natal Department of Economic Development, Tourism and Environmental Affairs, Pietermaritzburg.

Grottoli, E., Biausque, M., Jackson, D.W.T., and Cooper, A., 2023: Long term drivers of shoreline change over two centuries on a headland-embayment beach. *Earth Surface Processes and Landforms*, 48 (14), 2500-2520.

Hashmi, S.G.M.D. and Ahmed, S.R., 2018: GIS-based analysis and modelling of coastline erosion and accretion along the coast of Sindh Pakistan. *Journal of Coastal Zone Management*, 21(1), 1-7.

Hellemaa, P., 1999: The Development of Coastal Dunes and their Vegetation in Finland, Unpublished Masters Dissertation, University of Helsinki, Finland.

Heritage, G.L. and van Niekerk, A.W., 1995: Drought conditions and sediment transport in the Sabie River. *Koedoe: African Protected Area Conservation and Science*, 38(2), 1-9.

Himmelstoss, E.A., Henderson, R.E., Kratzmann., and Farris, A.S., 2021: Digital Shoreline Analysis System version 5.1 user guide. *U.S Geological Survey software release*.

Hinkel, J., Nicholls, R.J., Tol, R.S.J., Wang, Z.B., Hamilton, J.M., and Boot, G., 2013: A global analysis of erosion of sandy beaches and sea-level rise: An application of DIVA. *Global and Planetary Change*, 111, 150-158.

Hird, S., Stokes, C., and Masselink, G., 2021: Emergent coastal behaviour results in extreme duen erosion decoupled from hydrodynamic forcing. *Marine Geology,* 444, #106667.

Hobday, D.K. and Orme, A.R., 1974: The Port Dunford Formation: A major Pleistocene barrier-lagoon complex along the Zululand coast. *Transaction of the Geological Society of South Africa*, 17, 141-149.

Hossain, S.K.A., Mondal, I., Thakur, S., Linh, N.T.T., and Anh, D.T., 2022: Assessing the multi-decadal shoreline dynamics along the Purba Medinipur-Balasore coastal stretch, India by integrating remote sensing and statistical methods. *Acta Geophysica,* 70, 1701-1715.

Hossen, F, Md. and Sultana, N., 2023: Shoreline change detection using DSAS technique: Case of Saint Martin Island, Bangladesh. *Remote Sensing Applications: Society and Environment, 30, #100943.*

Hugo, P. and Luger, S., 2019: Numerical modelling to understand the causes of the beach erosion at Big Bay, Bloubergstrand. Civil *Engineering*, 27(4), 41-46.

Isha, I.B. and Adib, M.R.M., 2020: Application of Geospatial Information System (GIS) using Digital Shoreline Analysis System (DSAS) in determining shoreline changes. *IOP Conference Series: Earth and Environmental Science*, #616.

Islam, M.S. and Crawford, T.W., 2022: Assessment of spatio-temporal empirical forecasting performance of future shoreline positions. *Remote Sensing,* 14(24), #6364.

Jackson, D.W.T., Cooper, J.A.G. and Green, A.N., 2014: A preliminary classification of coastal sand dunes of the KwaZulu-Natal coast. *Journal of Coastal Research*, Special Issue 70(10070), 718-722.

Kelbe, B., 2010: Hydrology and water resources of the Richards Bay EMF area. Report by Hydrological Research & Training cc. Mtunzini. South Africa.

Jonkman, S.N., Hillen, M., Nicholls, R., and Ledden, M., 2013: Costs of adapting coastal defences to sea level rise – New estimates and their implications. *Journal of Coastal Research*, 290, 1212-1226.

Kilar, H., 2022: Shoreline change assessment using DSAS technique: A case study of the coast of Meric Delta, NW Turkiye. *Regional Studies in Marine Science*, 57, #102737.

Kim, J., Muphy, E., Nistor, I., Ferguson, S., and Provan, M., 2021: Numerical analysis of storm surges on Canada's western Arctic coastline. *Journal of Marine Science and Engineering*, 9, #326.

King Cetshwayo District Municipality Integrated Development Plan 2023/2023 – 2026/2027. Richards Bay. South Africa.

Knight, J. and Burningham., 2019: Sand dunes and ventifacts on the coast of South Africa. *Aeolian Research*, 39, 44-58.

Knight, J., 2023: Nature-based solutions for coastal resilience in South Africa. *South African Geographic Journal*, 106(1), 21-50.

Kwa-Zulu Natal Department of Economic Development, Tourism, and Environmental Affairs (KZN EDTEA), 2023: Draft KwaZulu-Natal Coastal Management Programme (2023-2028). Pietermaritzburg.

Kwa-Zulu Natal Department of Economic Development, Tourism, and Environmental Affairs (KZN EDTEA)., 2017: KwaZulu-Natal Coastal Management Programme. KZNEDTEA, Pietermaritzburg.

Leuci, R., Wiles, E., Thackery, Z., and Veila, G: 2022: Trends in sandy beach variability Ethekwini Municipality South Africa. *Journal of Sea Research*, 179 (2022), #102149.

Long, J.W. and Plant, N.G., 2012: Extended Kalman Filter Framework for forecasting shoreline evolution. *Geophysical Research Letters*, 39(13), #L13603.

Luck-Vogel, M., Le Roux, A., and Ludick, C: 2019: Green Book: The impact of climate changes on coastal zones, CSIR. Pretoria. Available from: https://pta-gis-2-web1.csir.co.za/portal2/apps/GBCascade/index.html?appid=167c6e4cdd784527b5291b642ed73531

Luijendijk, A., Hagenaars, G., Ranasinghe, R., Baart, F., Donchyts, G., and Aarninkhof, S., 2018: The state of the world's beaches. *Scientific Reports*, 8, #6641.

Ma, P. and Li, G., 2023: Comparison and analysis of detection methods for typhoon – storm surges based on tide gauge data – taking coasts of China as examples. *International Journal of Environmental Research and Public Health*, 451, #012067.

MacHutchon, M., 2015: Geophysical monitoring of coastal erosion and cliff retreat of Monwabisi Beach, False Bay, South Africa. *South African Journal of Geomatics*, 4(2), 80-95.

Mafi-Gholami, D., Baharlouii, M., and Mahmoudi, B., 2017: A review of shoreline change models for predicting coastal erosion and accretion. *Conference at the 4th International Conference on the Environmental Planning and Management*, Tehran: Iran.

Mather, A. and Stretch, D.D., 2012: A perspective on sea level rise and coastal storm surge from southern and eastern Africa: A case study near Durban, South Africa. *Water*, 4, 237-259.

Maselink, G., Russell, P., Rennie, A., Brook, S. and Spencer, T., 2020: Impacts of climate change on coastal geomorphology and coastal erosion relative to the coastal and marine environment around the UK. *MCCIP Science Review*, 2020, 258-189.

Maun, M.A., 2009: *The biology of coastal sand dunes*, Oxford University Press, United States of America.

McGwynne, L.E. De Ruyck, A.M.C., Kerley, G.I.H., and McLachlan, A., 1996: KwaZulu-Natal coastal dunes: Ecological dynamics, human impacts, and guidelines for planners. *Town and Regional Planning Supplement*, 43, 1-98.

Medina, Y.G.Z., Rocha, W.P., Armenta, S.A.M., and Ocha, C.F., 2023: Assessment and forecast of shoreline change using geospatial techniques in the Gulf of California. *Land,* 12, #782.

Mehlhorn, P., Viehberg, F., Kirsten, K., Newman, B., Frentzel, P., Gildeeva, O., Green, A., Hahn, A., and Torsten, H., 2021: Spatial distribution and consequences of contaminants in harbour sediments – A case study from Richards Bay Harbour, South Africa. *Marine Pollution Bulletin,* 172, #112764.

Meyer, R., Talma, A.S., Duvenhage, A.W.A., Eglington, B.M., Taljaard, J., and Botha, J.F., 2001: Geohydrological investigation and evaluation of the Zululand Coastal Aquifer. Report to the Water Research Commission. Available from: 221-1-01.pdf (wrc.org.za)

Mol, N., Smithen, C., van Huyssteen, M., Hale, T. and De Beer, E., 2013: Final scoping report: Richards Bay Mining: Zulti South project – EMP amendment, EIA, WULA, NNR certification and planning and development Act. *SRK Consulting,* Project No #439550.

Morton, R. A. and Miller, T. L., 2005: National assessment of shoreline change: Part 2: Historical shoreline changes and associated coastal land loss along the U.S. Southeast Atlantic Coast: U.S. *Geological Survey Open-file Report,* 2005-1401.

Murray, J., Adam, E., Woodborne, S., Miller, D., Xulu, S., and Evans, M., 2023: Monitoring shoreline changes along the southwestern coast of South Africa from 1937 to 2020 using varied remote sensing data and approaches. *Remote Sensing*, 15, #317

Mutaqin, B., 2017: Shoreline changes analysis in Kuwaru coastal area, Yogyakarta, Indonesia: An application of the digital shoreline analysis system. *International Journal of Sustainable Development Planning*, 12(7), 1203-1214.

Naicker, D. and Teurlings, P., 2014: Proposed Richards Bay Port expansion programme within the uMhlathuze local municipality in KwaZulu-Natal province – Draft Scoping Report. AECOM SA (Pty)Ltd project #14C00389.

Nassar, K., Mahmod, W.E., Fath, H., Masria, A., Nadaoka, K. and Negm, A., 2019: Shoreline change detection using DSAS technique: Case of north Sinai coast, Egypt. *Marine Georesources & Geotechnology,* 137(1), 81-95.

Nathaniel, P. and Baxter, B., 2025: Scoping and Environmental impact reporting process for the development of new berth 605 and associated infrastructure to support the CHF, Port of Richards Bay, KwaZulu-Natal. Project No #43102871.

O'Leary, B.C., Fonseca, C., Cornet, C.C., de Vries, M.B., Degia, A.K., Failler, P., Furlan, E., Garrabou, J., Gil, A., Hawkins, J.P., Krause-Jensen, D., LeRoux, X., Peck, M.A., Perez, G., Quieros, A.M., Rozynski, G., Sanchez-Archilla, A., Simide, R., Pinto. I.S., Tregaraot, E., and Roberts, C.M., 2023: Embracing nature-based solutions to promote resilient marine and coastal ecosystems. *Nature-Based Solutions*, 3(2023), #100044.

Oppenheimer, M., Glavovic, B.C., Hinkel, J., van de Wal, R., Magnan, A.K., Abd-Elgawad, A., Cai, R., Cifuentes-Jara, M., DeConto, R.M., Ghosh, T., Hay, J., Isla, F., Marzeion, B., Meyssignac, B.,, and Sebesvari, Z., 2019: Sea Level Rise and Implications for Low-Lying Islands, Coasts and Communities. *In: IPCC Special Report on the Ocean and Cryosphere in a Changing Climate.* Cambridge University Press, UK and New York, NY, USA, pp. 321-445.

Oyedotun, T.D., 2014: Shoreline geometry: DSAS as a tool for historical trend analysis. In: Geomorphological Techniques, Clarke, L. and Nield J.M. (eds), British Society for Geomorphology, London, 1-12.

Palalane, J; 2016: Processes of long-term coastal evolution and their mathematical modelling: Application to the Mozambique coast, Unpublished PhD thesis, Lund University, Sweden.

Pilkey, H. and Cooper, J.A.G., 2004: Society and sea level rise. *Science*, 303, 1781-2.

Pranzini, E. and Margeta, E.J., 2022: Groynes, breakwaters, artificial reefs, and jetties. Available from: https://adriadapt.eu/adaptation-options/groynes-breakwaters-artificial-reefs-and-jetties/

Pringle, W.J., Wirasaet, D., Roberts, K.J. and Westerink, J., 2021: Global storm tide modelling with ADCIRC v55: unstructured mesh design and performance. *Geoscientific Model Development*, 14, 1125-1145.

Rautenbach, C., Daniels, T., de Vos, M.A. and Barnes, M., 2020: A coupled wave, tide and storm surge operational forecasting system for South Africa: Validation and physical description. *Natural Hazards*, 103, 7-8.

Rezaie, A.M. and Haque, A., 2022: Development of storm surge inundation model and database for enhanced climate services in Bangladesh. *Frontiers in Water*, 4, #887631.

Roolason, V., Patterson, D. and Huxley, C., 2010: Assessing shoreline response to sea level rise: An alternative to the Bruun Rule. In *19th NSW Coastal Conference (pp 1-20).*

Rosati, J.D., Dean, R.G., and Walton, T.L., 2013: The modified Bruun Rule extended for landward transport. *U.S Army Research*, #219.

Saad, R., Gerard J.A. and Gerard, P., 2021: Detection of shoreline changes using DSAS technique and remote sensing: A case study of Tyre Southern Lebanon. *Journal of Oceanography and Marine Science*, 9(11), 1-18.

Schoonees, J.S. and Theron, A.K., 2002: Development of an accurate longshore sediment transport model. *Journal of the South African Institute of Civil Engineering*, 44(3), 12-17.

Schoonees, J.S., Theron, A.K., and Bevis, D., 2006: Shoreline accretion and sand transport at groynes inside the port of Richards Bay, *Coastal Engineering*, 53, 1045-1058.

Sebastian, A., Proft, J., Dietrich, J.C., Du, W., Bedient, P.B. and Dawson, C.N., 2014: Characterizing hurricane storm surge behavior in Galveston Bay using the SWAN + ADCIRC model. *Coastal Engineering,* 88, 171-181.

Simmonis, J, 2016: Contributing factors driving beach erosion, Zululand Observer, Richards Bay. Available from: Contributing factors driving beach erosion | Zululand Observer (citizen.co.za)

Singhvi, A., Luijendijk, A.P., van Oudenhoven, A.P.E., 2022: The grey-green spectrum: A review of coastal protection interventions. *Journal of Environmental Management,* 311, #114824.

Smith, A., Bundy, S.C. and Cooper, A., 2016: Apparent dynamic stability of the southeast African coast despite sea level rise. *Earth Surfaces Processes and Landforms*, 41(11), 1494-1503.

Smith, A.M., Guastella, L.A., Botes, Z.A., Bundy, S.C. and Mather, A.A., 2014: Forecasting cyclic erosion on a multi-annual to multi-decadal scale: Southeast African coast. *Estuarine, Coastal and Shelf Science*, 150(Part A), 86-91.

Smith, A.M., Mather, A.A., Bundy, S.C., Cooper, J.A.G., Guastela, L.A., Ramsay, P.J. and Theron, H., 2010: Contrasting styles of well-driven coastal erosion: examples from KwaZulu-Natal, South Africa. *Geological Magazine*, 147(6), 940-953.

Smith, A., Guastella, L.A., Bundy, S.C. and Mather A.A., 2007: Combined marine storm and Saros spring high tide erosion events along the KwaZulu-Natal coast in March 2007. *Journal of Science*, 103, 274-277.

Tadesse, M., Wahl, T. and Cid, A., 2020: Data-driven modelling of global storm surges. *Frontiers in Marine Science*, 7, #260.

Taylor, R., Kelbe, B., Haldorsen, S., Botha, G., Wejden, B., Vaeret, L., and Simonsen, M., 2006: Groundwater dependent ecology of the shoreline of the subtropical Lake St Lucia estuary. *Environmental Geology*, 49, 588-600.

Tinley, K.L., 1985: Coastal dunes of South Africa. *South African National Scientific Program Report*, 109, 1-297.

Toledo, I., Pagan J.I., Aragones, L., and Crespo, M.B., 2024: Doing nothing is no solution: Coastal erosion management in Guardamar del Segura (Spain). *Marine Policy*, 169(2024), #106340.

Transnet National Port Authority, No Date: Company Brochure. Available from : https://www.transnetnationalportsauthority.net/OurPorts/RichardsBay/Documents/Richards%20Bay%20Port%20Brochure.pdf

Transnet National Ports Authority, 2022: Port Development Framework Plans Update, Cape Town.

Transnet National Ports Authority, 2019: Media release: unique port sand bypass system mimics nature successfully. Available from: https://www.transnetnationalportsauthority.net/Corporate%20Affairs/Press%20Releases/Sand%20bypass%2015-4-2019.pdf

Tsai, Y., 2022: Monitoring 23-years of shoreline changes of the Zengwun Estuary in Southern Taiwan using time-series Landsat data and edge detection techniques. *Science of the Total Environment*, 839, #156310.

Umhlathuze local Municipality, 2024: 5th generation: Spatial Development Framework 2022/2023 – 2026/2027.

United Nations., 2017: Percentage of total population living in coastal areas. Available from: www.un.org

USGS., 2024: Digital Shoreline Analysis System. Available from: https://www.usgs.gov/centers/whcmsc/science/digital-shoreline-analysis-system-dsas

van Rijn, L.C., 2014: A simple general expression for longshore transport of sand, gravel, and shingle. *Coastal Engineering*, 90, 23-29.

Wahl, J.L., 2016: Evaluation of storm surge components at Saldanha Bay. Unpublished Masters dissertation. University of Stellenbosch, South Africa.

Ware, C.I., 2001: Evolution of the northern KwaZulu-Natal coastal dune cordon; evidence from the fine-grained sediment fraction, Unpublished Masters dissertation, University of KwaZulu-Natal, Durban, South Africa.

Weerts, S.P., 2002: Habitat utilization by juvenile fishes in uMhlathuze Estuary and Richards Bay Harbour, Unpublished Masters dissertation. University of Zululand, South Africa.

Wells, C.P., 2015: Modelling sand bypassing schemes on the Kwa-Zulu Natal coast, Unpublished Masters dissertation. University of Kwa-Zulu Natal, South Africa.

Woods Hole Sea Grant Program (WHSGP)., 2011: Longshore Sediment Transport. Cape Cod, Massachusetts, USA. Available from: https://seagrant.whoi.edu/wp-content/uploads/2015/02/LST_report_web.pdf

Wolf, T., Outten, S., Mangin, F., Chen, L. and Nilsen, J.E.O., 2023: Analysis of storm surge along the Norwegian coast. *Frontiers in Earth Science*, 11, #1037826.

Zamborn, J.A., 1989: The dolos breakwater block. *Landmarks in Water Engineering Practice*. *Die Siviele Ingenieur in Suid Afrika*, 31, 317-318.

Appendix 1:

Table of standardised field headings from DSAS

DSAS Statistics	Description
NSM	Net shoreline movement
SCE	Shoreline change envelope
EPR	End point rate
EPRunc	Uncertainty of the end point rate
LRR	Linear regression rate
LSE	Standard error of linear regression
LCI	Confidence interval of linear regression
LR2	*R*-squared of linear regression
WLR	Weighted linear regression
WSE	Standard error of linear regression
WCI	Confidence interval of weighted linear regression
WR2	*R*-squared of weighted linear regression

*Shaded entries are uncertainty and statistical parameters

Appendix 2:

Shoreline rates and statistics as calculated by DSAS for uMhlathuze Estuary for 123 transects cast.

OBJECTID	Trans Order	ShrCount	LRR	LR2	LCI	LSE	EPR	EPRunc	NSM	SCE	WLR	WR2	WCI	WSE	TCD	Shape_Length
1	5	8	-0.16	0.01	1.43	24.98	-0.06	0.23	-2.65	62.84	-0.66	0.13	1.75	4.26	200	371.7529815
2	6	8	-0.17	0.01	1.39	24.27	-0.02	0.23	-1.06	57.5	-0.67	0.14	1.65	4.01	250	367.7345739
3	7	8	-0.12	0.01	1.44	25.11	0.01	0.23	0.57	60.54	-0.67	0.14	1.63	3.96	300	371.1112306
4	8	8	-0.06	0	1.51	26.33	0.05	0.23	2.19	65.6	-0.57	0.1	1.68	4.08	350	376.526058
5	9	8	0.03	0	1.55	27	0.12	0.23	5.51	69.7	-0.47	0.07	1.74	4.24	400	381.0091836
6	10	8	0.1	0	1.61	28.11	0.17	0.23	7.51	73.82	-0.39	0.04	1.86	4.54	450	385.5235351
7	11	8	0.16	0.01	1.71	29.74	0.21	0.23	9.5	80.17	-0.37	0.03	1.98	4.83	500	391.0957646
8	12	8	0.17	0.01	1.76	30.69	0.28	0.23	12.68	81.26	-0.31	0.02	2.08	5.07	550	392.2802659
9	13	8	0.13	0.01	1.8	31.3	0.37	0.23	16.71	79.1	-0.31	0.02	2.15	5.23	600	391.6440142
10	14	8	0.16	0.01	1.81	31.57	0.42	0.23	19.12	78.87	-0.26	0.01	2.17	5.28	650	392.9482319
11	15	8	0.19	0.01	1.82	31.64	0.42	0.23	18.98	79.66	-0.27	0.02	2.13	5.19	700	395.278805
12	16	8	0.19	0.01	1.81	31.57	0.41	0.23	18.26	79.81	-0.27	0.02	2.17	5.3	750	396.9880094
13	17	8	0.18	0.01	1.78	30.96	0.36	0.23	16.09	80.33	-0.33	0.02	2.18	5.3	800	399.117731
14	18	8	0.2	0.01	1.78	31.06	0.38	0.23	17.15	81.34	-0.33	0.02	2.26	5.5	850	402.2689515
15	19	8	0.24	0.02	1.76	30.71	0.43	0.23	19.37	81.32	-0.26	0.01	2.26	5.5	900	406.1472341
16	20	8	0.29	0.03	1.72	29.91	0.45	0.23	20.29	81.45	-0.23	0.01	2.19	5.34	950	410.185151
17	21	8	0.29	0.03	1.71	29.88	0.47	0.23	21.3	81.77	-0.1	0	2.19	5.32	1000	412.9384164
18	22	8	0.35	0.04	1.72	30.02	0.53	0.23	23.96	83.93	-0.07	0	2.13	5.2	1050	417.2473589

OBJECTID	Trans Order	ShrCount	LRR	LR2	LCI	LSE	EPR	EPRunc	NSM	SCE	WLR	WR2	WCI	WSE	TCD	Shape_Length
19	23	8	0.38	0.05	1.74	30.31	0.59	0.23	26.49	84.95	-0.04	0	2.14	5.21	1100	420.4096149
20	24	8	0.35	0.04	1.75	30.42	0.62	0.23	27.84	83.07	0	0	2.15	5.25	1150	422.5067667
21	25	8	0.36	0.04	1.73	30.21	0.65	0.23	29.21	81.55	0.08	0	2.12	5.15	1200	426.195805
22	26	8	0.38	0.05	1.73	30.12	0.68	0.23	30.54	80.38	0.14	0	2.09	5.1	1250	430.2206745
23	27	8	0.41	0.05	1.76	30.74	0.69	0.23	31.01	82.23	0.24	0.01	2.11	5.15	1300	437.0915176
24	28	8	0.5	0.07	1.78	31.11	0.75	0.23	33.75	85.54	0.36	0.03	2.09	5.08	1350	444.372756
25	29	8	0.53	0.09	1.72	29.93	0.83	0.23	37.27	82	0.44	0.04	2.01	4.9	1400	444.1347946
26	30	8	0.45	0.07	1.69	29.54	0.77	0.23	34.46	78.71	0.46	0.05	2.06	5.03	1450	444.1712919
27	31	8	0.45	0.07	1.66	28.88	0.71	0.23	32.04	78.46	0.43	0.05	1.97	4.81	1500	445.5717033
28	32	8	0.47	0.07	1.64	28.57	0.69	0.23	31.09	77.66	0.47	0.05	1.97	4.8	1550	445.3373604
29	33	8	0.54	0.1	1.62	28.25	0.73	0.23	32.94	79.37	0.5	0.06	1.94	4.73	1600	447.4698796
30	34	8	0.65	0.13	1.66	28.96	0.79	0.23	35.77	84.44	0.63	0.09	2.01	4.89	1650	453.2180694
31	35	8	0.78	0.18	1.65	28.85	0.87	0.23	39.35	87.38	0.82	0.16	1.86	4.52	1700	460.8184455
32	36	8	0.73	0.17	1.62	28.21	0.89	0.23	40	87.18	0.85	0.19	1.77	4.3	1750	461.2447847
33	37	8	0.7	0.16	1.59	27.74	0.91	0.23	40.85	87.59	0.88	0.22	1.65	4.02	1800	462.3919651
34	38	8	0.69	0.15	1.64	28.65	0.93	0.23	41.75	92.12	0.93	0.25	1.62	3.93	1850	467.9975438
35	39	8	0.66	0.13	1.75	30.42	0.95	0.23	42.9	96.24	1.04	0.25	1.78	4.33	1900	473.2037115
36	40	8	0.72	0.14	1.74	30.3	0.99	0.23	44.38	95.37	1.14	0.27	1.86	4.53	1950	479.7534667
37	41	8	0.78	0.17	1.72	30.04	0.95	0.23	42.88	96.98	1.11	0.28	1.78	4.33	2000	488.7791804
38	42	8	0.84	0.19	1.7	29.63	0.92	0.23	41.3	96.4	1.13	0.28	1.8	4.37	2050	497.5941289

OBJECTID	Trans Order	ShrCount	LRR	LR2	LCI	LSE	EPR	EPRunc	NSM	SCE	WLR	WR2	WCI	WSE	TCD	Shape_Length
39	43	8	0.9	0.22	1.68	29.22	0.91	0.23	40.95	93.61	1.2	0.28	1.93	4.7	2100	506.0492112
40	44	8	0.95	0.25	1.64	28.65	0.9	0.23	40.67	88.77	1.26	0.27	2.09	5.08	2150	511.4483654
41	45	8	1.09	0.33	1.56	27.14	1.01	0.23	45.58	84.95	1.37	0.28	2.16	5.27	2200	516.2546477
42	46	8	1.23	0.4	1.51	26.24	1.19	0.23	53.38	85.69	1.46	0.33	2.1	5.11	2250	520.666405
43	47	8	1.29	0.43	1.49	26.03	1.31	0.23	58.97	83.79	1.53	0.35	2.06	5.03	2300	522.4712016
44	48	8	1.34	0.46	1.46	25.45	1.41	0.23	63.23	83.77	1.58	0.39	1.97	4.81	2350	523.5935512
45	49	8	1.37	0.49	1.39	24.31	1.48	0.23	66.51	82.52	1.6	0.41	1.91	4.65	2400	523.9422063
46	50	8	1.38	0.5	1.38	24.03	1.55	0.23	69.79	81.25	1.67	0.41	1.99	4.84	2450	524.3656348
47	51	8	1.42	0.52	1.35	23.47	1.61	0.23	72.55	81.99	1.72	0.44	1.96	4.77	2500	526.9629598
48	52	8	1.45	0.56	1.28	22.26	1.57	0.23	70.56	81.89	1.72	0.47	1.82	4.45	2550	529.4004481
49	53	8	1.47	0.59	1.21	21.13	1.52	0.23	68.55	81.05	1.7	0.49	1.72	4.19	2600	531.0743946
50	54	8	1.43	0.57	1.24	21.66	1.49	0.23	67.15	81	1.7	0.5	1.71	4.17	2650	532.2030161
51	55	8	1.46	0.57	1.28	22.34	1.56	0.23	70.22	84.08	1.78	0.55	1.6	3.91	2700	532.4381461
52	56	8	1.57	0.59	1.3	22.69	1.73	0.23	77.78	88.2	1.93	0.61	1.54	3.75	2750	533.715334
53	57	8	1.7	0.61	1.36	23.72	1.82	0.23	81.8	95.59	2.05	0.65	1.5	3.65	2800	541.1790135
54	58	8	1.77	0.62	1.4	24.36	1.88	0.23	84.45	99.22	2.13	0.66	1.53	3.73	2850	545.2120545
55	59	8	1.8	0.61	1.43	24.94	1.94	0.23	87.12	101.03	2.21	0.64	1.67	4.06	2900	546.5151369
56	60	8	1.9	0.63	1.47	25.55	2.01	0.23	90.26	106.17	2.31	0.63	1.77	4.31	2950	550.9732339

OBJECTID	Trans Order	ShrCount	LRR	LR2	LCI	LSE	EPR	EPRunc	NSM	SCE	WLR	WR2	WCI	WSE	TCD	Shape_Length
57	61	8	2.01	0.66	1.45	25.28	2.08	0.23	93.49	110.95	2.43	0.64	1.84	4.49	3000	555.0936598
58	62	8	2.09	0.69	1.4	24.43	2.1	0.23	94.5	113.16	2.48	0.63	1.91	4.65	3050	557.6598387
59	63	8	2.11	0.7	1.37	23.92	2.03	0.23	91.16	114.27	2.39	0.6	1.97	4.79	3100	560.411378
60	64	8	2.13	0.71	1.37	23.82	1.95	0.23	87.77	116.27	2.26	0.58	1.92	4.68	3150	563.3733304
61	65	8	2.14	0.71	1.35	23.6	1.93	0.23	86.91	116.11	2.14	0.56	1.9	4.64	3200	564.1704899
62	66	8	2.09	0.7	1.35	23.59	1.92	0.23	86.2	112.6	2	0.54	1.85	4.5	3250	561.6253768
63	67	8	2.04	0.67	1.44	25.04	1.93	0.23	86.84	110	1.91	0.52	1.82	4.44	3300	560.306092
64	68	8	2.05	0.67	1.42	24.8	1.96	0.23	88.28	108.65	1.9	0.49	1.93	4.71	3350	561.2588411
65	69	8	2.14	0.71	1.36	23.79	1.99	0.23	89.72	112.71	1.99	0.52	1.9	4.62	3400	567.6308139
66	70	8	2.22	0.75	1.3	22.63	1.99	0.23	89.74	117.28	2.13	0.57	1.86	4.53	3450	574.5158624
67	71	8	2.36	0.77	1.29	22.44	1.99	0.23	89.7	127.07	2.19	0.6	1.77	4.31	3500	581.8716006
68	72	8	2.45	0.78	1.29	22.56	2.03	0.23	91.33	133.31	2.31	0.62	1.8	4.38	3550	585.8955206
69	73	8	2.47	0.75	1.44	25.17	2.06	0.23	92.48	139.55	2.41	0.59	1.99	4.84	3600	591.7463975
70	74	8	2.53	0.72	1.56	27.17	2.08	0.23	93.52	144.58	2.38	0.58	2.01	4.9	3650	596.389964

OBJECTID	Trans Order	ShrCount	LRR	LR2	LCI	LSE	EPR	EPRunc	NSM	SCE	WLR	WR2	WCI	WSE	TCD	Shape_Length
71	75	8	2.62	0.73	1.61	28	2.14	0.23	96.14	147.99	2.42	0.59	2.02	4.91	3700	599.4395921
72	76	8	2.68	0.72	1.69	29.4	2.23	0.23	100.23	151.3	2.52	0.58	2.14	5.2	3750	602.5041332
73	77	8	2.79	0.71	1.78	31.04	2.34	0.23	105.4	156.98	2.65	0.58	2.24	5.45	3800	607.9733938
74	78	8	2.9	0.71	1.84	32.11	2.47	0.23	111.19	162.38	2.77	0.6	2.27	5.54	3850	613.1804709
75	79	8	3.04	0.73	1.86	32.36	2.6	0.23	116.98	166.86	2.91	0.63	2.24	5.47	3900	617.487251
76	80	8	3.03	0.73	1.83	31.97	2.62	0.23	117.86	166.36	2.91	0.61	2.34	5.7	3950	619.9522416
77	81	8	2.98	0.73	1.81	31.49	2.57	0.23	115.52	166.48	2.9	0.57	2.54	6.19	4000	623.0667883
78	82	8	2.98	0.74	1.78	30.97	2.51	0.23	113	167.46	2.88	0.55	2.59	6.31	4050	625.2191388
79	83	8	2.99	0.74	1.77	30.81	2.48	0.23	111.4	168.44	2.83	0.55	2.53	6.17	4100	626.5932385
80	84	8	3.02	0.74	1.8	31.3	2.53	0.23	114.03	170.36	2.89	0.56	2.56	6.23	4150	628.9249873
81	85	8	3.11	0.76	1.76	30.75	2.67	0.23	120.02	170.32	3.01	0.62	2.33	5.69	4200	631.6327555
82	86	8	3.15	0.75	1.81	31.46	2.8	0.23	126.01	170.16	3.13	0.64	2.35	5.73	4250	634.3561283
83	87	8	3.25	0.77	1.8	31.33	2.94	0.23	132.2	170.8	3.25	0.7	2.14	5.21	4300	637.9968971

OBJECTID	Trans Order	ShrCount	LRR	LR2	LCI	LSE	EPR	EPRunc	NSM	SCE	WLR	WR2	WCI	WSE	TCD	Shape_Length
84	88	8	3.37	0.78	1.79	31.17	3.06	0.23	137.91	171.54	3.34	0.76	1.88	4.59	4350	641.7943775
85	89	8	3.48	0.8	1.75	30.55	3.19	0.23	143.47	173.96	3.46	0.78	1.86	4.52	4400	645.4666873
86	90	8	3.62	0.82	1.69	29.42	3.3	0.23	148.62	179.1	3.59	0.8	1.8	4.39	4450	649.0659109
87	91	8	3.73	0.83	1.68	29.25	3.36	0.23	151.36	182.66	3.64	0.82	1.71	4.16	4500	652.967562
88	92	8	3.78	0.82	1.75	30.54	3.34	0.23	150.35	185.88	3.55	0.82	1.65	4.02	4550	657.0057133
89	93	8	3.84	0.82	1.82	31.64	3.31	0.23	148.87	190.03	3.44	0.81	1.67	4.07	4600	661.0535138
90	94	8	3.85	0.81	1.88	32.79	3.28	0.23	147.38	193.21	3.37	0.78	1.77	4.31	4650	663.0134575
91	95	8	3.87	0.79	1.98	34.59	3.28	0.23	147.41	196.2	3.33	0.76	1.87	4.55	4700	664.1293646
92	96	8	3.86	0.77	2.13	37.12	3.26	0.23	146.67	198.61	3.23	0.73	1.98	4.82	4750	664.6774198
93	97	8	3.85	0.77	2.11	36.82	3.24	0.23	145.93	196.36	3.14	0.7	2.05	5	4800	660.5726631
94	98	8	3.89	0.8	1.97	34.29	3.23	0.23	145.21	194.31	3.07	0.68	2.1	5.13	4850	656.477147
95	99	8	3.85	0.76	2.15	37.54	3.26	0.23	146.59	193.93	3.01	0.66	2.18	5.3	4900	653.9525478
96	100	8	3.88	0.75	2.27	39.51	3.31	0.23	148.77	194.29	2.99	0.66	2.16	5.25	4950	652.1212451

OBJECTID	Trans Order	ShrCount	LRR	LR2	LCI	LSE	EPR	EPRunc	NSM	SCE	WLR	WR2	WCI	WSE	TCD	Shape_Length
97	101	8	3.94	0.77	2.16	37.68	3.35	0.23	150.95	194.65	3.09	0.68	2.11	5.14	5000	650.2898279
98	102	8	4.05	0.79	2.08	36.33	3.41	0.23	153.58	195.69	3.14	0.7	2.04	4.97	5050	650.7788046
99	103	8	4.15	0.8	2.08	36.25	3.54	0.23	159.17	196.08	3.17	0.71	2.01	4.9	5100	652.0664842
100	104	8	4.17	0.8	2.1	36.55	3.58	0.23	160.89	196.45	3.18	0.71	2.05	4.98	5150	653.3541223
101	105	8	4.19	0.8	2.09	36.38	3.61	0.23	162.61	198.07	3.34	0.74	1.99	4.84	5200	655.8843997
102	106	8	4.2	0.8	2.1	36.57	3.65	0.23	164.07	200.85	3.49	0.75	1.99	4.84	5250	659.1536847
103	107	8	4.18	0.79	2.18	38.02	3.68	0.23	165.4	204.9	3.64	0.75	2.09	5.09	5300	662.3986569
104	108	8	4.2	0.79	2.19	38.15	3.7	0.23	166.65	208.19	3.81	0.75	2.2	5.36	5350	664.9188661
105	109	8	4.33	0.84	1.88	32.78	3.7	0.23	166.61	211.33	3.96	0.75	2.26	5.5	5400	667.2985301
106	110	8	4.45	0.85	1.9	33.15	3.73	0.23	168.05	213.94	3.99	0.73	2.41	5.87	5450	669.6889783
107	111	8	4.4	0.81	2.14	37.3	3.78	0.23	170.07	214.73	3.92	0.71	2.5	6.09	5500	672.0907666
108	112	8	4.45	0.78	2.36	41.16	3.82	0.23	172.1	215.92	3.87	0.67	2.68	6.53	5550	674.6271597
109	113	8	4.51	0.76	2.55	44.43	3.86	0.23	173.79	217.48	3.8	0.63	2.9	7.07	5600	675.7096992

OBJECTID	Trans Order	ShrCount	LRR	LR2	LCI	LSE	EPR	EPRunc	NSM	SCE	WLR	WR2	WCI	WSE	TCD	Shape_Length
110	114	8	4.43	0.73	2.68	46.69	3.89	0.23	174.86	214.25	3.66	0.64	2.74	6.67	5650	676.8040582
111	115	8	4.39	0.69	2.91	50.73	3.92	0.23	176.43	210.49	3.55	0.62	2.77	6.74	5700	677.90994
112	116	8	4.33	0.64	3.24	56.48	3.96	0.23	178.01	207.73	3.42	0.59	2.86	6.97	5750	678.6743069
113	117	8	4.25	0.59	3.56	62.13	3.99	0.23	179.49	223.26	3.3	0.55	2.97	7.24	5800	677.8236723
114	118	8	4.22	0.58	3.58	62.46	4.02	0.23	181.05	225.02	3.25	0.55	2.92	7.11	5850	678.5795725
115	119	8	4.27	0.6	3.48	60.58	4.06	0.23	182.48	221.01	3.2	0.54	2.93	7.14	5900	680.7064992
116	120	8	4.29	0.61	3.41	59.44	4.07	0.23	182.96	218.55	3.24	0.55	2.92	7.11	5950	681.8389797
117	121	8	4.29	0.62	3.36	58.53	4.08	0.23	183.46	216.1	3.36	0.57	2.93	7.13	6000	682.9713175
118	122	8	4.36	0.64	3.25	56.59	4.09	0.23	183.97	208.89	3.5	0.57	3.03	7.37	6050	684.1037279
119	123	8	4.45	0.66	3.16	55.06	4.07	0.23	183.26	210.41	3.63	0.57	3.18	7.74	6100	684.0131429
120	124	8	4.69	0.64	3.54	61.75	4.01	0.23	180.46	241.24	3.93	0.52	3.78	9.22	6150	698.0701186
121	125	8	4.94	0.62	3.87	67.52	3.95	0.23	177.69	268.75	4.14	0.5	4.15	10.11	6200	723.6730427
122	126	8	5.26	0.64	3.94	68.69	3.88	0.23	174.82	288.32	4.49	0.5	4.48	10.92	6250	749.8730173

OBJECTID	Trans Order	ShrCount	LRR	LR2	LCI	LSE	EPR	EPRunc	NSM	SCE	WLR	WR2	WCI	WSE	TCD	Shape_Length
123	127	8	5.46	0.62	4.24	73.82	3.83	0.23	172.48	302.33	4.86	0.49	4.91	11.96	6300	778.8185302

Shoreline rates and statistics as calculated by DSAS for South Dunes for 78 transects cast.

OBJECTID	TransOrder	ShrCount	LRR	LR2	LCI	LSE	EPR	EPRunc	NSM	SCE	WLR	WR2	WCI	WSE	TCD	Shape_Length
1	3	8	2	0.52	1.94	33.73	3.15	0.23	141.78	141.78	2.32	0.49	2.37	5.76	100	830.1807
2	4	8	1.89	0.55	1.71	29.77	2.94	0.23	132.09	132.09	2.21	0.53	2.07	5.04	150	822.9336
3	5	8	1.87	0.64	1.41	24.59	2.72	0.23	122.39	122.39	2.13	0.59	1.79	4.36	200	815.6685
4	6	8	1.72	0.71	1.09	18.92	2.36	0.23	106.02	106.02	1.95	0.68	1.34	3.26	250	801.7432
5	7	8	1.47	0.74	0.88	15.31	2.09	0.23	94.27	94.27	1.91	0.67	1.33	3.23	300	784.8589
6	8	8	1.3	0.71	0.83	14.5	1.97	0.23	88.61	88.61	1.91	0.62	1.51	3.67	350	773.4728
7	9	8	1.2	0.56	1.06	18.41	2.05	0.23	92.07	92.07	2.04	0.48	2.1	5.12	400	771.4943
8	10	8	1.16	0.47	1.24	21.6	2.06	0.23	92.55	92.55	2.22	0.43	2.55	6.22	450	769.6675
9	11	8	1.04	0.4	1.26	22.01	1.75	0.23	78.86	79.03	2.12	0.38	2.69	6.55	500	762.647
10	12	8	0.78	0.29	1.23	21.49	1.4	0.23	63.07	74.61	1.91	0.34	2.64	6.43	550	763.6792
11	13	8	0.39	0.1	1.19	20.78	1.06	0.23	47.58	70.24	1.49	0.26	2.52	6.14	600	764.4886
12	14	8	0.09	0.01	1.14	19.83	0.7	0.23	31.44	62.84	1.11	0.18	2.37	5.76	650	765.7736
13	15	8	0.01	0	0.98	17.15	0.45	0.23	20.09	45.48	0.97	0.21	1.88	4.59	700	752.3365
14	16	8	-0.07	0.01	0.98	17	0.27	0.23	12.04	46.52	0.92	0.21	1.81	4.41	750	754.0117
15	17	8	-0.44	0.13	1.14	19.82	-0.26	0.23	-11.76	58.28	0.68	0.1	2.02	4.92	800	755.8686

OBJECTID	TransOrder	ShrCount	LRR	LR2	LCI	LSE	EPR	EPRunc	NSM	SCE	WLR	WR2	WCI	WSE	TCD	Shape_Length
16	18	8	-0.78	0.26	1.33	23.25	-0.83	0.23	-37.26	80.7	0.39	0.03	2.15	5.24	850	756.4609
17	19	8	-1.15	0.35	1.58	27.54	-1.36	0.23	-61.34	99.98	0.02	0	2.21	5.38	900	753.9512
18	20	8	-1.55	0.37	2.04	35.58	-2.02	0.23	-90.91	127.54	-0.35	0.02	2.41	5.86	950	753.2148
19	21	8	-1.99	0.37	2.57	44.8	-2.73	0.23	-122.68	158.75	-0.63	0.05	2.85	6.95	1000	754.1909
20	22	8	-2.46	0.4	3	52.34	-3.46	0.23	-155.92	189.26	-0.99	0.09	3.19	7.77	1050	754.5911
21	23	8	-2.81	0.41	3.33	58.1	-4.08	0.23	-183.45	209.25	-1.36	0.15	3.25	7.91	1100	751.014
22	24	8	-3.1	0.43	3.59	62.61	-4.51	0.23	-202.92	226.35	-1.64	0.19	3.38	8.23	1150	751.6928
23	25	8	-3.43	0.44	3.84	66.85	-4.91	0.23	-221.09	245.36	-1.85	0.21	3.64	8.87	1200	754.336
24	26	8	-3.76	0.46	4.09	71.36	-5.29	0.23	-238.08	269.6	-2.04	0.21	3.98	9.68	1250	762.2617
25	27	8	-3.95	0.45	4.38	76.42	-5.61	0.23	-252.66	284.28	-2.12	0.2	4.24	10.33	1300	760.6851
26	28	8	-4.08	0.45	4.46	77.68	-5.81	0.23	-261.6	288.61	-2.34	0.24	4.17	10.15	1350	760.233

OBJECTID	TransOrder	ShrCount	LRR	LR2	LCI	LSE	EPR	EPRunc	NSM	SCE	WLR	WR2	WCI	WSE	TCD	Shape_Length
27	29	8	-4.21	0.47	4.49	78.24	-5.97	0.23	-268.7	295.1	-2.57	0.28	4.12	10.03	1400	765.5566
28	30	8	-4.26	0.47	4.53	79.04	-6.09	0.23	-273.94	294.18	-2.73	0.31	4.04	9.85	1450	763.4799
29	31	8	-4.26	0.46	4.65	81.07	-6.16	0.23	-277.18	301.15	-2.78	0.32	4.08	9.94	1500	767.5435
30	32	8	-4.31	0.44	4.81	83.89	-6.32	0.23	-284.43	310.41	-2.9	0.33	4.14	10.09	1550	770.9888
31	33	8	-4.3	0.43	4.95	86.36	-6.39	0.23	-287.4	314.17	-2.86	0.31	4.26	10.38	1600	769.1271
32	34	8	-4.25	0.41	5.11	89.14	-6.42	0.23	-289	313.43	-2.75	0.28	4.37	10.64	1650	762.8136
33	35	8	-4.19	0.39	5.25	91.46	-6.47	0.23	-290.99	318.22	-2.67	0.26	4.46	10.86	1700	762.0162
34	36	8	-4.21	0.38	5.36	93.43	-6.62	0.23	-297.99	323.63	-2.67	0.26	4.53	11.03	1750	761.2619
35	37	8	-4.28	0.38	5.45	95.01	-6.83	0.23	-307.17	329.18	-2.73	0.26	4.61	11.24	1800	759.8355
36	38	8	-4.36	0.38	5.55	96.68	-7.05	0.23	-317.41	334.55	-2.81	0.26	4.74	11.54	1850	758.2263

OBJECTID	TransOrder	ShrCount	LRR	LR2	LCI	LSE	EPR	EPRunc	NSM	SCE	WLR	WR2	WCI	WSE	TCD	Shape_Length
37	39	8	-4.41	0.37	5.72	99.68	-7.27	0.23	-327.28	340.9	-2.92	0.27	4.83	11.76	1900	757.5981
38	40	8	-4.54	0.38	5.82	101.49	-7.48	0.23	-336.69	348.97	-3.15	0.3	4.8	11.7	1950	758.6581
39	41	8	-4.71	0.39	5.85	101.94	-7.63	0.23	-343.53	357.96	-3.36	0.33	4.8	11.68	2000	760.0743
40	42	8	-4.84	0.4	5.89	102.66	-7.75	0.23	-348.84	363.06	-3.5	0.35	4.8	11.7	2050	757.5763
41	43	8	-4.8	0.41	5.77	100.65	-7.63	0.23	-343.34	360.68	-3.45	0.35	4.72	11.49	2100	757.7802
42	44	8	-4.73	0.41	5.62	97.97	-7.46	0.23	-335.56	355.23	-3.34	0.34	4.67	11.38	2150	758.483
43	45	8	-4.62	0.42	5.48	95.47	-7.31	0.23	-328.85	349.78	-3.26	0.34	4.53	11.03	2200	759.1876
44	46	8	-4.48	0.41	5.33	92.97	-7.16	0.23	-322.08	344.12	-3.27	0.36	4.37	10.64	2250	759.7375
45	47	8	-4.38	0.42	5.18	90.24	-7.01	0.23	-315.43	334.88	-3.26	0.37	4.24	10.34	2300	756.3718
46	48	8	-4.32	0.42	5.04	87.76	-6.89	0.23	-309.98	326.65	-3.24	0.38	4.18	10.17	2350	752.8778

OBJECTID	TransOrder	ShrCount	LRR	LR2	LCI	LSE	EPR	EPRunc	NSM	SCE	WLR	WR2	WCI	WSE	TCD	Shape_Length
47	49	8	-4.21	0.42	4.9	85.42	-6.72	0.23	-302.24	318.14	-3.2	0.38	4.11	10.02	2400	749.2547
48	50	8	-4.12	0.43	4.77	83.15	-6.54	0.23	-294.46	309.66	-3.17	0.37	4.13	10.07	2450	745.6573
49	51	8	-4.05	0.43	4.61	80.43	-6.39	0.23	-287.66	301.41	-3.1	0.37	4.05	9.86	2500	742.3322
50	52	8	-3.83	0.44	4.34	75.67	-6.05	0.23	-272.05	287.54	-2.9	0.36	3.86	9.41	2550	741.4012
51	53	8	-3.54	0.43	4.11	71.57	-5.66	0.23	-254.55	273.18	-2.68	0.34	3.73	9.09	2600	741.7857
52	54	8	-3.25	0.4	3.94	68.61	-5.27	0.23	-237.28	258.77	-2.46	0.3	3.75	9.13	2650	743.684
53	55	8	-2.97	0.38	3.76	65.47	-4.92	0.23	-221.49	244.32	-2.29	0.28	3.66	8.91	2700	745.6058
54	56	8	-2.72	0.37	3.55	61.81	-4.57	0.23	-205.66	229.82	-2.18	0.28	3.5	8.52	2750	747.5511
55	57	8	-2.32	0.35	3.13	54.51	-3.91	0.23	-175.73	199.21	-1.92	0.26	3.25	7.91	2800	744.9191
56	58	8	-1.95	0.35	2.65	46.26	-3.24	0.23	-145.8	168.89	-1.68	0.24	2.96	7.21	2850	742.2686

OBJECTID	TransOrder	ShrCount	LRR	LR2	LCI	LSE	EPR	EPRunc	NSM	SCE	WLR	WR2	WCI	WSE	TCD	Shape_Length
57	59	8	-1.59	0.36	2.14	37.26	-2.56	0.23	-115.17	138.54	-1.42	0.24	2.53	6.17	2900	739.6302
58	60	8	-1.22	0.35	1.66	28.89	-1.85	0.23	-83.28	107.63	-1.14	0.21	2.22	5.41	2950	736.9574
59	61	8	-0.89	0.33	1.26	21.96	-1.21	0.23	-54.65	76.6	-0.95	0.17	2.11	5.14	3000	734.2981
60	62	8	-0.55	0.22	1.03	17.95	-0.65	0.23	-29.1	56.45	-0.69	0.11	1.99	4.85	3050	732.2154
61	63	8	-0.22	0.04	1.03	18.01	0.05	0.23	2.03	55.57	-0.24	0.01	2.06	5.01	3100	731.6683
62	64	8	0.12	0.01	1.19	20.76	0.66	0.23	29.89	54.14	0.13	0	2.06	5.02	3150	732.5564
63	65	8	0.53	0.13	1.4	24.38	1.26	0.23	56.88	73.83	0.55	0.07	2.02	4.91	3200	755.1963
64	66	8	0.8	0.23	1.48	25.79	1.64	0.23	73.93	81	0.95	0.22	1.82	4.43	3250	769.55
65	67	8	1.03	0.33	1.48	25.74	1.92	0.23	86.38	86.38	1.37	0.46	1.5	3.66	3300	777.1878
66	68	8	1.23	0.38	1.56	27.23	2.15	0.23	96.95	96.95	1.63	0.53	1.54	3.76	3350	784.8475
67	69	8	1.31	0.38	1.67	29.05	2.33	0.23	105.04	105.04	1.75	0.53	1.63	3.97	3400	791.4174
68	70	8	1.36	0.4	1.67	29.06	2.38	0.23	106.9	106.9	1.78	0.58	1.52	3.71	3450	792.6404
69	71	8	1.39	0.41	1.68	29.23	2.41	0.23	108.5	108.5	1.82	0.62	1.43	3.48	3500	793.9086
70	72	8	1.49	0.45	1.65	28.73	2.55	0.23	114.66	114.66	2.05	0.71	1.3	3.18	3550	795.1974
71	73	8	1.64	0.51	1.61	28.05	2.73	0.23	123	123	2.3	0.78	1.23	2.99	3600	796.5079
72	74	8	1.79	0.57	1.56	27.13	2.86	0.23	128.67	128.67	2.39	0.8	1.21	2.96	3650	797.8399

OBJECTID	TransOrder	ShrCount	LRR	LR2	LCI	LSE	EPR	EPRunc	NSM	SCE	WLR	WR2	WCI	WSE	TCD	Shape_Length
73	75	8	1.86	0.6	1.51	26.29	2.9	0.23	130.65	130.65	2.47	0.8	1.24	3.01	3700	800.2285
74	76	8	1.9	0.62	1.48	25.72	2.94	0.23	132.36	132.36	2.46	0.8	1.25	3.04	3750	803.0457
75	77	8	1.97	0.63	1.5	26.09	3.04	0.23	137.02	137.02	2.53	0.77	1.38	3.37	3800	805.8848
76	78	8	2.04	0.62	1.58	27.59	3.22	0.23	144.88	144.88	2.7	0.75	1.56	3.81	3850	808.7551
77	79	8	2.08	0.61	1.66	29	3.38	0.23	151.9	151.9	2.87	0.74	1.71	4.16	3900	811.6871
78	80	8	2.17	0.63	1.66	28.99	3.51	0.23	157.87	157.87	2.92	0.74	1.71	4.17	3950	814.4686

Shoreline rates and statistics as calculated by DSAS for Alkantstrand for 6 transects cast.

OBJECTID	TransOrder	ShrCount	LRR	LR2	LCI	LSE	EPR	EPR unc	NSM	SCE	WLR	WR2	WCI	WSE	TCD	Shape_Length
1	2	8	-2.87	0.82	1.32	23.05	-3.33	0.23	-149.73	149.73	-2.73	0.81	1.31	3.26	50	214.7413
2	3	8	-3.15	0.81	1.52	26.5	-3.68	0.23	-165.75	166.35	-2.9	0.8	1.44	3.59	100	220.6967
3	4	8	-3.24	0.81	1.57	27.31	-3.77	0.23	-169.68	170.08	-2.97	0.79	1.51	3.77	150	224.9504
4	5	8	-3.32	0.84	1.47	25.58	-3.81	0.23	-171.38	171.38	-3.01	0.82	1.42	3.55	200	228.8612
5	6	8	-3.41	0.85	1.4	24.46	-3.87	0.23	-174.17	176.38	-3.03	0.82	1.44	3.59	250	232.5635
6	7	8	-3.48	0.84	1.5	26.16	-3.91	0.23	-176.09	184.52	-2.96	0.76	1.64	4.1	300	231.721

Shoreline rates and statistics as calculated by DSAS for Alkantstrand North for 203 transects cast.

OBJECTID	TransOrder	ShrCount	LRR	LR2	LCI	LSE	EPR	EPR unc	NSM	SCE	WLR	WR2	WCI	WSE	TCD	Shape_Length
1	2	8	-4.28	0.8	2.16	37.68	-4.55	0.25	-204.66	204.66	-4.88	0.77	2.63	5.55	50	278.835
2	3	8	-4.53	0.81	2.16	37.73	-4.86	0.25	-218.65	218.65	-5.09	0.81	2.49	5.24	100	299.7328
3	4	8	-4.64	0.82	2.17	37.9	-4.86	0.25	-218.69	218.69	-5.14	0.82	2.39	5.03	150	311.9315
4	5	8	-4.6	0.85	1.95	34.04	-4.64	0.25	-208.66	208.66	-5.15	0.81	2.5	5.26	200	317.813
5	6	8	-4.73	0.85	1.95	34.04	-4.76	0.25	-213.98	213.98	-5.37	0.79	2.73	5.75	250	335.3866
6	7	8	-4.72	0.87	1.85	32.21	-4.76	0.25	-214.18	214.18	-5.33	0.8	2.68	5.64	300	341.1754
7	8	8	-4.59	0.89	1.64	28.59	-4.86	0.25	-218.8	218.8	-5.15	0.79	2.66	5.61	350	349.7413
8	9	8	-4.4	0.9	1.5	26.17	-4.6	0.25	-207.15	207.15	-4.98	0.77	2.68	5.65	400	345.6103
9	10	8	-4.29	0.89	1.52	26.45	-4.28	0.25	-192.76	192.76	-4.97	0.74	2.93	6.16	450	341.6658
10	11	8	-4.13	0.89	1.42	24.8	-4.19	0.25	-188.45	188.45	-4.78	0.75	2.74	5.77	500	339.9991
11	12	8	-4.02	0.9	1.33	23.14	-4.18	0.25	-187.93	187.93	-4.58	0.78	2.41	5.07	550	341.3104
12	13	8	-3.97	0.92	1.18	20.62	-4.14	0.25	-186.44	186.44	-4.39	0.84	1.95	4.1	600	340.3059
13	14	8	-3.92	0.94	1.03	17.96	-4.09	0.25	-184.03	184.03	-4.25	0.88	1.59	3.35	650	338.3939

OBJECTID	TransOrder	ShrCount	LRR	LR2	LCI	LSE	EPR	EPRunc	NSM	SCE	WLR	WR2	WCI	WSE	TCD	Shape_Length
14	15	8	-3.79	0.95	0.89	15.48	-3.96	0.25	-178.05	178.05	-4.04	0.9	1.33	2.8	700	333.4547
15	16	8	-3.7	0.94	0.91	15.82	-3.76	0.25	-169.36	169.36	-3.87	0.91	1.18	2.48	750	325.6467
16	17	8	-3.67	0.93	1.03	18.03	-3.74	0.25	-168.18	168.18	-3.9	0.88	1.44	3.04	800	320.8008
17	18	8	-3.58	0.91	1.15	20.02	-3.75	0.25	-168.76	168.76	-3.89	0.85	1.66	3.49	850	317.7078
18	19	8	-3.52	0.9	1.18	20.55	-3.78	0.25	-170.02	170.02	-3.73	0.88	1.38	2.9	900	315.0712
19	20	8	-3.57	0.88	1.33	23.09	-3.9	0.25	-175.68	175.68	-3.71	0.9	1.22	2.56	950	317.7248
20	21	8	-3.63	0.83	1.66	28.87	-3.91	0.25	-175.82	175.82	-3.63	0.9	1.19	2.52	1000	315.5953
21	22	8	-3.58	0.84	1.53	26.69	-3.92	0.25	-176.41	176.41	-3.52	0.91	1.1	2.31	1050	314.1627
22	23	8	-3.57	0.86	1.44	25.12	-3.91	0.25	-175.73	175.73	-3.47	0.91	1.07	2.25	1100	312.7401
23	24	8	-3.51	0.87	1.34	23.37	-3.91	0.25	-175.88	175.88	-3.4	0.92	1.03	2.17	1150	314.2789
24	25	8	-3.56	0.88	1.31	22.87	-3.94	0.25	-177.17	177.17	-3.49	0.92	1	2.1	1200	317.8347
25	26	8	-3.6	0.89	1.29	22.53	-3.95	0.25	-177.79	177.79	-3.57	0.93	0.98	2.07	1250	321.0421
26	27	8	-3.53	0.89	1.26	22.05	-3.88	0.25	-174.73	174.73	-3.5	0.93	0.97	2.04	1300	322.3894

OBJECTID	TransOrder	ShrCount	LRR	LR2	LCI	LSE	EPR	EPR unc	NSM	SCE	WLR	WR2	WCI	WSE	TCD	Shape_Length
27	28	8	-3.44	0.89	1.23	21.46	-3.8	0.25	-171.15	171.15	-3.42	0.93	0.95	2.01	1350	323.5041
28	29	8	-3.32	0.88	1.21	21.18	-3.67	0.25	-165.03	165.03	-3.28	0.92	0.95	2.01	1400	321.6765
29	30	8	-3.22	0.88	1.17	20.45	-3.61	0.25	-162.47	162.47	-3.2	0.92	0.97	2.03	1450	322.6244
30	31	8	-3.08	0.87	1.18	20.57	-3.48	0.25	-156.54	156.54	-3	0.9	0.99	2.09	1500	319.6817
31	32	8	-2.93	0.86	1.17	20.38	-3.25	0.25	-146.26	146.26	-2.8	0.89	1	2.1	1550	318.1544
32	33	8	-2.88	0.85	1.2	20.88	-3.17	0.25	-142.63	142.63	-2.66	0.84	1.16	2.43	1600	319.9157
33	34	8	-2.87	0.85	1.21	21.13	-3.11	0.25	-139.91	139.91	-2.62	0.83	1.18	2.49	1650	322.0255
34	35	8	-2.8	0.85	1.19	20.78	-2.99	0.25	-134.68	134.68	-2.57	0.85	1.1	2.31	1700	321.844
35	36	8	-2.75	0.84	1.19	20.78	-2.9	0.25	-130.65	130.65	-2.58	0.87	0.99	2.09	1750	322.9274
36	37	8	-2.78	0.79	1.42	24.8	-2.87	0.25	-129.1	129.56	-2.64	0.86	1.07	2.26	1800	324.4335
37	38	8	-2.65	0.82	1.26	21.89	-2.82	0.25	-126.78	126.78	-2.53	0.87	0.98	2.07	1850	324.089
38	39	8	-2.53	0.77	1.38	23.99	-2.66	0.25	-119.86	119.86	-2.37	0.84	1.04	2.19	1900	318.4253
39	40	8	-2.48	0.75	1.43	25	-2.61	0.25	-117.59	117.96	-2.26	0.8	1.15	2.41	1950	315.9407

OBJECTID	TransOrder	ShrCount	LRR	LR2	LCI	LSE	EPR	EPR unc	NSM	SCE	WLR	WR2	WCI	WSE	TCD	Shape_Length
40	41	8	-2.48	0.76	1.4	24.43	-2.64	0.25	-118.74	118.74	-2.24	0.77	1.21	2.54	2000	318.8559
41	42	8	-2.45	0.76	1.38	24.04	-2.51	0.25	-112.91	112.91	-2.17	0.77	1.17	2.47	2050	314.5455
42	43	8	-2.53	0.78	1.35	23.54	-2.57	0.25	-115.66	115.66	-2.29	0.82	1.09	2.29	2100	314.6789
43	44	8	-2.46	0.76	1.39	24.21	-2.56	0.25	-115.27	115.27	-2.14	0.74	1.25	2.64	2150	311.2115
44	45	8	-2.5	0.78	1.33	23.1	-2.68	0.25	-120.52	120.52	-2.25	0.79	1.14	2.41	2200	313.4019
45	46	8	-2.23	0.76	1.24	21.66	-2.32	0.25	-104.47	107.27	-2	0.79	1.04	2.19	2250	297.1557
46	47	8	-2.31	0.76	1.29	22.51	-2.44	0.25	-109.58	109.58	-2.07	0.78	1.1	2.31	2300	300.7803
47	48	8	-2.24	0.75	1.31	22.83	-2.3	0.25	-103.71	103.71	-1.92	0.71	1.23	2.6	2350	296.7098
48	49	8	-2.29	0.79	1.19	20.81	-2.32	0.25	-104.39	104.39	-2.01	0.77	1.1	2.32	2400	300.2806
49	50	8	-2.56	0.82	1.22	21.2	-2.65	0.25	-119.29	119.47	-2.35	0.82	1.11	2.33	2450	319.9378
50	51	8	-2.55	0.84	1.13	19.7	-2.66	0.25	-119.67	119.67	-2.35	0.82	1.1	2.31	2500	324.5171
51	52	8	-2.29	0.84	1	17.36	-2.31	0.25	-103.98	103.98	-2.03	0.78	1.06	2.24	2550	312.8623
52	53	8	-2.2	0.86	0.88	15.27	-2.29	0.25	-103.27	103.27	-2.01	0.82	0.94	1.98	2600	315.2544

OBJECTID	TransOrder	ShrCount	LRR	LR2	LCI	LSE	EPR	EPRunc	NSM	SCE	WLR	WR2	WCI	WSE	TCD	Shape_Length
53	54	8	-2.18	0.84	0.94	16.45	-2.27	0.25	-102.16	102.16	-1.99	0.82	0.95	1.99	2650	316.6797
54	55	8	-2.11	0.81	1.03	17.91	-2.18	0.25	-98.09	98.09	-1.91	0.79	0.99	2.08	2700	315.8804
55	56	8	-2	0.77	1.08	18.82	-1.95	0.25	-87.56	95.12	-1.94	0.86	0.78	1.64	2750	314.18
56	57	8	-1.87	0.74	1.12	19.51	-1.92	0.25	-86.57	96.22	-1.8	0.82	0.83	1.75	2800	311.17
57	58	8	-1.86	0.71	1.17	20.44	-1.94	0.25	-87.15	95.17	-1.72	0.78	0.92	1.94	2850	305.6122
58	59	8	-1.92	0.74	1.13	19.73	-2.13	0.25	-96	96	-1.73	0.73	1.07	2.24	2900	307.6688
59	60	8	-1.98	0.77	1.09	19.08	-2.14	0.25	-96.17	96.17	-1.83	0.81	0.89	1.88	2950	305.8117
60	61	8	-1.97	0.75	1.12	19.56	-1.93	0.25	-86.83	87.52	-1.86	0.83	0.85	1.79	3000	296.3897
61	62	8	-1.97	0.76	1.11	19.31	-1.92	0.25	-86.25	87.86	-1.87	0.83	0.85	1.79	3050	299.7497
62	63	8	-2	0.75	1.16	20.14	-1.96	0.25	-88.06	90.6	-1.91	0.82	0.9	1.9	3100	302.839
63	64	8	-2.26	0.74	1.34	23.33	-2.26	0.25	-101.48	106.85	-2.32	0.85	0.98	2.06	3150	312.4851
64	65	8	-2.14	0.69	1.42	24.77	-2.14	0.25	-96.45	109.66	-2.15	0.83	0.97	2.05	3200	311.8392
65	66	8	-2.03	0.66	1.46	25.5	-2.01	0.25	-90.53	107.57	-1.99	0.81	0.97	2.05	3250	309.6234
66	67	8	-1.95	0.66	1.41	24.53	-1.9	0.25	-85.68	98.48	-1.81	0.76	1.01	2.13	3300	307.6922
67	68	8	-2.05	0.69	1.36	23.72	-2.06	0.25	-92.58	99.13	-1.87	0.76	1.05	2.22	3350	313.5287
68	69	8	-2.09	0.77	1.14	19.95	-2.18	0.25	-98.05	98.05	-1.93	0.81	0.94	1.98	3400	318.2389
69	70	8	-2.18	0.81	1.06	18.44	-2.26	0.25	-101.72	101.72	-2.09	0.87	0.81	1.7	3450	321.4892
70	71	8	-2.33	0.81	1.13	19.75	-2.34	0.25	-105.35	105.35	-2.12	0.8	1.05	2.22	3500	324.1273

OBJECTID	TransOrder	ShrCount	LRR	LR2	LCI	LSE	EPR	EPR unc	NSM	SCE	WLR	WR2	WCI	WSE	TCD	Shape_Length
71	72	8	-2.32	0.8	1.15	20.05	-2.4	0.25	-108.03	108.03	-2.06	0.77	1.13	2.39	3550	327.7375
72	73	8	-2.22	0.82	1.04	18.17	-2.36	0.25	-106.05	106.05	-2.1	0.86	0.85	1.8	3600	332.8065
73	74	8	-2.03	0.82	0.94	16.34	-2.23	0.25	-100.21	100.21	-1.98	0.9	0.68	1.43	3650	333.2895
74	75	8	-1.84	0.83	0.82	14.32	-2.01	0.25	-90.55	90.55	-1.89	0.92	0.56	1.19	3700	338.7804
75	76	8	-1.79	0.8	0.89	15.45	-1.74	0.25	-78.47	87.17	-1.72	0.89	0.62	1.3	3750	346.9768
76	77	8	-1.92	0.8	0.95	16.58	-1.71	0.25	-77.12	91.21	-1.73	0.84	0.75	1.58	3800	353.8174
77	78	8	-2.1	0.78	1.11	19.39	-1.87	0.25	-84.27	103.57	-1.8	0.74	1.07	2.26	3850	363.0455
78	79	8	-2.17	0.76	1.22	21.3	-1.96	0.25	-88.02	111.2	-1.87	0.73	1.14	2.41	3900	368.3985
79	80	8	-2.1	0.73	1.27	22.21	-1.95	0.25	-87.89	111.54	-1.77	0.65	1.29	2.71	3950	367.1727
80	81	8	-2.08	0.72	1.28	22.34	-1.98	0.25	-89.11	113.39	-1.78	0.65	1.29	2.72	4000	368.3054
81	82	8	-2.11	0.75	1.22	21.18	-2.06	0.25	-92.7	113.87	-1.9	0.73	1.16	2.44	4050	373.3777
82	83	8	-2.19	0.77	1.21	21.12	-2.16	0.25	-97.16	117.12	-2.02	0.77	1.12	2.35	4100	380.2865
83	84	8	-2.27	0.76	1.26	21.94	-2.21	0.25	-99.44	120.41	-2.08	0.78	1.09	2.3	4150	384.9303
84	85	8	-2.32	0.75	1.35	23.47	-2.23	0.25	-100.14	122.8	-2.08	0.77	1.14	2.41	4200	387.639
85	86	8	-2.31	0.75	1.33	23.2	-2.23	0.25	-100.51	119.71	-1.98	0.71	1.27	2.68	4250	389.9633
86	87	8	-2.33	0.76	1.32	23.03	-2.3	0.25	-103.41	117.93	-2.02	0.73	1.24	2.62	4300	390.665
87	88	8	-2.29	0.74	1.36	23.71	-2.19	0.25	-98.63	116.33	-1.96	0.71	1.24	2.62	4350	389.2319

OBJECTID	TransOrder	ShrCount	LRR	LR2	LCI	LSE	EPR	EPR unc	NSM	SCE	WLR	WR2	WCI	WSE	TCD	Shape_Length
88	89	8	-2.06	0.68	1.43	24.91	-1.91	0.25	-85.74	114.12	-1.74	0.65	1.27	2.68	4400	383.4819
89	90	8	-1.76	0.58	1.5	26.14	-1.55	0.25	-69.7	108.26	-1.44	0.55	1.29	2.72	4450	374.0821
90	91	8	-1.87	0.54	1.72	29.91	-1.75	0.25	-78.71	129.13	-1.67	0.59	1.4	2.94	4500	384.3183
91	92	8	-1.86	0.56	1.66	28.98	-1.69	0.25	-76.11	126.78	-1.75	0.67	1.21	2.56	4550	380.8774
92	93	8	-1.74	0.52	1.65	28.8	-1.5	0.25	-67.47	117.18	-1.59	0.65	1.15	2.43	4600	366.5437
93	94	8	-1.7	0.48	1.78	31.03	-1.28	0.25	-57.67	116.24	-1.43	0.52	1.37	2.89	4650	356.9966
94	95	8	-1.75	0.43	2	34.91	-1.22	0.25	-55.1	127.93	-1.52	0.5	1.52	3.2	4700	358.6849
95	96	8	-1.63	0.46	1.77	30.78	-1.15	0.25	-51.78	115.96	-1.58	0.58	1.35	2.85	4750	358.5042
96	97	8	-1.67	0.52	1.61	28.04	-1.38	0.25	-62.28	108.17	-1.68	0.67	1.17	2.47	4800	355.3066
97	98	8	-1.72	0.52	1.66	28.85	-1.51	0.25	-68	110.3	-1.71	0.68	1.17	2.45	4850	352.9735
98	99	8	-1.71	0.5	1.7	29.63	-1.56	0.25	-70.42	113.6	-1.68	0.67	1.18	2.48	4900	354.3462
99	100	8	-1.7	0.58	1.45	25.26	-1.55	0.25	-69.97	105.11	-1.62	0.71	1.04	2.19	4950	355.1191
100	101	8	-1.88	0.66	1.34	23.42	-1.6	0.25	-71.93	105.99	-1.85	0.8	0.93	1.96	5000	360.2007
101	102	8	-1.97	0.66	1.41	24.5	-1.5	0.25	-67.71	107.69	-1.89	0.78	1.01	2.14	5050	361.0193
102	103	8	-2.12	0.61	1.69	29.46	-1.66	0.25	-74.88	129.34	-2.01	0.75	1.16	2.44	5100	372.7604
103	104	8	-2.26	0.64	1.69	29.41	-1.9	0.25	-85.52	134.15	-2.13	0.77	1.16	2.44	5150	378.421
104	105	8	-2.38	0.66	1.69	29.4	-2.15	0.25	-96.64	138.6	-2.25	0.79	1.16	2.44	5200	384.1922
105	106	8	-2.45	0.65	1.79	31.28	-2.22	0.25	-99.81	143.88	-2.3	0.77	1.24	2.62	5250	386.9937
106	107	8	-2.6	0.62	2.02	35.29	-2.39	0.25	-107.49	158.92	-2.42	0.73	1.46	3.06	5300	392.3766

OBJECTID	TransOrder	ShrCount	LRR	LR2	LCI	LSE	EPR	EPR unc	NSM	SCE	WLR	WR2	WCI	WSE	TCD	Shape_Length
107	108	8	-2.43	0.57	2.13	37.1	-2.12	0.25	-95.57	162.7	-2.28	0.7	1.51	3.17	5350	395.3961
108	109	8	-2.37	0.56	2.09	36.48	-2.06	0.25	-92.89	155.33	-2.15	0.67	1.51	3.18	5400	388.1015
109	110	8	-2.41	0.64	1.82	31.65	-2.35	0.25	-105.59	146.42	-2.22	0.71	1.41	2.98	5450	391.0001
110	111	8	-2.4	0.65	1.75	30.58	-2.36	0.25	-106.39	141.04	-2.21	0.73	1.34	2.82	5500	389.3218
111	112	8	-2.35	0.65	1.74	30.37	-2.31	0.25	-104.11	138.24	-2.17	0.73	1.31	2.75	5550	388.8359
112	113	8	-2.32	0.62	1.83	31.92	-2.21	0.25	-99.26	140.56	-2.14	0.73	1.32	2.77	5600	389.562
113	114	8	-2.04	0.61	1.63	28.45	-1.97	0.25	-88.6	125.64	-1.82	0.65	1.32	2.78	5650	387.9171
114	115	8	-1.87	0.59	1.55	27.01	-1.83	0.25	-82.2	121.43	-1.71	0.64	1.27	2.67	5700	388.9786
115	116	8	-1.71	0.53	1.6	27.85	-1.57	0.25	-70.7	119.07	-1.63	0.67	1.14	2.41	5750	384.4396
116	117	8	-1.65	0.54	1.53	26.68	-1.48	0.25	-66.52	108.9	-1.65	0.73	0.99	2.09	5800	375.6479
117	118	8	-1.58	0.55	1.44	25.03	-1.51	0.25	-67.85	97.57	-1.55	0.73	0.94	1.98	5850	367.6908
118	119	8	-1.69	0.58	1.43	24.98	-1.75	0.25	-78.83	96.46	-1.65	0.75	0.95	2	5900	365.4369
119	120	8	-1.83	0.57	1.59	27.67	-1.9	0.25	-85.31	104.31	-1.79	0.74	1.05	2.21	5950	363.4558
120	121	8	-1.93	0.53	1.82	31.67	-1.88	0.25	-84.66	119.85	-1.95	0.73	1.18	2.48	6000	364.9726
121	122	8	-2.05	0.48	2.14	37.35	-1.91	0.25	-86.16	142.42	-2.1	0.7	1.38	2.9	6050	369.804
122	123	8	-2.24	0.48	2.34	40.79	-2.15	0.25	-96.6	161.8	-2.31	0.7	1.51	3.19	6100	377.0138
123	124	8	-2.26	0.51	2.2	38.33	-2.17	0.25	-97.53	153.31	-2.3	0.73	1.41	2.98	6150	371.8791
124	125	8	-2.26	0.54	2.09	36.44	-2.17	0.25	-97.77	150.66	-2.35	0.75	1.35	2.84	6200	372.3877

OBJECTID	TransOrder	ShrCount	LRR	LR2	LCI	LSE	EPR	EPRunc	NSM	SCE	WLR	WR2	WCI	WSE	TCD	Shape_Length
125	126	8	-2.15	0.49	2.18	38.01	-1.91	0.25	-86.17	156.87	-2.24	0.71	1.43	3.02	6250	373.8108
126	127	8	-2.05	0.5	2.03	35.3	-1.84	0.25	-82.89	152.05	-2.12	0.69	1.41	2.96	6300	375.2646
127	128	8	-1.98	0.54	1.81	31.55	-1.79	0.25	-80.58	141.52	-2.04	0.71	1.31	2.75	6350	371.4166
128	129	8	-1.93	0.58	1.64	28.52	-1.74	0.25	-78.22	132.06	-1.96	0.73	1.18	2.49	6400	365.4159
129	130	8	-1.95	0.62	1.52	26.56	-1.78	0.25	-80.06	128.18	-1.97	0.75	1.12	2.37	6450	362.6173
130	131	8	-2.08	0.71	1.34	23.28	-2	0.25	-90.22	123.09	-2.12	0.83	0.97	2.03	6500	359.8466
131	132	8	-2.18	0.71	1.38	24.02	-2.09	0.25	-94.09	126.14	-2.24	0.85	0.94	1.99	6550	355.9693
132	133	8	-2.2	0.71	1.4	24.36	-2.05	0.25	-92.27	125.1	-2.28	0.86	0.93	1.96	6600	350.6423
133	134	8	-2.11	0.69	1.4	24.46	-1.89	0.25	-84.92	118.79	-2.15	0.84	0.92	1.94	6650	339.4994
134	135	8	-2.18	0.72	1.35	23.53	-2.05	0.25	-92.15	116.9	-2.19	0.86	0.87	1.84	6700	334.7275
135	136	8	-2.13	0.72	1.31	22.88	-2.02	0.25	-90.88	113.92	-2.16	0.87	0.85	1.78	6750	329.9738
136	137	8	-2.37	0.76	1.34	23.4	-2.36	0.25	-106.24	113.53	-2.49	0.87	0.97	2.05	6800	324.6296
137	138	8	-2.71	0.77	1.48	25.8	-2.9	0.25	-130.52	130.52	-2.88	0.88	1.06	2.23	6850	328.0338
138	139	8	-2.46	0.77	1.33	23.13	-2.56	0.25	-115.12	121.89	-2.55	0.89	0.88	1.86	6900	327.772
139	140	8	-1.96	0.67	1.39	24.21	-1.79	0.25	-80.41	119.61	-2.03	0.82	0.95	2.01	6950	326.2784
140	141	8	-1.86	0.64	1.39	24.22	-1.64	0.25	-73.86	117.91	-1.93	0.79	0.99	2.08	7000	327.8263
141	142	8	-1.78	0.66	1.27	22.12	-1.54	0.25	-69.21	109.89	-1.88	0.8	0.94	1.98	7050	329.1942
142	143	8	-1.68	0.67	1.17	20.42	-1.41	0.25	-63.34	101.32	-1.71	0.8	0.84	1.78	7100	328.4952

OBJECTID	TransOrder	ShrCount	LRR	LR2	LCI	LSE	EPR	EPR unc	NSM	SCE	WLR	WR2	WCI	WSE	TCD	Shape_Length
143	144	8	-1.66	0.69	1.11	19.3	-1.4	0.25	-62.98	96.94	-1.59	0.81	0.77	1.63	7150	328.6893
144	145	8	-1.63	0.67	1.15	19.97	-1.39	0.25	-62.69	98	-1.55	0.79	0.81	1.7	7200	328.4881
145	146	8	-1.69	0.64	1.27	22.12	-1.47	0.25	-66.23	104.48	-1.61	0.77	0.88	1.85	7250	327.0929
146	147	8	-1.72	0.69	1.16	20.15	-1.54	0.25	-69.14	99.57	-1.65	0.81	0.79	1.66	7300	325.1004
147	148	8	-1.65	0.76	0.94	16.3	-1.53	0.25	-68.84	88.53	-1.59	0.86	0.65	1.36	7350	322.6924
148	149	8	-1.64	0.76	0.92	16.11	-1.53	0.25	-68.79	88.68	-1.57	0.85	0.67	1.4	7400	322.0691
149	150	8	-1.73	0.76	0.97	16.85	-1.59	0.25	-71.34	93.73	-1.72	0.88	0.65	1.37	7450	323.1479
150	151	8	-1.85	0.7	1.21	21.16	-1.57	0.25	-70.75	104.97	-1.8	0.84	0.8	1.69	7500	318.2702
151	152	8	-1.96	0.72	1.22	21.26	-1.6	0.25	-72.14	106.9	-1.87	0.84	0.82	1.73	7550	315.0775
152	153	8	-2.07	0.78	1.09	18.92	-1.72	0.25	-77.59	103.32	-1.95	0.86	0.78	1.63	7600	314.3141
153	154	8	-2.08	0.78	1.1	19.19	-1.72	0.25	-77.4	103.27	-1.96	0.87	0.77	1.61	7650	308.5375
154	155	8	-2.03	0.78	1.08	18.85	-1.68	0.25	-75.68	102.07	-1.92	0.87	0.73	1.54	7700	302.6944
155	156	8	-1.92	0.75	1.11	19.38	-1.51	0.25	-67.9	97.47	-1.79	0.85	0.76	1.59	7750	292.0731
156	157	8	-1.83	0.74	1.09	19	-1.51	0.25	-68.1	96.99	-1.67	0.82	0.77	1.62	7800	286.5055
157	158	8	-1.83	0.67	1.29	22.53	-1.51	0.25	-67.87	106.25	-1.61	0.73	0.98	2.07	7850	282.6458
158	159	8	-1.79	0.67	1.24	21.63	-1.43	0.25	-64.5	101.71	-1.58	0.75	0.91	1.92	7900	280.1761
159	160	8	-1.7	0.65	1.24	21.56	-1.28	0.25	-57.76	96.97	-1.47	0.72	0.92	1.94	7950	278.8562
160	161	8	-1.73	0.65	1.27	22.2	-1.38	0.25	-62.27	103.15	-1.57	0.73	0.97	2.03	8000	285.4791
161	162	8	-1.76	0.65	1.28	22.39	-1.47	0.25	-66.1	104.57	-1.64	0.76	0.93	1.97	8050	288.4686
162	163	8	-2.01	0.67	1.42	24.74	-1.73	0.25	-77.71	117.08	-1.9	0.78	1.01	2.13	8100	299.7317

OBJECTID	TransOrder	ShrCount	LRR	LR2	LCI	LSE	EPR	EPR unc	NSM	SCE	WLR	WR2	WCI	WSE	TCD	Shape_Length
163	164	8	-2.13	0.64	1.58	27.59	-1.74	0.25	-78.23	122.61	-2	0.78	1.07	2.26	8150	303.6063
164	165	8	-2.15	0.54	2	34.8	-1.54	0.25	-69.27	138.8	-1.96	0.68	1.34	2.82	8200	309.5554
165	166	8	-2.16	0.49	2.22	38.65	-1.48	0.25	-66.82	151.07	-1.95	0.63	1.49	3.14	8250	320.3003
166	167	8	-1.92	0.52	1.85	32.3	-1.34	0.25	-60.1	130.5	-1.72	0.64	1.28	2.7	8300	324.5173
167	168	8	-1.78	0.52	1.72	29.95	-1.22	0.25	-54.72	121.36	-1.68	0.65	1.22	2.57	8350	325.6579
168	169	8	-1.83	0.59	1.53	26.68	-1.4	0.25	-62.91	116.03	-1.87	0.66	1.34	2.81	8400	331.8196
169	170	8	-1.88	0.69	1.25	21.82	-1.51	0.25	-67.93	105.67	-1.86	0.75	1.06	2.23	8450	330.775
170	171	8	-1.96	0.74	1.16	20.22	-1.61	0.25	-72.56	106.25	-1.85	0.83	0.85	1.79	8500	328.2314
171	172	8	-1.8	0.85	0.77	13.37	-1.56	0.25	-70.13	82.08	-1.64	0.86	0.65	1.38	8550	319.9567
172	173	8	-1.86	0.82	0.88	15.39	-1.65	0.25	-74.46	91.46	-1.73	0.84	0.75	1.58	8600	319.3114
173	174	8	-1.89	0.86	0.76	13.18	-1.7	0.25	-76.67	86.79	-1.78	0.87	0.68	1.43	8650	317.2932
174	175	8	-1.89	0.89	0.67	11.63	-1.69	0.25	-75.83	81.82	-1.81	0.91	0.58	1.22	8700	314.3413
175	176	8	-1.85	0.89	0.64	11.16	-1.59	0.25	-71.53	77.76	-1.82	0.93	0.49	1.02	8750	308.3192
176	177	8	-1.71	0.89	0.59	10.35	-1.46	0.25	-65.64	70.77	-1.61	0.93	0.46	0.96	8800	298.3088
177	178	8	-1.75	0.88	0.64	11.07	-1.63	0.25	-73.52	78.23	-1.61	0.83	0.71	1.5	8850	299.4329
178	179	8	-1.83	0.81	0.87	15.25	-1.67	0.25	-74.97	89.5	-1.61	0.76	0.9	1.89	8900	293.7273
179	180	8	-1.81	0.74	1.08	18.76	-1.58	0.25	-70.92	96.37	-1.54	0.68	1.06	2.23	8950	288.8247
180	181	8	-1.74	0.69	1.15	20.13	-1.37	0.25	-61.66	96.07	-1.52	0.73	0.93	1.97	9000	283.7957
181	182	8	-1.64	0.67	1.15	20.11	-1.22	0.25	-54.95	92.79	-1.51	0.74	0.89	1.87	9050	282.4565
182	183	8	-1.53	0.66	1.1	19.25	-1.08	0.25	-48.68	85.65	-1.46	0.74	0.86	1.8	9100	278.2314

OBJECTID	TransOrder	ShrCount	LRR	LR2	LCI	LSE	EPR	EPR unc	NSM	SCE	WLR	WR2	WCI	WSE	TCD	Shape_Length
183	184	8	-1.48	0.53	1.4	24.43	-0.93	0.25	-41.88	98.05	-1.42	0.65	1.04	2.19	9150	273.5365
184	185	8	-1.46	0.46	1.57	27.45	-0.89	0.25	-40.05	105.44	-1.39	0.6	1.12	2.37	9200	266.8646
185	186	8	-1.44	0.5	1.43	25.01	-0.95	0.25	-42.86	99.91	-1.38	0.65	1.02	2.14	9250	261.4036
186	187	8	-1.44	0.61	1.14	19.89	-1.16	0.25	-51.99	92.89	-1.39	0.72	0.87	1.84	9300	264.5094
187	188	8	-1.47	0.63	1.12	19.46	-1.24	0.25	-55.74	94.04	-1.38	0.69	0.94	1.97	9350	265.7908
188	189	8	-1.43	0.62	1.12	19.44	-1.1	0.25	-49.63	88.66	-1.29	0.7	0.84	1.76	9400	258.4319
189	190	8	-1.37	0.6	1.12	19.53	-1.04	0.25	-46.93	84.68	-1.16	0.63	0.88	1.86	9450	255.217
190	191	8	-1.58	0.65	1.15	20.12	-1.33	0.25	-59.73	96.8	-1.44	0.7	0.94	1.97	9500	267.8557
191	192	8	-1.8	0.59	1.51	26.26	-1.4	0.25	-63.19	116.71	-1.67	0.71	1.05	2.21	9550	273.4743
192	193	8	-1.9	0.59	1.6	27.83	-1.44	0.25	-64.7	121.53	-1.78	0.73	1.07	2.26	9600	277.1764
193	194	8	-1.88	0.58	1.61	28.1	-1.42	0.25	-63.86	121.28	-1.75	0.72	1.09	2.29	9650	278.6659
194	195	8	-1.81	0.53	1.7	29.65	-1.43	0.25	-64.17	126.61	-1.71	0.68	1.17	2.47	9700	283.348
195	196	8	-1.62	0.48	1.7	29.66	-1.2	0.25	-54.02	118.29	-1.52	0.64	1.14	2.4	9750	277.5643
196	197	8	-1.61	0.47	1.71	29.86	-1.24	0.25	-55.59	121.68	-1.54	0.62	1.2	2.52	9800	282.1549
197	198	8	-1.52	0.47	1.63	28.34	-1.16	0.25	-52.25	115.28	-1.41	0.59	1.17	2.46	9850	279.9055
198	199	8	-1.41	0.45	1.55	27.04	-1.06	0.25	-47.7	108.16	-1.25	0.53	1.16	2.45	9900	275.0142
199	200	8	-1.42	0.43	1.62	28.27	-1.09	0.25	-49.09	112.97	-1.23	0.48	1.28	2.7	9950	274.9974
200	201	8	-1.47	0.4	1.81	31.58	-1.22	0.25	-55.07	127.65	-1.29	0.39	1.6	3.37	10000	281.7143
201	202	8	-1.42	0.37	1.85	32.22	-1.19	0.25	-53.44	130.12	-1.28	0.37	1.67	3.53	10050	284.1808
202	203	8	-1.34	0.35	1.84	32.15	-1.08	0.25	-48.39	127.88	-1.24	0.37	1.62	3.42	10100	281.6099

OBJECTID	TransOrder	ShrCount	LRR	LR2	LCI	LSE	EPR	EPR unc	NSM	SCE	WLR	WR2	WCI	WSE	TCD	Shape_Length
203	204	8	-1.24	0.3	1.91	33.21	-0.92	0.25	-41.58	126.98	-1.12	0.31	1.65	3.49	10150	276.6713